A CYTOLOGICAL AND HISTOCHEMICAL STUDY OF THE HOST-PARASITE INTERACTION OF *ENDOCRONARTIUM HARKNESSII* ON HARD PINES

BY

© ANTHONY ARTHUR HOPKIN

A Thesis

Submitted to the Faculty of Graduate Studies
in partial fulfillment of the
requirements for the degree of
Doctor of Philosophy

Department of Botany
University of Manitoba
Winnipeg, Manitoba
R3T 2N2

ISBN 0-315-33984-5

A CYTOLOGICAL AND HISTOCHEMICAL STUDY OF THE HOST-PARASITE INTERACTION OF ENDOCRONARTIUM HARKNESSII ON HARD PINES

BY

ANTHONY ARTHUR HOPKIN

A thesis submitted to the Faculty of Graduate Studies of the University of Manitoba in partial fulfillment of the requirements of the degree of

DOCTOR OF PHILOSOPHY

TABLE OF CONTENTS

List of Abbreviations

Al	-	amorphous layer
ANS	-	1-aniline-8-Napthalene - sulphuric acid
AP	-	appressorium
C	-	collar
CP	-	phosphotungstic acid in chromic acid
CU	-	cuticle
CW	-	host cell wall
EHM	-	extrahaustorial matrix
EM	-	extrahaustorial membrane
ER	-	endoplasmic reticulum
G	-	Golgi bodies
Glut	-	gluteraldehyde
H	-	haustorium
HB	-	haustorial body
HMC	-	haustorial mother cell
HN	-	haustorial neck
H O	-	Hydrogen peroxide
IH	-	intercellular hyphae
L	-	lipid
N	-	nucleus
OsO	-	osmium tetroxide
PA	-	periodic acid
PACP	-	periodic acid - chromic acid - phosphotungstic acid
PA-SP	-	periodic acid - silver proteinate
PA-TCH-SP	-	periodic acid - thiocarbohydrazide - silver proteinate
PbC	-	lead citrate
PTA	-	phosphotungstic acid
S	-	septum
SITS	-	4-acetoamido-4'-isothiocyana-tostibene-2, 2'-disulfonic acid
SV	-	subcuticular vesicle
TCH	-	thiocarbohydrazide
TCH-SP	-	thiocarbohydrazide - silver proteinate
UA	-	uranyl acetate
V	-	vesicle
VA	-	vacuole
WGL	-	wheat germ lectin
WGL-gold	-	gold-bound wheat germ lectin
WL	-	wall layer

Acknowledgements

I wish to express my appreciation to Dr. James Reid, my supervisor and mentor. I am deeply indebted to him for his guidance during the course of this study, and for his efforts in the preparation of this manuscript. I would also like to thank the other members of the Advisory Committee; Drs. J. Chong and D. Harder for their advice and access to their facilities, Dr. Y. Hiratsuka for the interest he has shown in me, and Dr. D. Punter for his patience and advice.

I am also grateful to Dr. A. Olchowecki for his preparation of the color plates in this thesis, and for advice on photographic techniques, related and unrelated to this thesis. And also to Mrs. J. Gourlay for her persistance in the typing of this thesis.

A special note of gratitude to Prof. Mike Sumner for his encouragement, advice and friendship.

Finally, I would like to express my sincere appreciation to my wife Joanne, for her understanding and sacrifice in our five years of marriage.

This study was sponsored by the Canadian Forestry Service under a PRUF contract granted to Dr. J. Reid, for which the author is extremely grateful.

ABSTRACT

The host- parasite interaction of Endocronartium harknessii (Moore) Y. Hirst. on hard pines was investigated using light and electron microscopy.

The nature of the haustorium was studied using histochemical procedures: PACP, PA-TCH-SP, WGL - gold and cellulase extraction. Haustoria were also examined in UA/PbC stained material by electron microscopy, and fresh, freeze sectioned, and fixed, epoxy-embedded material was selectively stained and examined using fluorescence and brightfield microscopy. The study also focused on the infection process of the rust fungus on juvenile seedlings, as well as host responses in both compatible and incompatible reactions.

Infection of the host was direct, through the cuticle followed by production of a subcuticular vesicle from which a mycelium developed between the cuticle and epidermis. Haustoria were formed from the mycelium, infecting adjacent epidermal cells. Subsequent to this, hyphae grew between epidermal cells and ramified through the cortex, ultimately infecting the vascular tissue.

Light and electron microscopy were also used to help elucidate the process of host cell penetration and haustorial development. The penetration peg which developed from an apparently unspecialized hyphal element appeared as a narrowed tubular structure that penetrated the host cell wall through mechanical and possibly enzymatic action. The incipient haustorium also displayed a peg-like appearance, though in later stages of development, swelling occurred in its distal portion resulting in the appearance

of a globose to lobed haustorial body delimited by a narrow, septate neck region.

Histochemical tests provided evidence for a degree of specialization of the haustorial neck as compared to the intercellular hyphae. The neck region does not possess a neck ring as reported for D- haustoria, but some evidence of a barrier to apoplastic transport in this region is provided by the use of the fluorochrome SITS. The haustorial body was surrounded by an invaginated portion of the host plasmalemma which was separated from the haustorium by the extrahaustorial matrix. Histochemical tests showed this matrix to be composed of polysaccharides with 1,4 and beta-1,3 linkages, as well as lipids.

Observations on the compatible reaction failed to detect an elaborate alteration of the host ER system in infected cells. However host ER was closely associated with the haustorium and may be directly continuous with the extrahaustorial matrix. A number of host cells appeared to react to invading haustoria by the production of collars, which were apparently composed of material similar to that in host cell walls.

Resistance of the Japanese black pine to E. harknessii was also examined. The host generally appeared to restrict the mycelium to the cortex, most infected cells being necrotic. Periderm formation in the cortex seemed to provide an effective barrier between the mycelium and host vascular tissue. However, some evidence of vascular tissue infection was observed, although in most cases this resulted in a complete breakdown of the host cell protoplasm.

LIST OF FIGURES

GENERAL INTRODUCTION

Endocronartium harknessii (J.P. Moore) Y. Hirat. is an autoecious, endocyclic rust that induces globose branch and stem galls to form on hard pines. The rust, commonly known as western gall rust or pine-to-pine gall rust, is considered to be the most common and destructive stem rust in western Canada (Ziller 1974). Although there have been frequent reports of damage caused by this rust (e.g. Hiratsuka and Powell 1976; Ziller 1974), damage is usually restricted to a few acres and often only associated with tree nurseries.

In the past, *E. harknessii* was commonly confused with *Cronartium quercuum* (Berk.) Miyabe ex Shirai, the eastern gall rust. For years *E. harknessii* was believed to be restricted to the western half of North America with the heteroecious *C. quercuum* predominating in the eastern half of the continent. The two rusts produce morphologically indistinguishable galls, and the fact that the true range of *E. harknessii* also extended into eastern North America only became apparent after Anderson and French (1965) developed a technique to separate the two rusts on the basis of aeciospore germ-tube morphology. The common name, western gall rust, is a misnomer as the rust is widely distributed in eastern Canada and the northeastern United States, as well as western North America and northern Mexico. Although this pathogen is presently confined to North America, it does pose a potential threat to susceptible *Pinus* spp. in other parts of the world due to its pine-to-pine habit (Hiratsuka and Powell 1976).

Unlike C. quercuum, E. harknessii has a reduced nuclear cycle. Using the ontogenic system of nomenclature prepared by Cummins (1959) which emphasizes the position of the spore states in the life cycle, the infective spores of E. harknessii are aecioid teliospores. These functional teliospores are morphologically aeciospores but, on germination, produce a germ tube which functions as the basidiospore (Hiratsuka 1969). The germ tube penetrates directly through the cuticle of the current years shoots and leaders (Nelson 1970), successful infection causing woody galls, witches brooms, stunting, and tree mortality. New teliospores are produced on the galls one or two years after initial infection and are then dispersed.

A number of hard pines are known to be susceptible to E. harknessii; Pinus banksiana Lamb., P. contorta Dougl., P. jeffreyi A. Murr., P. mugo Turra, P. ponderosa Laws., P. radiata D. Don and P. sylvestris L., are all found to be naturally infected. Some southern pines, including P. elliottii Engelm. var. elliottii and P. taeda L., two economically important species, are also susceptible when artificially inoculated. However, E. harknessii is not indigenous to the southern United States and Pinus species such as P. virginiana Mill., which one might expect to serve as a bridging host species, do not appear to be susceptible to the rust (Wenner and Merrill 1984).

While western gall rust has long been considered a forest management problem, the biology and the nature of the interaction of the rust fungus with its hosts are poorly understood. Thus,

while tree breeders are producing superior quality stock, there is a danger that the genetic base of hard pine forests is being reduced in a manner which will make them more susceptible to rusts such as E. harknessii. To minimize possible future problems in intensively managed forests, it is important to fully understand the biology and host-parasite relationships of pathogens such as E. harknessii.

The purpose of this study was, therefore, to carry out a cytological study of western gall rust on hard pines, and specifically investigate:

1) the infection and colonization of host tissues;

2) the nature and degree of specialization of the haustorium; and

3) the nature of presumptive resistant and susceptible host reactions to the rust.

Thus, the general aim of the study was to apply light and electron microscopic techniques to obtain information that might help in the understanding of this tree disease and its causal agent, as well as to obtain information basic to the development of successful control practices.

LITERATURE REVIEW

I. History and Occurrence of *Endocronartium harknessii*

Peridermium harknessii J.P. Moore, the cause of Western gall rust, appears to have been first fully described in Harkness (1884) on *Pinus ponderosa* Laws. and later reported by Hedgcock (1912) on *P. jeffreyi*. The true life cycle of the rust was not then understood and, as it was only found on pine hosts, it was considered to be in the imperfect state. Consequently it was placed in the genus *Peridermium*, and for years included in the *Cronartium coleosporioides* Diet. and Holow. complex (Arthur 1934; Cummins 1962). In 1926, York reported the occurrence of a *Peridermium* sp. on *P. sylvestris* in a tree plantation near Woodgate, New York. This rust was well established in the plantation, though its specific identity was unknown, hence it became known as the Woodgate gall rust (York 1929). Not until 1957 did Boyce determine that this rust was identical to *P. harknessii*.

Early workers (Meinecke 1916, 1920, 1929; Weir and Hubert 1917) suggested that *P. harknessii* (= *E. harknessii*) exhibited facultative heteroecism, infecting *Castilleja miniata* Dougl. as the alternate host. However, this was subsequently disputed by Lorbeer (1955), Wagner (1964), and Zalasky and Riley (1963). Wagner(1964) suggested surface contamination of *C. miniata* by *P. stalactiforme* Arth. & Kern (=*Cronartium coleosporioides*) that was present in the same area from which the *Castilleja* plants were taken, may have resulted in the apparent heteroecism observed by Meinecke (1929). Some early reports suggested that *P. harknessii* was autoecious

(Fromme 1916; McKenzie 1942), and as early as 1932 Jackson even suspected the rust of having an endo-type life cycle. However, the other endocyclic rusts, Endophyllum spp. and Kunkelia spp., all produce basidiospores; this made the acceptance of P. harknessii as an endocyclic rust contentious, since it was not then clear whether the infectious spores were functioning as teliospores.

Hiratsuka et al. (1966) demonstrated that aeciospores of P. harknessii germinate directly, with the germ tube apparently functioning as both the metabasidium and as a functional basidiospore following meiotic division of the germinating spore's nucleus. However, Christenson (1968), in a similar study, suggested that nuclear division was mitotic. True (1938) also reported a grouping of the two nuclei in the infectious spore with no apparent fusion, indicating the possibility of parasexuality.

Hiratsuka (1969) suggested that since the aecioid teliospores of P. harknessii and those of Peridermium pini (Pers) Lev., both produce functional basidiospores upon germination, they should not be assigned to the imperfect genus Peridermium. Hiratsuka felt the unique characteristics of these two apparently endocyclic rusts made them worthy of inclusion in a new, discrete genus, and he therefore created Endocronartium to accommodate endo-species which were morphologically similar to the species of the imperfect genus Peridermium Lk.

II. Host Colonization and Haustorium Development

Host penetration by germinating rust basidiospores was first described by DeBary (1863); other early reports include those by Robinson (1913) and Waterhouse (1921). Later Allen (1930, 1932a, 1932b, 1934, 1935) in a series of papers concerning several species of the genus Puccinia, provided detailed descriptions of basidiospore infections. Other early work that contributed to the understanding of the process of infection by basidiospore germlings, and subsequent host colonization, were the light microscopic investigations of Gymnosporangium juniperi-virginianae Schw. on Malus spp. by Reed and Grabill (1915) and Nusbaum (1935).

Infections derived from basidiospore germlings usually occur as a result of direct penetration through the cuticle and epidermis, with the subsequent production of an intracellular vesicle within the epidermis; the latter was described as a primary hypha by Allen (1935) and Nusbaum (1935).

In all reported instances, inter- and intracellular structures form in the host when infection hyphae, produced from the intracellular vesicle (primary hypha), exited from the epidermal cell directly into adjacent cells or intercellular spaces. The initial penetration of the epidermal cell by the basidiospore germling appears to be due to enzymatic action (Gold and Mendgen 1984a; Gray et al. 1983). Conversely, the outgrowth of the intracellular hypha from the infected cell may be due to a

mechanical process as described for Uromyces appendiculatus (Pers.) Unger var. appendiculatus (Gold and Mendgen 1984b).

In contrast to the direct penetration process reported for basidiospore germlings of most rusts, Clinton and McCormick (1919), and Patton and Johnson (1970), state that monokaryotic infections of pine needles by C. ribicola A. Fisch. occur indirectly through stomata in a manner similar to urediniospore derived infections. Sato et al. (1980) reported direct host penetration by infection hyphae arising from the promycelium of Uromyces aloes (Cooke) P. Magnus. The latter is a microcyclic rust that germinates without producing basidiospores, although its method of infection is similar to that of directly penetrating basidiospore germlings of other rusts.

The infection process of an endocyclic rust has not been described previously, although early stages of infection of P. sylvestris by the Woodgate Peridermium (True 1938) may have actually dealt with E. harknessii (Boyce 1957). As well, Van der Kamp (1970) provided some information on the early colonization of P. sylvestris by Peridermium pini, also believed to be an endocyclic rust (Hiratsuka 1969), but he did not describe the infection process.

The ultrastructure of the infection process as it relates to M- haustoria has not been well studied. Recently Gold and Mendgen (1984a) and Gray et al. (1983) described basidiospore infection and early colonization of U. appendiculatus appendiculatus and Cronartium quercuum (Berk.) Miyabe ex Shirai f. sp. fusiforme

Burdsall and Snow respectively, using electron microscopy. Similarly, Kohno et al. (1977) investigated the ultrastructure of the infection process of the microcyclic rust Kuehneola japonica (Diet.) Diet. on Rosa sp.

Little is known about the formation of the penetration peg and the subsequent development of M- haustoria in monokaryotic stages of rust infections. Most information relating to the ultrastructure of this process deals with dikaryotic infections, although even here information is restricted to reports on Uromyces phaseoli (Pers.) Wint. var. vignae (Barcl.) Arth. (Heath and Heath 1975); Melampsora lini (Pers.) Lév. (Littlefield and Bracker 1972) and Puccinia graminis Pers. f. sp. tritici Eriks. and Henn. and P. coronata Cda. f. sp. avenae Eriks. (Chong 1981). These authors report that penetration pegs appear to originate as localized evaginations from the haustorial mother cells. Heath and Heath (1975), and Littlefield and Bracker (1972) report that only the inner wall layer of the haustorial mother cell is involved in the production of the penetration peg. However, Chong (1981) reported that both the inner and middle wall layers of the mother cell are continuous throughout the penetration region.

Littlefield and Heath (1979) suggested that penetration pegs grow by "tip growth", but apical vesicles similar to those deemed responsible for apical growth of hyphae (Grove and Bracker 1970) were not evident. However Littlefield and Bracker (1972) noted the presence of multivesicular structures in the penetration pegs of M. lini.

The morphology of penetration pegs has been described for the developing M- haustoria of C. ribicola (Robb et al. 1975b); Puccinia poarum Niels. (Al-Keshraji and Losel 1981) and Puccinia sorghi Schw. (Rijkenberg and Truter 1973); the penetration pegs of the latter two rusts show no significant reduction in diameter where they penetrate the host cell wall. Conversely the penetration peg of C. ribicola appears not unlike those of D-haustoria, at least during the initial stages of penetration.

The ontogeny of M- haustoria is not reported in any detail at the ultrastructural level. Again, most information regarding haustorial ontogeny comes from studies of D- haustoria. Chong (1981) described stages of early haustorial formation in P. graminis tritici and P. coronata avenae, and showed the peg-like morphology of the incipient haustorium prior to swelling of the body. Heath and Heath (1975) provided information on development of the D-haustorial neck and body of U. phaseoli vignae, as well as a schematic representation of host cell penetration and subsequent development of the haustorium. However, perhaps the most instructive study was reported by Littlefield (1972) who used light microscopy to visualize the ontogeny of the D- haustoria of M. lini, and for the first time showed all stages of development.

III. Intracellular Structures

Bushnell (1972) defines the fungal haustorium as: "a specialized organ which is formed inside a living host cell as a branch of an extracellular (or intercellular) hypha or thallus,

which terminates in that host cell, and which probably has a role in the interchange of substances between host and fungus".

Fungal haustoria were first described by DeBary (1863), who recognized these organs as specialized structures responsible for the maintenance of the host/parasite relationship. However, DeBary also used the term to describe the exterior anchoring organs (appressoria) of species of Cystopus Lev. [= Albugo (Pers.) Roussel ex S.F. Gray]. The first description of haustoria in the Uredinales, and definitive recognition of them as feeding organs, was by Ward (1882) in his study of the morphology of Hemileia vastatrix Berk. & Br. However, Karling (1932) appears to have been the first author to restrict the term haustorium to the feeding organs of parasites. At present it is still believed that the haustorium is an organ of absorption, although direct evidence for this is lacking (Harder and Chong 1984).

Some autoradiographic studies strongly suggest the transfer of substances between the rust haustorium and its host cell (Ehrlich and Ehrlich 1970; Favoli and Marte 1973; Mendgen 1974, 1977; Mendgen and Heitefuss 1975; Onoe et al. 1973). However in none of these studies could it be verified that the route of transfer was indeed through the haustorium.

Haustorial morphology and the ultrastructure of host/parasite relationships in the rusts have been thoroughly reviewed by Bracker and Littlefield (1973), Bushnell (1972), Harder and Chong (1984), and Littlefield and Heath (1979), with the latter two authors markedly refining the terminology employed with respect to the

haustorium. They also proposed that haustoria originating from aeciospore or urediniospore infections be designated as dikaryotic or D-haustoria and those from basidiospore infections as monokaryotic or M-haustoria. Some authors (Al-Khesraji and Lösel 1981; Gold and Littlefield 1979; Gold and Mendgen 1984b; Kohno et al. 1976; and Rijkenberg and Truter 1973) use the term intracellular hyphae to describe M-haustoria because of their less specialized nature in comparison with D-haustoria, and their often hypha-like appearance. Harder (1978) used the designation P-(pycnial) haustoria for haustoria produced in basidiospore infections. Recently Gold (1983) proposed the term H-(haploid) haustoria, which would equate to M-haustoria to emphasize the point that such haustoria are peculiar to the haploid stage of the life cycle. Other authors (e.g. Chong 1981; Harder and Chong 1984) have adopted the terminology proposed by Bushnell (1972), as modified by Littlefield and Heath (1979), and this terminology will be used in this text.

Monokaryotic or M-haustoria

M-haustoria, as reported from early light microscopic studies (Allen 1930, 1932a, b; Colley 1918; Dodge 1922; Pady 1935a, b) appeared more filamentous and tortuous than D-haustoria, but such studies provided little information on their actual structural features. Further, the early ultrastructural studies on M-haustoria (Boyer and Isaac 1964; Longo and Naldini 197 ; Moore and McAlear 1961; Orcival 1969) show cross sections of M-haustoria that appear similar to those produced in uredinial and telial stages

(D-haustoria). However, recent workers have produced evidence that suggests M-haustoria are less specialized than D-haustoria.

Ultrastructural studies have been carried out on the M-haustoria of rusts from a number of different genera Cronartium flaccidum (Alb. & Schw.) Wint. (Longo et al. 1982); C. ribicola (Boyer and Isaac 1964; Robb et al. 1975b); Gymnosporangium haraeanum Syd. (Kohno et al. 1976); Kuehneola japonica (Kohno et al. 1977); Kunkelia nitens (Schw.) Arth. (Glidewell and Mims 1979); Melampsora epitea Thuem. (Spiers and Hopcroft 1985); M. pinitorqua (Braun) Rostr. (Jonsson et al 1978; Longo and Naldini 1972); Peridermium pini (Walles 1974); Puccinia recondita Rob. ex Desm. f. sp. tritici (Gold et al.1979); P. sorghi (Rijkenberg and Truter 1973); Uromyces appendiculatus appendiculatus (Gold 1983; Gold and Mendgen 1984b). However, only in a few cases have direct comparisons been made between M-and D-haustoria of the same species of rust: e.g. Cronartium comandrae Pk. (Tainter 1985); C. quercuum fusiforme (Gray 1982; Gray et al. 1982); Puccinia coronata avenae (Chong 1981; Chong et al. 1981); P. poarum (Al-Khesraji and Losel 1980; Al-Khesraji and Lösel 1981); P. podophylli Schw. (Borland and Mims 1980).

In general, ultrastructural studies have shown M-haustoria to be distinctly different from their dikaryotic counterparts. Harder (1978) suggested that the differences in morphology between the two types of haustoria might be due to modifications induced by host cell responses in the alternate hosts. However, Borland and Mims (1980) discounted this hypothesis since their study of the

autoecious, macrocyclic rust P. podophylli showed that similar differences existed between haustoria produced by hyphae of different nuclear conditions within the same host.

M-haustoria are typically septate with the septum often close to the point of penetration (Littlefield and Heath 1979); however septa may be variously positioned and, unlike D-haustoria, M-haustoria are often filamentous and lack a definite neck band. However, like D-haustoria, M-haustoria generally terminate within the host cell, although there are reports of intracellular hyphae exiting from the host cell. (Allen 1935; Colley 1918; Gold and Littlefield 1979; Gold et al. 1979).

A very marked difference between D- and M-haustoria is that the latter are reported to originate from morphologically unspecialized, terminal intercellular hyphae (Harder and Chong 1984), which do not differ structurally from other intercellular hyphal elements. However, Gold and Mendgen (1984) note exceptions to reports that mother cells of M-haustoria are terminal.

Harder and Chong (1984) list the general characteristics of M-haustoria of cereal rusts, many of which are similar to those already mentioned herein, and while it would be tempting to suggest these features could also be characteristic of the M-haustoria of many other rusts regardless of their hosts, this is not likely to prove true. Great variation can exist among M-haustoria of different genera, or even between species of the same genus; indeed exceptions might be found with respect to all characteristics assumed to be common.

Ultrastructural studies of C. ribicola by Robb et al. (1975a, b) show tubular, though often twisted M-haustoria in pine callus tissue. An ill defined neckband was present in some haustoria. This inconclusive observation is the only report of a possible neck-band in M-haustoria.

M-haustoria similar in morphology to those of C. ribicola are reported for C. flaccidum (Longo et al. 1982) and M. pinitorqua (Longo and Naldini 1972). However, Jonsson et al. (1978) reported that unlike those of C. ribicola, the haustoria of M. pinitorqua are slightly constricted where they enter the host cell, although Coffey (in Littlefield and Heath 1979) and Longo and Naldini-Longo (1975) illustrate that the M-haustoria of this rust are not constricted at their bases. While the degree of constriction of the haustorial neck is in question, all studies dealing with M-haustoria of M. pinitorqua and C. ribicola report a septum located near the point of entry into the host cell.

Ultrastructural studies of basidiospore infections of Puccinia coronata avenae (Chong et al. 1981; Harder 1978), P. poarum (Al-Khesraji and Lösel 1981), P. sorghi (Rijkenberg and Truter 1973), and Uromyces appendiculatus (Gold and Mendgen 1984a) all report finger-like haustoria showing little or no constriction at the proximal end. These haustoria were also septate although the septa were frequently observed only in more distal regions of the haustorial bodies. This situation is also characteristic of the M-haustoria of Gymnosporangium haraeanum (= G. asiaticum Miyabe ex

Yamada) on Japanese pear (Kohno et al. 1976), but this rust shows another variation in being binucleate.

Although the M-haustoria of cereal rusts are generally believed to be "essentially unaltered hyphae that invade and grow inside a host cell" (Harder and Chong 1984), those of some other macrocyclic rusts exhibit morphological features suggestive of a degree of specialization. Gray et al.(1982) note that while M-haustoria of C. quercuum fusiforme appear less specialized than those derived from dikaryotic mycelium, they are constricted at the point of penetration into the host cell and possess a distinct neck-like region and an expanded haustorial body. Interestingly, the M-haustoria of two rusts closely related to C. quercuum, C. ribicola (Robb et al. 1975b) and C. comandrae (Tainter 1985), exhibit characteristics considered more typical of M-haustoria (Harder and Chong 1984) than those displayed by C. quercuum in being hypha-like in appearance.

The majority of reports concerning M-haustoria relate to macrocylic rusts, although a few studies do concern rusts with reduced nuclear cycles. One such rust is Peridermium pini (= Endocronartium pini) which is believed to be the autoecious counterpart of C. flaccidum (Hiratsuka 1969). Van der Kamp (1969) observed that the aecioid teliospores produced septate uninucleate intercellular hyphae, which subsequently produced haustoria. Walles (1974) undertook the first ultrastructural study of this rust, and found that the haustoria produced from the terminal ends of intercellular hyphae were typical of M-haustoria in being

septate, but lacked the characteristic filamentous shape of M-haustoria. Walles described the haustoria of P. pini as having a constricted proximal portion corresponding to a haustorial neck, with the distal portion expanding into a "sac-like formation". He also noted that the haustorial mother cell differed from the intercellular hyphae in shape; the distal portion being narrow and bent at right angles to the host cell wall.

An ultrastructural investigation of the endocyclic rust Kunkelia nitens, (Glidewell and Mims 1979), again revealed a haustorial septum positioned near the point of host-cell penetration, but the haustorium itself was not constricted at this point, and was coiled and lobed in the more distal portions.

In those cases where median sections have been photographed, M-haustorial septa typically appear plugged. Gray et al. (1982) observed that such septa of C. quercuum were "occluded by a pulley-wheel shaped plug", and Walles (1974) observed similar plugs in the haustorial septa of P. pini, but suggested they were Woronin-bodies typical of ascomycete septa (Bracker 1967). Jonsson et al. (1978) reported that septa of intercellular hyphae of M. pinitorqua were occluded by Woronin bodies, but they did not mention the haustorial septal plug. Coffey (in Littlefield and Heath 1979) stated that the M-haustorial septum of this latter rust could have both plugged and unplugged pores, possibly indicating that the plug has some function. In the only other study in which median sections were reported, Borland and Mims (1980) found that

the haustorial septum of Puccinia podophylli is occluded by an electron dense substance.

M-haustoria, like their dikaryotic counterparts, cause an invagination of the host plasmalemma after penetrating the host cell wall; the membrane forms an extension of itself around the entire intracellular haustorium. Referred to as the extrahaustorial membrane, it is believed to be composed of newly synthesized membrane material rather than simply representing a stretching of the pre-existing plasmalemma (Harder and Chong 1984).

Although this extrahaustorial membrane is continuous with the plasmalemma, studies of D-haustoria employing PACP treatment clearly show the former membrane possesses special characteristics which are different from those of the plasmalemma (Littlefield and Bracker 1972; Littlefield and Heath 1979). Further, Harder and Mendgen (1982) have shown the extrahaustorial membranes of D-haustoria are deficient in sterols when compared to the unaltered plasmalemma, while Spencer-Phillips and Gay (1981) found ATP-ase activity was lacking in extrahaustorial membranes of Uromyces appendiculatus appendiculatus and Erysiphe graminis DC. ex Merat; similar results have been reported for Albugo candida (Pers.ex Fr.) Kuntze (= A. cruciferarum S.F. Gray) (Woods and Gay 1983). The authors suggest that this modification may allow the haustorium to control efflux from the host cell. However, to date no definitive tests have been carried out on the extrahaustorial membranes of M-haustoria of rusts.

The cell walls of both M- and D-haustoria are generally separated from the extrahaustorial membrane by a zone of uncertain origin, the extrahaustorial matrix (Bushnell 1972). The extrahaustorial matrix of C. quercuum (Gray et al. 1982), P. coronata avenae (Chong et al. 1981) and U. appendiculatus appendiculatus (Gold and Mendgen 1984b)show different degrees of staining in regions both distal and proximal to the mother cell. Chong (1981), employing histochemical tests, showed that various regions were quite distinct in composition, suggesting regional levels of specialization. Alternatively, ultrastructural studies of conventionally stained M-haustoria of C. ribicola (Robb et al. 1975b), C. flaccidum (Longo et al. 1982), Gymnosporangium haraeanum (Kohno et al. 1976), Peridermium pini (Walles 1974), and Puccinia sorghi (Rijkenberg and Truter 1973) suggest such extrahaustorial matrices are of uniform composition, though histochemical staining may prove otherwise.

The composition and origin of the extrahaustorial matrix is a subject of much speculation. Boyer and Isaac (1964) in their study of C. ribicola suggested the extrahaustorial matrix was fungal in origin because they felt it was similar to the material surrounding the intercellular hyphae. However, their observations were made from cross sections, thus making it difficult to determine what region of the haustorium they were observing.

Rijkenberg and Truter (1973) found no distinction could be made between the host collar and the extrahaustorial matrix in M-haustoria of Puccinia sorghi, thus implying a host origin. Kohno

et al. (1976) stated that the M-haustoria of Kuehneola japonica are surrounded by what appears to be callose-like material, and they felt this encapsulation was deposited directly between the extrahaustorial membrane and fungal wall of older haustoria. They also reported that in younger haustoria the extrahaustorial membrane was closely appressed to the haustorial wall, thus the existance of a true matrix is questionable in this instance. Harder (1978) noted a similarity in the staining of the contents of host vesicles associated with extrahaustorial membranes and the contents of the extrahaustorial matrix in M- haustoria of Puccinia coronata avenae. Further evidence that the extrahaustorial matrix is of host origin comes from the discovery of cellulose in the extrahaustorial matrix of the D-haustoria of P. coronata avenae (Chong et al. 1981). However, the matrices of M-haustoria have not been examined to the same degree and the origin of the region is still uncertain.

IV Host Responses

Cytoplasmic changes

Host responses in compatible reactions are still poorly understood, with the majority of studies having concentrated on the incompatible reaction. Much of what is known about haustorium induced changes to the host cytoplasm was reviewed by Littlefield and Heath (1979) and more recently by Harder and Chong (1984). However, most information presently available concerns the effects caused by dikaryotic infections.

The manner by which haustoria derive nutrients from their host cells is still uncertain. However, Harder et al. (1978) showed that the extrahaustorial matrix of P. graminis tritici is directly continuous with the host endoplasmic reticulum. Subsequently, Chong et al. (1981) demonstrated that cellulose is a common constituent of both the host ER and the extrahaustorial matrix of P. coronata avenae. Although such a direct connection of the matrix with the host ER is not observed in most rust infections, vesicles believed to be ER cisternae are commonly associated with the extrahaustorial membrane in several rusts (Littlefield and Heath (1979). Heath and Heath (1971) reported such cisternae contain material similar in electron lucency to that of the matrix, and Chong and Harder (1982) observed similar vesicles aggregated around the haustorial neck of P. coronata avenae; other workers such as Coffey et al. (1983) have observed vesicles associated with the necks of young haustoria.

An association of M- haustoria with host ER is not as apparent, though Chong (1981) reported the presence of some ER cisternae near the M- haustoria of P. coronata avenae. Gold and Mendgen (1984b) also reported the occurrence of Golgi bodies in the host cytoplasm near the penetration and exit sites of the intracellular hyphae of U. appendiculatus.

Harder et al. (1978) and Harder and Chong (1984) discussed the occurrence of membrane complexes associated with the haustorial bodies of P. coronata and P. graminis and suggested these complexes were open to the host ER system. Although such membrane complexes nor direct connections between the extrahaustorial matrices and host endoplasmic reticula have been reported in other rust/host systems, large numbers of tubules were noted in the host cytoplasm associated with the haustorium of M. lini (Coffey et al. 1972) and the intracellular mycelium of the tropical corn rust Physopella zeae (Heath and Bonde 1983). Future investigations may provide further evidence of the nature of these associations, and their frequency in compatible reactions.

Perhaps the most commonly reported association of a host organelle with the haustorium concerns the nucleus. This was reported in early light microscopic studies of M- haustoria (Allen 1932b; Colley 1918), and is a feature commonly reported in ultrastructural studies (Littlefield and Heath 1979; Chong and Harder 1982; Gold and Mendgen 1984b). Littlefield and Heath (1979) suggest this association is more common in monokaryotic infections, but Al-Khesraji and Lösel (1981) noted the converse in their study

of Puccinia poarum. Al-Khesraji and Lösel also presented evidence which suggested that nuclei associated with haustoria may be altered in size and form; there are no similar reports of such a phenomenon in other rust infections.

A number of reports detail alterations in the ultrastructure of chloroplasts after infection. Robb et al. (1975a) found increased numbers of plastoglobuli in pine callus tissue chloroplasts adjacent to M- haustoria of C. ribicola, while Heath (1974) reported a general breakdown and swelling of chloroplasts in infected cowpea leaves, an increase in plastoglobuli, and the occurrence of large starch grains, not evident in uninfected controls. Degeneration of chloroplasts in leaves of Populus tremula L. infected with Melampsora pinitorqua was also observed by Mlodzianowski and Siwecki (1975), but these authors also noted starch degeneration accompanied by production of glycogen in the chloroplasts, as well as abnormally large plastoglobuli. The production and increase in plastoglobuli appears to be a general feature of chloroplast degeneration in dikaryotic infections.

Collars

Collar development is a common host response to both M- and D- haustoria. Two types of collars (designated types I and II) can be discerned, which differ in both morphology and ontogeny.

In dikaryotic infections, collars appear to be separated from the wall of the haustorial neck by the host plasmalemma, the latter being folded back along the haustorial neck. These collars are

designated as type I (Littlefield and Heath 1979), and it has been suggested they are produced by the coalescence of vesicles containing collar material with the host plasmalemma about the site of penetration (Harder and Chong 1984). Some type I collars contain membranous material, believed to represent excess membrane derived from the collar-forming vesicles (Heath and Heath 1971). Chong et al. (1981) also observed host endoplasmic reticula associated with the type I collars of the dikaryotic infections in P. coronata; earlier Heath and Heath (1971) had suggested the precursors of collar material might have been synthesized by the host ER.

Typically, type I collars contain fibrillar and electron lucent components (Littlefield and Heath 1979). Chong and Harder (1982) observed that while collars surrounding the haustorial necks of P. coronata had regions which reacted intensely to Thiery staining, they also contained electron lucent material; generally, such regions are believed to be composed of callose (Heslop-Harrison 1966) and evidence of callose in collars has also been obtained by light microscopy (Heath 1971, Coffey 1976).

Usually, collars associated with M- haustoria represent the second type, type II (Littlefield and Heath 1979). These are generally more fibrillar in nature (Harder 1978; Walles 1974) and lack membrane inclusions, but there is evidence of a callose component (Al-Khesraji and Lösel 1981). Type II collars are directly appressed to the haustorial neck wall, with no intervening plasmalemma. However, Gray et al. (1982) observed what they

considered to be the proximal portion of the extrahaustorial matrix intervening between the fungal wall and the collar in C. quercuum infections. Unlike type I collars, which probably are produced subsequent to penetration of the host cell wall, most authors suggest that type II collars develop before successful penetration has been completed (e.g. Harder 1978; Walles 1974), perhaps in a manner somewhat analogous to papilla formation in powdery mildew infections (Aist 1976).

Incompatible reactions

Resistance mechanisms to rust infection have been extensively studied in cereals and some dicotyledonous plants. There is copious literature on the subject, and much of the earlier ultrastructural work is reviewed by Littlefield and Heath (1979), Heath (1980) and Heath (1982). Comparable studies of rust resistance mechanisms in forest trees are limited, primarily to light microscopic investigations.

One of the earliest reports on a probably rust resistance mechanism in pines is that of Hutchinson (1935); he noted that specimens of Pinus sylvestris L. which showed reduced gall formation in response to infection by a Peridermium sp. also displayed tannin accummulation near the infected region. However, Boyer (1964) reported that phenolic accumulation in needles of P. strobus L. may not have been involved in resistance to C. ribicola. As well, Walkinshaw (1978) observed tannin accummulation in actively growing galls of some southern pines infected with C.

quercuum, indicating these probably did not play a role in resistance to this rust.

In other early reports, True (1938) and McKenzie (1942) described the anatomical reactions of P. sylvestris to a Peridermium rust (a Cronartium or Endocronartium), while Struckmeyer and Riker (1951), and Hoff and McDonald (1972) investigated resistance of P. strobus and P. armandii Franch., respectively, to C. ribicola. All these authors felt resistance was expressed by development of localized necrosis in the cortex with subsequent formation of wound periderm; a non-specific response by the host to injury.

Host responses exhibiting a higher degree of specificity were observed by Kinlock and Littlefield (1977) in the C. ribicola/P. lambertiana Dougl. interaction. Some individuals showed a definite hypersensitive response in the needles while in others, infected needles of resistant individuals developed localized necrotic zones in advance of the mycelium which appeared to restrict development of the pathogen. A similar response was seen at the ultrastructural level in pine callus tissue infected with C. ribicola (Robb et al. 1975a). These latter authors noted that the ultrastructural changes induced in the host cells occurred in advance of the infection and resembled an acceleration in normal senescence. However, this hypersensitive response in pine tissue was not as vigorous as that noted in cowpea infected with U. phaseoli vignae (Heath and Heath 1971; Heath 1972). There mycelial development appeared to be restricted to one or two haustoria and

there were no microscopic signs of infection. Although Miller et al. (1976) reported that some resistant families of slash pine showed no obvious sign of infection after artificial inoculation with C. quercuum, the authors could not demonstrate the mechanism of resistance.

Certain mechanisms of resistance to C. ribicola operate by preventing the rust from entering the main stem. McDonald and Hoff (1970) observed early shedding of infected needles of P. monticola Dougl. before the fungus could spread into the short shoot. Subsequently, Hoff and McDonald (1971) also observed resistance in western white pines which seemed to be a form of fungicidal reaction in the short shoot.

Perhaps the best understood of the pine/rust systems is that of the southern pines and C. quercuum. Jewell and Snow (1972), Jewell and Spiers (1976) and Miller et al. (1976) all found that anatomical resistance in one and two-year old infections was expressed by localized zones of dark-staining host cells, which delimited the rust infection. More recently Jewell et al. (1982) undertook a similar study of 30-90 day old infections and observed a similar expression of resistance in localized regions, which they referred to as resistance zones. However, Miller et al. (1976) also reported the occurrence of what might best be described as tolerance to this rust. In some seedlings the rust mycelium was obviously successful in reaching the cambium but failed to stimulate gall production; the host was apparently physiologically non-reactive.

In the only ultrastructural study of resistance to C. quercuum, Gray and Amerson (1983) examined the responses of juvenile seedlings of P. taeda L. derived from field resistant stock. They demonstrated that cell necrosis was instrumental in the expression of juvenile resistance in these seedlings, haustorial death occurring simultaneously with, or subsequent to host cell necrosis. They also suggested that the electron opaque material accompanying necrosis was a tannin or tannin precursor. Jonsson et al. (1978) studied resistance mechanisms in P. sylvestris to M. pinitorqua using ultrastructural techniques. They observed necrotic host cells containing dead haustoria, with host cell necrosis apparently preceding that of the haustoria. They also commonly observed as did Gray and Amerson (1983), that the intercellular hyphae remained unaffected by host cell necrosis. Indeed this latter observation appears to be common to many reports of rust resistance (Littlefield and Heath 1979).

Heath (1982) noted that a causal relationship between host and haustorium death is the most frequent explanation for the mechanism of incompatible reactions, where host cell necrosis is evident. However Harder et al. (1979) and Prusky et al. (1980) have observed the apparent necrosis of haustoria prior to that of the infected cell. Walles (1974) observed a similar phenomenon in the interaction between Peridermium pini and Pinus sylvestris, though only in a small fraction of the cells investigated.

Jonsson et al. (1978) also observed the encasement of haustoria by a reaction material, possibly callose. They felt this

might act as an effective resistance mechanism, similar to that observed in the incompatible reaction of the Queen Anne variety of cowpea to Uromyces phaseoli var. vignae (Heath 1971; Heath and Heath 1971). However, Littlefield and Heath (1979) suggested that encasement is a response to the presence of already moribund or dead haustoria.

MATERIALS AND METHODS

I. Plant Materials and Inoculation Procedures.

During the late spring of both 1984 and 1985, spore bearing galls of E. harknessii were collected from diseased specimens of P. banksiana, growing in the Belair Provincial Forest of Manitoba. After being allowed to air-dry overnight in the laboratory on paper, spores were tapped of the galls onto clean paper and sifted through cheesecloth to remove debris. Spores were subsequently collected in glass vials which were then hermetically sealed by means of a Blowpipe Torch (Unilab Inc.), and stored at -60°C in a deep freeze until required. All spore vials were identified as to source and date of collection by a tag placed inside the vial prior to sealing. In the early summer of each year, similar galls were collected from diseased specimens of P. contorta growing in the Banff/Jasper National Park area of Alberta. The galls were loosely wrapped in brown paper bags until they were returned to the laboratory (elapsed time a maximum of 72 hrs.), where they were treated as previously described, except that drying was not required.

When a spore population was selected for inoculation, vials were scored with a triangular file and broken open, after which spores could be removed.

Seeds of Pinus banksiana, P. contorta and P. thumbergii Parl. were planted, 6 to each 4 inch pot in a sandy loam soil (soil/sand/peat moss, 1:1:1) and placed in the greenhouse at

approximately 25 C. Seven to ten days after emergence, the seedlings were inoculated with a selected teliospore collection. Usually P. banksiana seedlings were inoculated with spores harvested from P. banksiana, and P. contorta seedlings with spores harvested from P. contorta; P. thumbergii, seedlings on separate occasions were inoculated with spores harvested from each source.

Seedlings were inoculated by misting the plants with distilled water, followed by the application of dried spores onto the hypocotyl with a camel hair brush. Inoculation was also attempted by suspending the spores in distilled water to which a drop of Tween 20 (Baker Chem.) had been incorporated, and applying the spore suspension with an atomizer. However, due to the hydrophobic nature of the spores this method was far less successful than the former technique. After inoculation the seedlings were again misted, placed in a shallow tray of water, covered in plastic to maintain high humidity, and incubated in the dark at 18 C in a growth cabinet (Controlled Environments Ltd., Model EF717) for 48 hours.

After incubation, inoculated seedlings were removed from the growth cabinet and returned to the greenhouse, then monitored for signs of infection over varying time periods.

II. Electron Microscopy.

A. Conventional fixation and staining for electron microscopy.

Two to three weeks after inoculation, reddish necrotic streaks became evident on the hypocotyls of infected seedlings. Seedlings showing such symptoms were selected for processing during the period from two to sixteen weeks post inoculation, and prior to any further treatment, were photographed using Ektachrome 160 film and a Wild M8 Stereo Microscope equipped with a Wild MPS Photoautomat system. The necrotic regions of the selected plants were then excised using a single edge razor blade broken 45° to the cutting edge (O'Brien and McCully 1981). This tissue was fixed in 3% Glutaraldehyde (Glut) in 0.025 M cacodylate buffer, pH 6.8, for one hour under partial vacuum at room temperature, followed by Glut fixation at 4 C for a further 48 hours. Tissue was either post-fixed for 4 hours at 4 C in 2% osmium tetroxide (OsO_4) in cacodylate buffer, or further processed without post-fixation. Further processing involved the dehydration of the fixed tissue in a graded ethanol or acetone series, followed by 3 successive changes in 100% propylene oxide (15 min each). The tissue was then infiltrated in successive changes of a propylene oxide/Epon Araldite mixture (Epon 812/Araldite 6005) of: 3:1; 1:1; 1:3 for 2 hours each. The specimen was then infiltrated for a further 24 hours in 2 changes of propylene oxide/Epon Araldite 1:3, followed by 5 d in 100% Epon Araldite. Following infiltration the specimen was polymerized at 70 C, under partial vacuum (10psi) for 16 hours.

Ultrathin sections were cut with a diamond knife on a Reichert OMU2 ultramicrotome. Sections were mounted on uncoated copper grids (75/300) and stained with a saturated solution of uranyl acetate (UA) in 50% methanol, followed by lead citrate (PbC).

Unless otherwise stated all electron microscopic examinations were carried out on an AEI 801 at an accelerating voltage of 60 kV. Photographic images were recorded on Kodak Electron Image 8.3 x 8.4 cm sheet film.

B. Plasmolysis of tissue.

In order to investigate the degree of attachment of the extrahaustorial membrane to the haustorium, tissue was plasmolyzed prior to fixation employing a method described by Coffey (1983). Infected hypocotyls were cut into 5 mm lengths, bisected longitudinally and then floated on a 0.8 M sucrose solution in the dark at 20°C for 16 hours. Small regions of tissue showing necrosis were excised and processed for electron microscopy as previously described, except that 0.8 M cacodylate buffer was used during glutaraldehyde fixation.

C. Periodic acid - chromic acid - phosphotungstic acid (PACP) staining (Roland et al. 1972).

Sections of Glut or Glut/OsO_4 fixed tissue were floated on 1% aqueous periodic acid for 30 min under high humidity (Nagahasi et al. 1978). Sections were then transferred through 5 changes of distilled water, 5 min each, using a platinum wire loop. The sections were subsequently floated on a solution of 1% phosphotungstic acid (PTA) in 10% chromic acid, transferred through 5 changes of distilled water, 5 min each, and mounted on copper grids. For control treatments, periodic acid oxidation or chromic acid and PTA were omitted; alternatively, hydrogen peroxide (H_2O_2) was used as an oxidizing agent. Hydrogen peroxide removes OsO_4 from the tissue, but does not specifically oxidize glycols to produce aldehydes as does periodic acid.

Phosphotungstic acid is an anionic stain whose specificity is strictly pH dependent, though the chemistry of the reaction is not well understood. Reviews on the subject can be found in Chong (1981), Hall (1978), and Hayat (1981). Van der Woude (1973) suggested that PACP reacts with glycolipids involved in the synthesis of cell wall polysaccharides. Pease (1966, 1970) and Rambourg (1967) used PTA to detect carbohydrates and glycoproteins in animal cells. However, Rambourg (1971) concluded that PACP treatment would only detect carbohydrates in glycol methacrylate embedded samples.

Recently Heslop-Harrison and Heslop-Harrison (1982) were able to showed that at low pH, PTA stained pectin-rich cell wall components in grass pollen tubes. However, in studies of host/parasite interactions the stain has generally been used to stain plasma membranes. Chong(1981), Hickey and Coffey (1978), Littlefield and Bracker (1972) and others have used the stain to show alterations in the host plasmalemma after its invagination by the haustorium.

D. Periodic acid- thiocarbohydrazide - silver proteinate (PA-TCH-SP) staining (Thiery 1967).

Ultrathin sections of tissue fixed in Glut/OsO_4 or Glut only, were floated on 1% aqueous periodic acid for 30 min in a high humidity chamber, and then washed in 5 changes of distilled water. Sections were then transferred to 0.2% thiocarbohydrazide (TCH) in 20% acetic acid for 0.2, 14 or 24 hours. They were then successively transferred through 10, 5 and 1% solutions of acetic

acid, 10 min each. These sections were then incubated on 1% aqueous silver proteinate for 30 min in the dark, transferred through 3 changes of distilled water and mounted on copper grids. Control sections were placed on 1% sodium borohydride either prior to oxidation to block endogenous aldehydes, or after periodic acid oxidation, to block aldehydes produced on the vicinal hydroxyl groups by oxidation. Other controls consisted of the elimination of either TCH or silver proteinate from the procedure, or the use of H_2O_2 as an oxidizing agent.

This method could be considered the ultrastructural equivalent of the periodic acid-Schiff's reaction. Periodic acid specifically oxidizes glycols with a 1-4 or 1-6 linkage and having vicinal hydroxyl groups, and produces aldehydes at the 2 and 3 carbons to which TCH will bind. Silver proteinate in turn binds to TCH and is reduced to metallic silver, resulting in the visualization of the reactive sites. Theoretically the degree of staining observable is dependent on the availability of the reactive sites to which TCH binds. Thiery (1969) suggested that the degree of polysaccharide branching, or the degree they are complexed to other substances such as lipids, is directly related to the time of exposure to TCH necessary to attain maximal staining. For example, a pure polysaccharide such as amylose should stain intensely after brief incubation in TCH as compared to amylopectin which would require a longer period of incubation in TCH. Amylopectin in turn would require a shorter incubation period in TCH than would glycoprotein, since aminoacids occupy many of the reactive sites resulting in reduced staining. There are some exceptions to this; cellulose,

because of the close association of its polymers forming micelles, shows reduced staining compared to other 1-4 glucans. Also, callose, a beta-1-3 glucan, does not react with PA-TCH-SP as vicinal hydroxyl groups are not present. Care must be taken in the interpretation of silver proteinate staining since, according to Thiery (1969), some fatty acids and polypeptides may also show a positive reaction.

E. Lectin-gold markers (Horisberger and Rosset 1977).

Wheat germ lectin conjugated to colloidal-gold (WGL) was generously provided by Dr.R. Rohringer (Research Station, Agriculture Canada, Winnipeg).

Infected tissue was fixed in 3% Glut without post-fixation in OsO_4 and processed as previously described. Ultrathin sections were floated for 2 hours on the gold-bound lectin in an appropriate buffer (Horisberger and Rosset 1977), and washed overnight in the same buffer. Sections were collected on copper grids, stained for 5 min with 2% aqueous UA, then washed. The control treatment consisted of floating the sections on a solution of the gold bound lectin in the presence of a chitin hydrolysate (N, N, C-triacetylchitriose, Sigma Chem.).

Wheat germ lectin binds specifically to chitin or its oligomers (Goldstein et al. 1975) and has been used successfully to localize chitin in fungal cell walls (e.g. Chong et al. 1985). In the presence of the appropriate hapten, the lectin should bind to

the hapten, precluding any attachment to reactive sites in the tissue, and indicating the specificity of the lectin.

F. Enzyme Treatments

Tissue was fixed in 3% Glut for 3 hours under partial vacuum at room temperature, washed in the appropriate buffer, and incubated in one of the following enzyme preparations (Hickey and Coffey 1978):

1. protease (Sigma, Type XIV) 5 mg/ml in 0.025 M Tris-HCL buffer pH 7.5; or
2. cellulase (Sigma, practical grade) 5 mg/ml in 0.05 M phosphate buffer pH 5.5.

Following enzyme treatment the tissue was washed in 0.025 M phosphate buffer pH 6.8, postfixed in phosphate buffered 2% OsO_4 and processed as previously described.

III Light Microscopy

A. Epoxy embedded sections.

For routine examination, 1 µm epoxy embedded sections were cut, using glass knives, on a JB4 Microtome (Sorvall Porter Blum). Sections were transferred to gelatin coated glass slides, the slides placed on a slide warmer, and the sections stained with 2% ethanolic crystal violet in ammonium oxalate (Gerhardt et al. 1981). Crystal violet, whose use in staining epoxy sections has not been previously reported, appears to possess the same

properties as toluidine blue (O'Brien et al. 1964), but provides superior contrast (M. Sumner pers. comm.). Epoxy sections were also stained with periodic acid-Schiff's reagent (PAS) and counterstained at 50 C with 1% aniline blue black (ABB) in 7% acetic acid, according to Fisher (1968) or, alternatively, with 2% crystal violet.

B. Fresh tissues.

To avoid the adverse effects of chemical fixatives (Feder and O'Brien 1968), fresh material was sectioned on a Pelcool freezing microtome (Measuring and Scientific Equipment Ltd.). Sections of 15-60 μm thickness were transferred to distilled water using a camel hair brush. Unstained material mounted in distilled water could be examined using phase contrast microscopy to differentiate haustoria from host tissue or, alternatively, fluorescence microscopy of appropriately stained material could be employed.

Fresh tissue sections to be examined using epifluorescence were stained with one of the following fluorochromes as described by Fulcher and Wong (1980).

1. 0.05% aniline blue (Polysciences) in 0.01 M phosphate buffer pH 8.5.

Aniline blue shows some specificity for beta-1-3 glucans. Specificity was increased by subjecting the tissue to PAS or calcofluor prior to staining with aniline blue (Smith and McCully 1978). Some tissue was also subjected to lyticase (5 mg/ml, Sigma

Chem.) prior to staining to determine whether fluorescence was induced by a beta-1-3 glucan.

2. 0.001% aqueous ANS (1-aniline-8-napthalene sulphuric acid, Sigma Chem.).

ANS is used to detect protein as this stain only fluoresces when absorbed to protein (Fulcher and Wong 1980).

3. 0.001% aqueous Nile blue A (Baker Chem.).

This fluorochrome is used to visualize storage lipids. It is known to induce an intense fluorescence in hexane soluble structures, and has a demonstrated affinity for cereal triglycerides (Fulcher and Wong 1980).

4. 0.01% aqueous calcofluor white (Polysciences).

Calcofluor is a well known general stain for cell walls (Hughes and McCully 1975) and has some specificity for mixed linkage beta-glucans (Wood and Fulcher 1980). Fresh sections were also stained with 0.001% acridine orange in 0.1 M boric acid - borax buffer pH 8.8 and counterstained with calcofluor to differentiate between fungal and host tissue; 0.5% aqueous malachite green could also be substituted for acridine orange.

5. 10 m aqueous SITS (4-acetamido-4′ -isothio-cyana-tostilbene-2, 2′ -disulfonic acid) (Polyscience).

SITS was used to determine whether a barrier to apoplastic transport was present in the haustorial neck (Heath 1976). This fluorochrome is believed to be restricted to the apoplast, and absence of any haustorial fluorescence in intact host cells is considered indicative of a tight junction between the extrahaustorial membrane and the haustorial neck.

C. Tissue clearing.

To observe initial penetration and early colony development, cleared tissue was examined with bright field microscopy. For observation, inoculated hypocotyls were excised and bisected, then cleared using a modified procedure of Shipton and Brown (1962). The hypocotyls were boiled for 1 min. in 0.1% trypan blue dissolved in a 1:1(v/v) mixture of glycerol and 95% ethanol. The specimens were then washed in 2 changes of 95% ethanol, followed by 2 changes of distilled water and placed in a sealed beaker containing a 70% aqueous solution of chloral hydrate for 3-5 days or until the specimen was sufficiently cleared. After clearing, the specimens were washed 3 times in distilled water, mounted in 50% glycerol beneath a coverslip (#1, 22 x 50 mm) and examined using brightfield microscopy.

D. Light microscopy and photomicrography

Fluorescence microscopy employed a Nikon Optiphot equipped with an episcopic fluorescence attachment, a high pressure mercury lamp and CF UV-F objectives. Sections stained with calcofluor, aniline blue, acridine orange or malachite green were examined

under UV light using a UV excitation filter (330-380 nm), dichroic mirror DM400 and a barrier filter transmitting above 420 nm. Sections stained with Nile blue or ANS were examined under blue light, excitation filter 410-485 nm, dichroic mirror 505, and a barrier filter transmitting above 515 nm. All fluorescent images were recorded on Ektachrome 200 ASA daylight film. Bright field and phase contrast microscopy was performed using a Carl Zeiss Photomicroscope. Photographic images were recorded on Panatomic-X 32 ASA film or Ektachrome 160 ASA tungsten corrected film.

C H A P T E R I

HOST COLONIZATION AND HAUSTORIUM DEVELOPMENT OF *ENDOCRONARTIUM HARKNESSII* ON HARD PINES

Introduction

Light microscopic investigations by workers such as Allen (1930, 1932a, 1932b, 1934, 1935), Miller *et al*. (1980), Reed and Grabill (1915) have contributed to our understanding of the process of infection and subsequent host colonization. With the exception of *C. ribicola* (Patton and Johnson 1970), host penetration in basidiospore infections is directly through the cuticle and epidermis. As *E. harknessii* is an endocyclic rust possessing aecioid teliospores which germinate directly without the production of basidiospores (Hiratsuka *et al*. 1966), the nature of its infection process has been uncertain. Evidence is presented here which is suggestive of a unique infection process among the rusts.

The ontogeny of M- haustoria has not been reported in any detail by previous workers, although there are some reports on the early development of the D- haustorium (Chong 1981; Heath and Heath 1975). As the morphologies of M- and D- haustoria are generally reported to be distinctly different, the former usually reported as appearing less specialized, this would presumably be reflected in its development. Reports of penetration pegs of M- haustoria (Al-Khesraji and Lösel 1981; Robb *et al*. 1975b) would seem to confirm this. Through a series of light and electron microscopic observations, some aspects of host cell penetration and early development of the haustorium of *E. harknessii* are reported here.

RESULTS

During these current infection studies, aecioid teliospores of E. harknessii germinated directly on the surface of the pine hypocotyl or cotyledon. However, as successful infection of the hypocotyl occurred more frequently, this study concentrated on infection of this region.

The teliospores produced elongate germ tubes that appeared to act as the infectious units of this rust, in effect behaving as functional basidiospores. The spores often produced a single germ tube with an appressorium at the point of infection (Fig. 1, arrow), although in many instances only a slight swelling was evident at the terminal end. The germ tubes could also appear branched (Fig. 2), but it is unclear whether every germ tube branch could produce a penetration structure, since only a single point of penetration was ever observed resulting from an individual spore. Penetration always occurred directly through the cuticle (Fig. 2, arrow), and although the production of appressoria over stomata was noted in other studies of E. harknessii (Y. Hiratsuka pers comm.), such was never observed during this investigation.

During penetration, a short narrowed infection peg issued from beneath either the well-defined appressorium (AP) or the terminal end of the germ tube. This penetrated the cuticle (Figs. 3 and 4) and then expanded beneath the cuticle, but above the epidermal cell wall, to produce what was apparently a subcuticular vesicle (SV); this became elongated and septate (Figs. 5 and 8). Hyphae

Legend

Figure 1. Calcofluor stained teliospore germling.

Figure 1. Teliospore germling producing a small appressorium (arrow) at the point of infection. Fluorescence microscopy. X800.

Figures 2-6. Phase contrast micrographs of the initial infection process, as visualized in cleared hypocotyls.

Figure 2. A branched teliospore germling infects the hypocotyl by direct penetration through the cuticle (arrow). X650.

Figure 3. A short narrowed infection peg (IP) is produced from the appressorium (AP) at the terminal end of the germ tube. X1600.

Figure 4. The IP expands to produce a subcuticular vesicle (SV) after penetration of the cuticle. X1600.

Figure 5. The SV develops into an elongate septate structure. X1600.

Figure 6. Hyphae (arrows) are produced from the SV and run parallel to the epidermal cells, producing haustoria along their length. X1600.

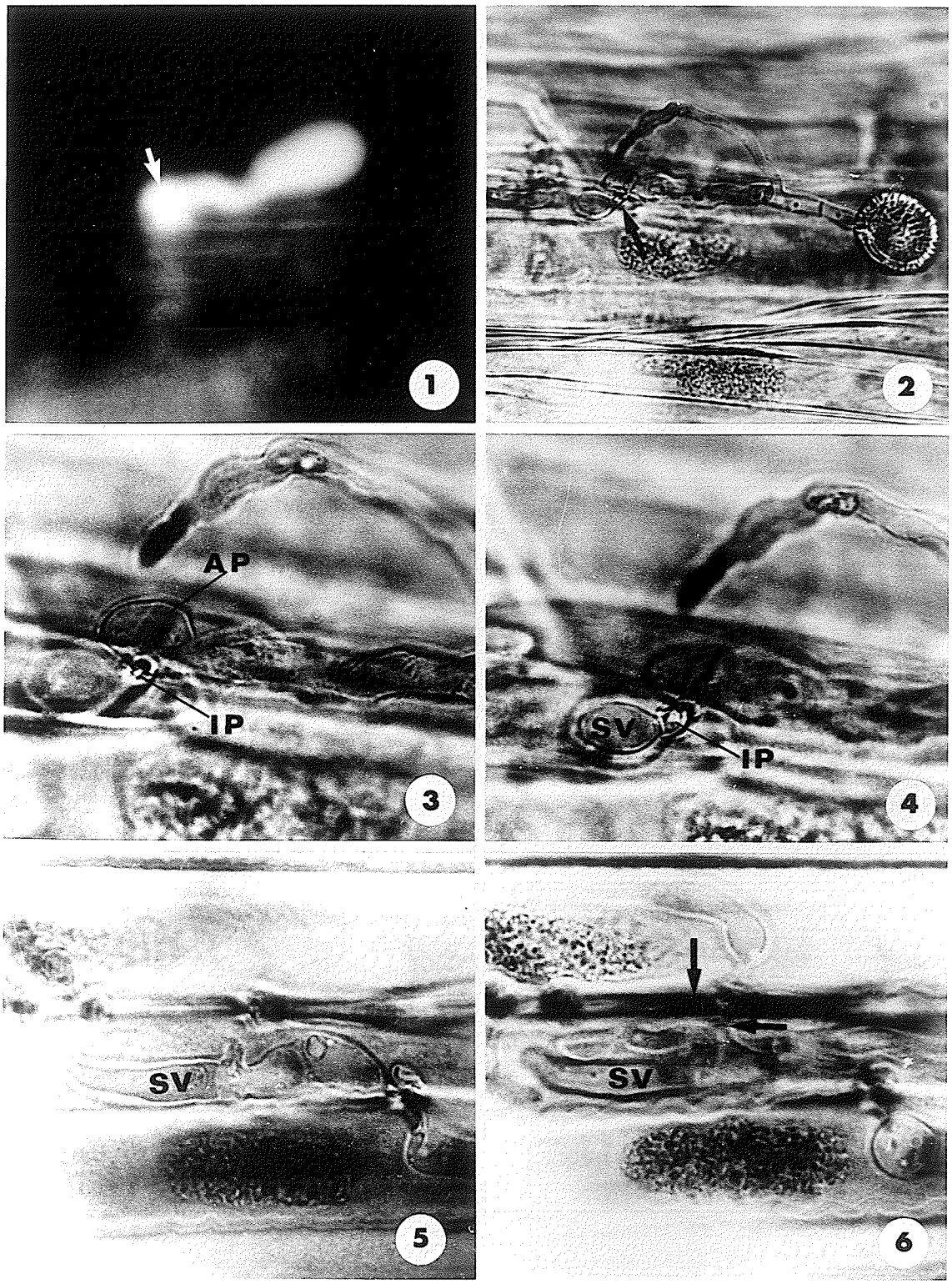
1
2
AP
IP
3
SV
IP
4
SV
5
SV
6

subsequently developed from the vesicle (Figs. 6 and 8, arrows) and these grew in a subcuticular manner either between the epidermal ridges (Figs. 6 and 7), or at right angles to the ridges (Figs. 8 and 9).

The subcuticular nature of the vesicle was not always evident in cleared tissues, and thin sections from the point of initial penetration were not observed. However, thin and ultrathin sections taken from tissue several days after inoculation, indicated that hyphae apparently produced from the vesicle (Figs. 6 and 8, arrows) were located between the host epidermis and cuticle; this implies the vesicle was subcuticular (Figs. 7 and 9).

The subcuticular mycelium extended in a lateral fashion and remained restricted to this location during the first 5-7 days of development (Fig. 10). However, the subcuticular hyphae produced haustoria from along their length; these developed within the adjacent epidermal cells by infection of the latter through their periclinal walls (Figs. 9 and 10). After the mycelium was well established in this subcuticular location, with many haustoria within the epidermal cells, intercellular hyphae grew between the anticlinal walls of the epidermis (Fig. 11), and became established in the outer cortex and produced haustoria in both the epidermal (Fig. 12) and cortical cells (Fig. 13).

The intercellular hyphae ramified throughout the cortex, intruding between cortical cells (Figs. 14 and 15) as they grew toward the vascular tissue. Upon reaching the vascular tissue, invasion of phloem, cambial and parenchymal cells occurred (Fig.

Legend

Figures 7-11. Early stages of host colonization.

Figure 7. Transmission electron micrograph of subcuticular hyphae. Glut/OsO_4. UA/Pb. X8800.

Figure 8. A cleared specimen showing a subcuticular vesicle (SV) producing hyphae (arrows) at right angles to the epidermal cells and subsequent development of a young colony in the hypocotyl. Phase contrast microscopy. X640.

Figure 9. An epoxy section of a subcuticular hypha (H) producing a haustorium (HB) in an epidermal cell. Bright field microscopy. X2000.

Figure 10. A cleared specimen showing the extent of the mycelium produced 5 to 7 days after inoculation. Phase contrast microscopy. X250.

Figure 11. An epoxy section showing the progression of intercellular hyphae (IH) between the anticlinal walls of the epidermis and between the epidermis and cortex. Bright field microscopy. X2000.

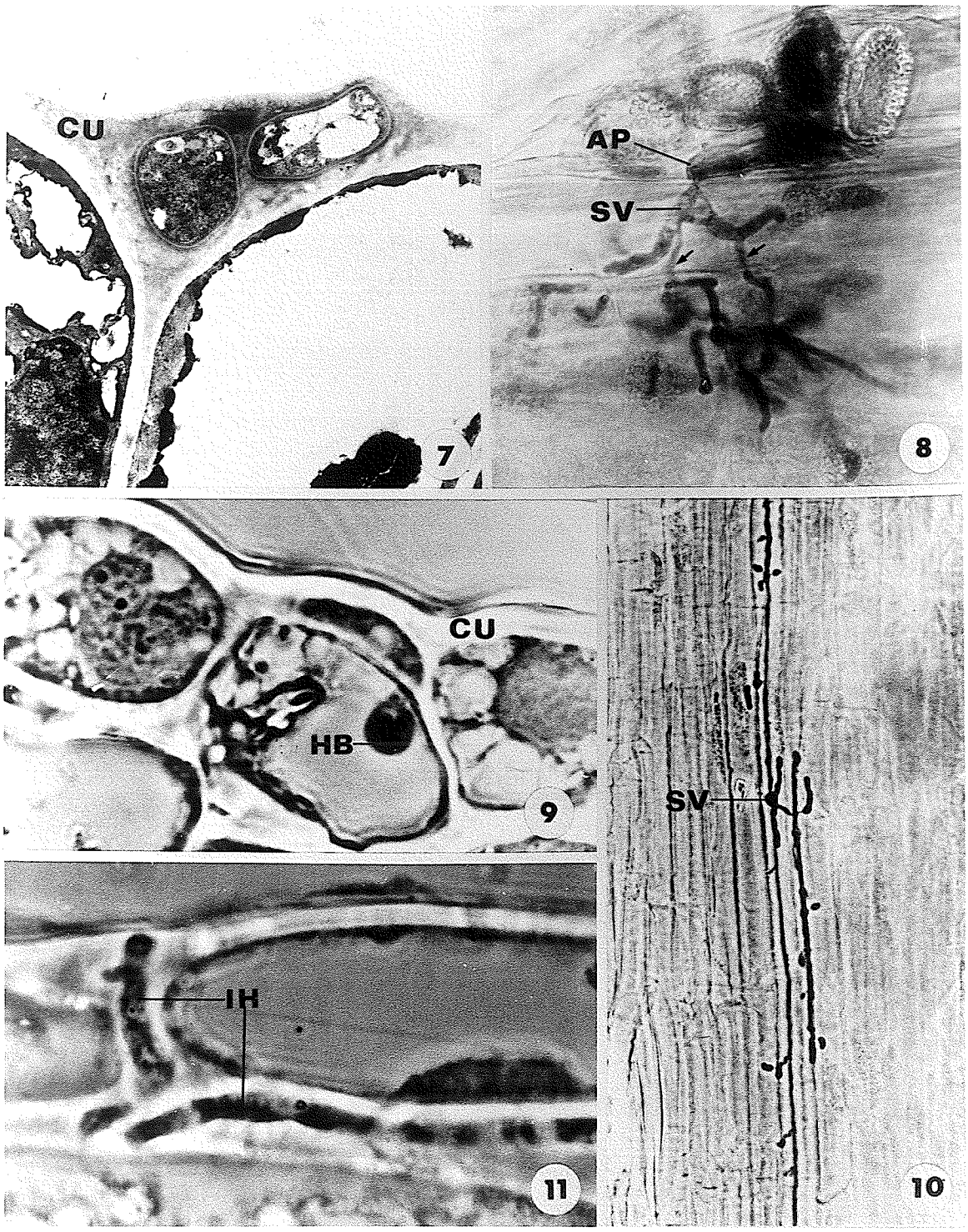
CU
7
AP
SV
8
CU
HB
9
SV
10
IH
11

Legend

Figures 12-13. Transmission electron micrographs of early stages of host colonization.

Figure 12. Haustorial invasion of an epidermal cell through the basal wall during the early stages of host colonization. Glut/OsO_4. UA/PbC. X5400.

Figure 13. Haustorial invasion of a cortical cell during the early stages of host colonization. Glut/OsO_4. UA/PbC. X4500.

Figures 14-15. Intrusion of intercellular hyphae between cortical cells.

Figure 14. Intercellular hyphae appear to ramify between the cells of the cortex, producing haustoria from successive pseudocells (arrows). Nomarski interference microscopy. X1600.

Figure 15. Transmission electron micrograph showing close contact between the host cells and the intercellular hyphae (IH). The host cell in contact with the IH appears flattened (arrow) suggesting a forcile separation of the cells. Glut/OsO_4. UA/PbC. X29700.

Figure 16. Light microscope photograph of infection of vascular tissue of the hypocotyl.

Figure 16. An epoxy section showing haustoria (arrows) infecting parenchyma cells in developing vascular tissue. Bright field microscopy. X250.

Figure 17. Light microscope photograph of points of haustorial production on hyphae.

Figure 17. A cleared specimen shows a terminally-produced haustorium (arrow) and others produced from intercalary cells. Phase contrast microscopy. X640.

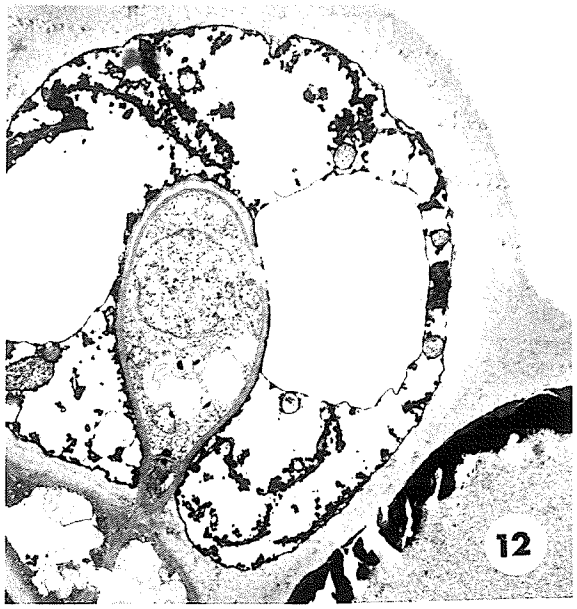
12

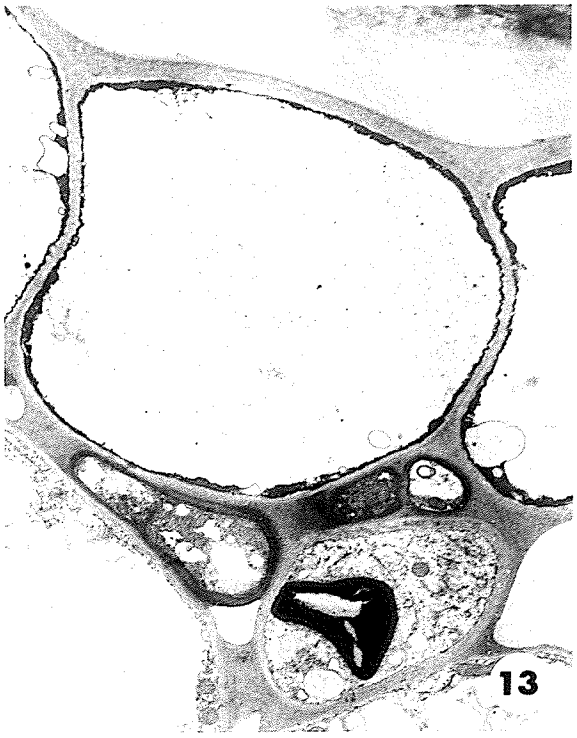
13

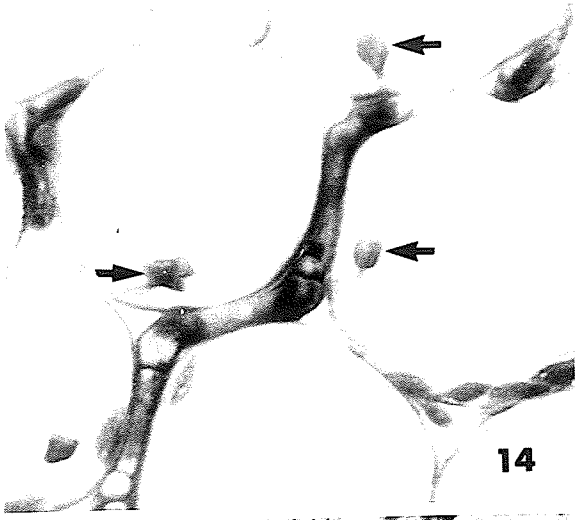
14

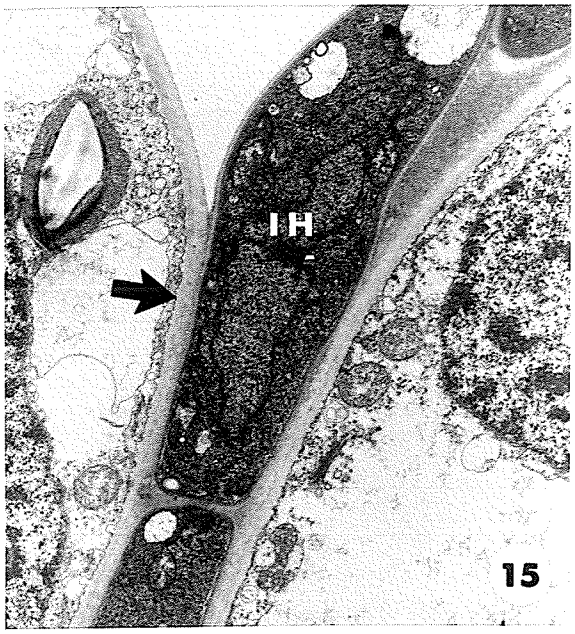
IH
15

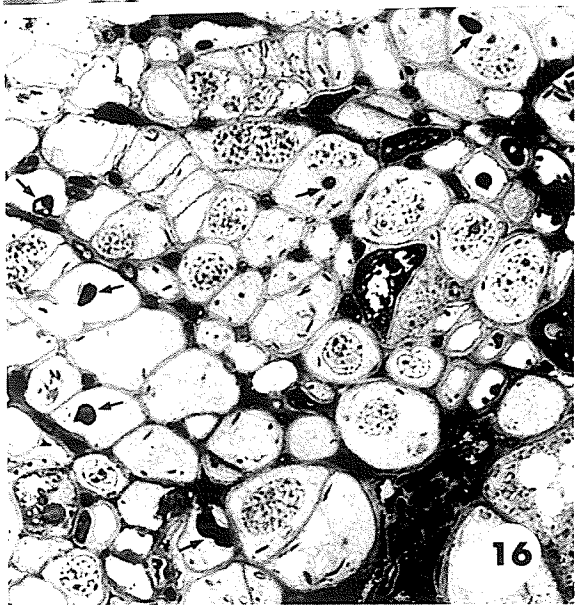
16

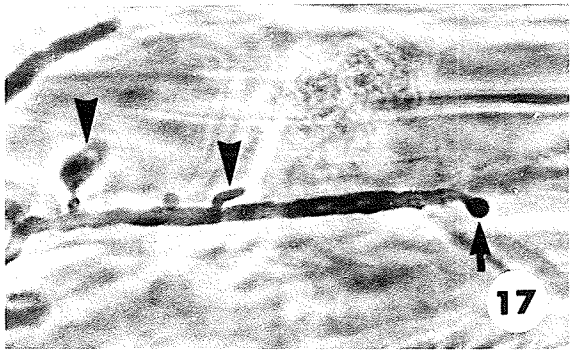
17

16). The infection and subsequent stimulation of the cambial tissue resulted in the production of woody galls in the susceptible host (True 1938).

The haustorial producing cells, the haustorial mother cells (HMC), did not display any obvious degree of specialization, but appeared similar to all other intercellular hyphal elements. While there were no obvious morphological features of the HMC that are unique to this rust, some aspects of their haustorial production were distinctive.

From examination of cleared specimens, it was apparent haustoria could be produced from terminal mother cells (Fig. 17, arrow), a feature commonly observed in other rusts regardless of their nuclear condition (Littlefield and Heath 1979); however, haustoria were also produced from intercalary locations along the hyphal elements (Fig. 17, arrowheads). In fact it was common to observe that a number of mature haustoria were produced from successive hyphal cells (Fig. 14, arrows), each of which had apparently functioned as a haustorial mother cell.

On occasion, individual haustorial mother cells of E. harknessii produced more than one haustorium. In Figure 18, two haustoria produced from the same HMC are visible, while in Figure 19 two haustoria are seen which developed in very close proximity to each other and from the same mother cell. In one instance, it appeared as though three haustoria were to be produced from a single HMC; in Figure 20 a mature haustorium is visible at the terminal end of the HMC (large arrow) as well as two laterally

Legend

Figures 18-21. Transmission electron micrographs of haustorial mother cells.

Figure 18. A haustorial mother cell (HMC) is shown producing two haustoria. Glut/OsO_4. UA/PbC. X6700.

Figure 19. Two haustoria are evident, originating from the same HMC in the same plane. Glut/OsO_4. UA/PbC. X8900.

Figure 20. A HMC with a mature haustorium (large arrow) at its terminal end and two laterally produced penetration pegs (small arrows). Glut/OsO_4. UA/PbC. X8200.

Figure 21. The haustorium and the HMC, each contain a single nucleus (N); note the normal appearance of the protoplasm in the HMC. Glut/PbC. X8900.

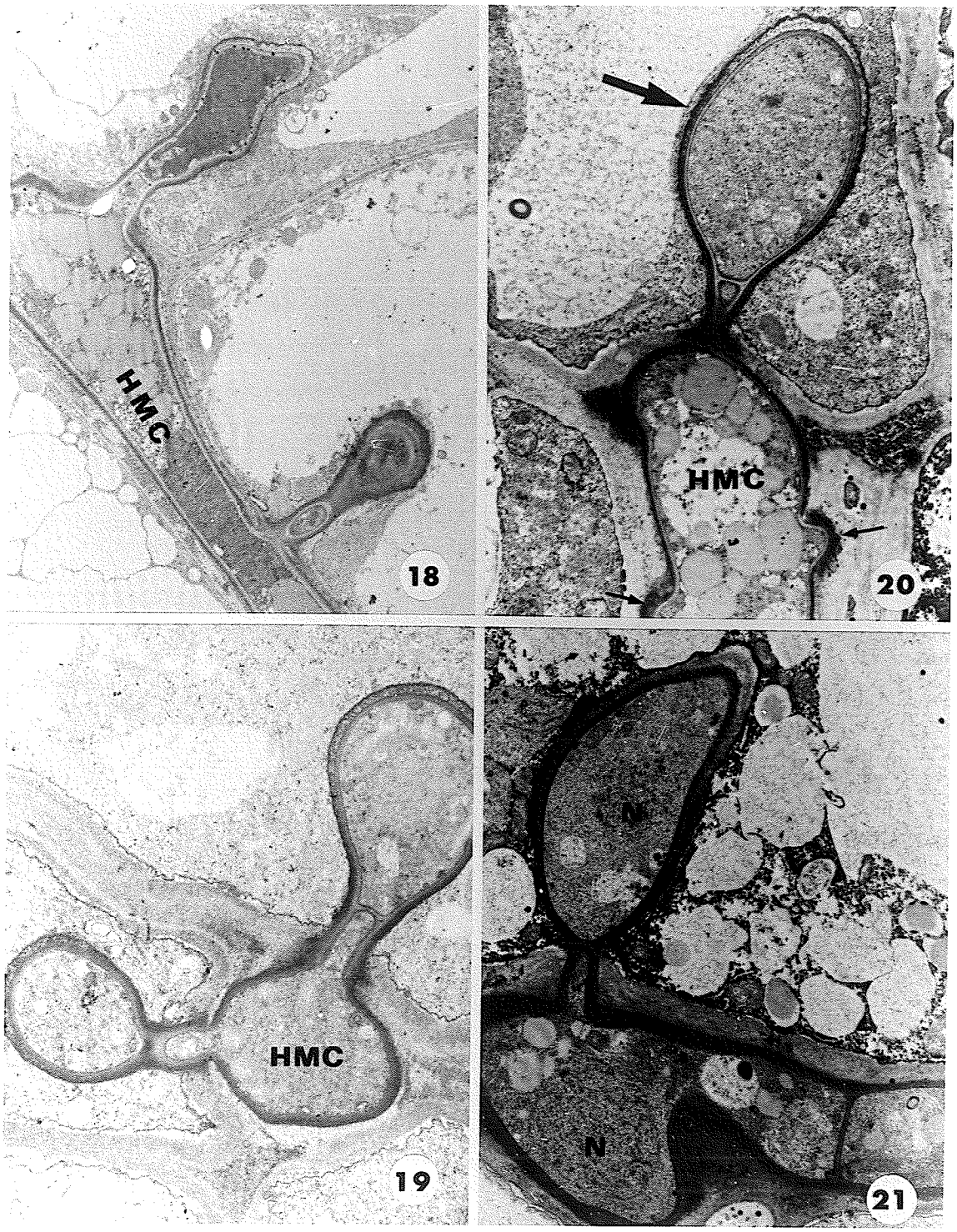
HMC
18
HMC
20
HMC
19
N
N
21

developing penetration pegs (arrows). While several haustoria could be produced from a common mother cell, apparently only one haustorium from each mother cell ever invades an individual host cell. While it was possible for a host cell to be invaded by more than one haustorium, these haustoria always originated from separate mother cells.

The HMC seems to retain its protoplasm after haustorial formation; vacuolate mother cells were usually associated with necrotic haustoria. The HMC was uninucleate (Fig. 21), as were all the pseudocells of the intercellular hyphae. Since the haustorium was also uninucleate this suggests that a nuclear division occurred in the HMC with subsequent migration of one daughter nucleus into the haustorium; however, this was not observed. It would be interesting to speculate how the number of haustoria produced per mother cell affects the number of nuclear divisions and vice versa.

The development of the M- haustoria of the rusts has not been previously described. The process in both M- and D- haustoria is ephemeral, and at the ultrastructural level serial sections are required in order to determine the true extent of development. However, in this study various stages were visualized making it possible to approximate the early development of the haustorium of E. harknessii.

At certain points of contact with the host cell wall, the HMC produced an evagination of its inner and outer wall layers (Figs. 22 and 23). Both wall layers remained continuous over the incipient penetration peg, the outer wall layer being PACP positive

on the hyphal wall and on the peg; however the outer layer appeared thickened immediately above the peg (Fig. 22, arrow). It is unlikely that this represents an actual thickening of the outer wall layer as it was not obvious in later stages of development (Figs. 23 and 24 inset). In fact it may have been altered host wall material that stained in a manner similar to the outer wall layer with PACP. On either side of the penetration peg, the host cell wall was more fibrillar in appearance (Fig. 22, arrowheads), again suggesting an induced alteration of the host cell wall during penetration. However, as the penetration peg continued to develop, an interruption between the outer layer of the hypha and the penetration peg was evident (Fig. 23, arrows), suggesting that the two regions might be forcibly pulled apart.

Near the point of penetration, the HMC appeared to be slightly invaginated around the site of the developing peg (Fig. 24, arrowheads), although this was not evident in the HMC at later stages of development (Fig. 25). It became increasingly evident at later stages of penetration peg development, that at the point of penetration the outer wall layer of the peg was not continuous with the outer wall layer of the HMC (Fig. 24 inset, arrowheads), but this outer layer remained continuous around the peg as it elongated (Fig. 24, arrow inset).

At the point of penetration, the host cell wall appeared to be invaginated, suggesting that some mechanical pressure was being applied during the penetration process (Fig. 24, arrow). However both the fibrillar appearance of the host wall around the peg,

noted earlier (Fig. 22), and the fact that the host cell wall did not always appear invaginated after penetration was complete (Fig. 25), suggest that the process is not wholly mechanical.

Emerging from the host cell wall the young M- haustorium still appeared peg-like (Fig. 26, arrow) but, as it matured, the terminal end showed increased swelling of the haustorial body (Fig. 27, arrow). The fine structure of the immature haustorium showed no evidence of septum formation, nor any evidence of nuclear or mitochondrial migration at this stage (Fig. 25). The outer wall layer that was evident in the penetration peg appeared to be continuous around the incipient haustorial body and neck region (Fig. 25, arrow), and showed no differentiation between it's distal and proximal regions.

During the final stages of development the haustorial body swelled becoming globose, and thus easily distinguished from the haustorial neck; the latter remained the same width as that of the original penetration peg (Fig. 28). At some point during the development of the haustorial body, organelles, including a nucleus, must migrate from the HMC and, subsequent to this, septal formation would occur in the haustorial neck. However evidence of such migration was not seen in any micrographs obtained. Ultimately the haustorial body of the mature haustorium developed a single lobe which never appeared branched or tortuous, and was always separated from the HMC by the narrowed neck region (Fig. 29).

Legend

Figures 22-25. Transmission electron micrographs of penetration peg and haustorial development.

Figure 22. An incipient penetration peg appearing as an evaginated portion of the HMC. Dark-staining material is evident adjacent to the developing peg (arrowheads). A thickened PACP positive region is evident immediately above the peg (arrow). Glut/OsO_4. PACP. X25000.

Figure 23. A developing penetration peg (PP) causing an inward displacement of the adjacent host-cell wall (CW). The dark-staining outer layer of the PP appears to be separated from a similar staining region of the HMC (arrows). Glut/OsO_4. PACP. X47,000.

Figure 24. The host cell wall appears invaginated during later stages of penetration peg development (arrow). The HMC appears to be slightly invaginated at the point of penetration (arrowheads). The inset shows a higher magnification micrograph of the PP. The outer wall layer of the peg appears uniform (arrows), and not thickened, but discontinuous from the HMC (arrowheads). Glut/OsO_4. UA/PbC. X13000. Inset X37000

Figure 25. An incipient hasutorium showing swelling in what will become the haustorial body. The young hasutorium is aseptate and is completely surrounded by an outer wall layer (arrow). Glut/OsO_4. UA/PbC. X17000.

Figures 26-29. Phase contrast micrographs of haustorial development as visualized in cleared host tissue.

Figure 26. A young haustorium with peg-like appearance (arrow). X1600.

Figure 27. An early stage of haustorial development showing swelling of the haustorial body (arrow). X1600.

Figure 28. A haustorium at a later stage of development showing a globose body and narrow septate (S) neck region. X1600.

Figure 29. A mature haustorium with a septate (S) narrow neck region terminating in a lobed haustorial body. X2000.

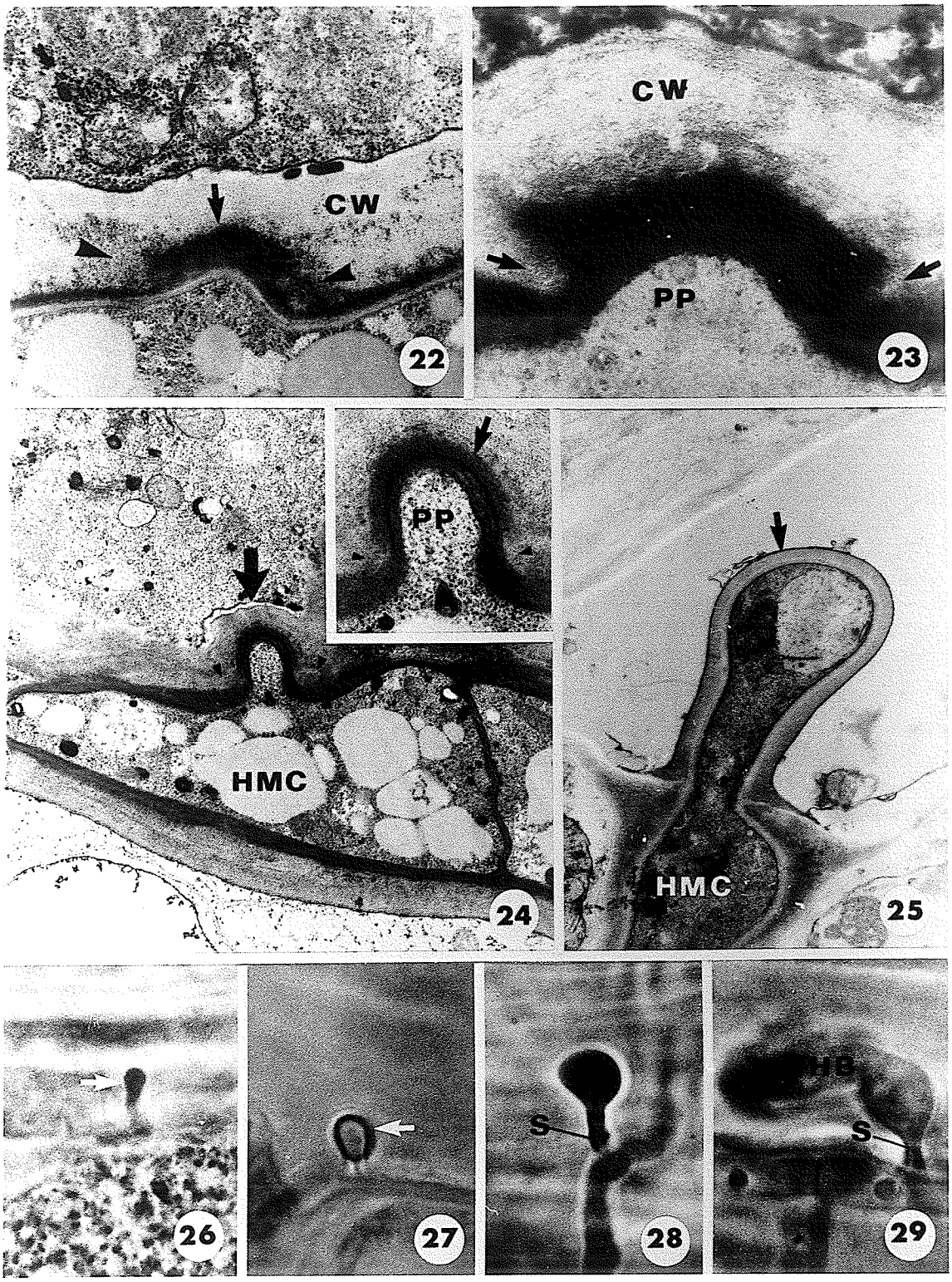
CW
22
CW
PP
23
PP
HMC
24
HMC
25
26
27
S
28
HB
S
29

DISCUSSION

In the rust fungi, with the notable exception of C. ribicola (Patton and Johnson 1970), all reports to date indicate that direct penetration of the cuticle is typical of basidiospore derived infections; in C. ribicola penetration of the host tissue occurs indirectly through stomata. Because of its endocylic nature E. harknessii does not produce basidiospores, but direct penetration of the cuticle occurs from the promycelium of the germinated teliospore as has previously been suggested by Hiratsuka et al. (1966). Direct penetration of host tissue from teliospore promycelia has only been reported previously for the microcyclic species Uromyces aloes (Sato et al. 1980). Here a narrow penetration peg developed from the promycelium without formation of an obvious appressorium. This penetration peg traversed the cuticle and entered the underlying epidermal cell where it produced an intracellular vesicle. This pattern is also typical of infection by basidiospore germlings of C. quercuum fusiforme (Gray et al. 1983; Miller et al. 1980), U. appendiculatus appendiculatus (Gold and Mendgen 1984a) and P. malvacearum (Allen 1935). In these monokaryotic infections, epidermal cells adjacent to the initial infected cell may be invaded laterally but, beyond this, hyphal development only appeared to occur in sub-epidermal tissues. The apparent initial spread of the mycelium of E. harknessii along the epidermal surface is in direct contrast to the above. A previous report (True 1938) described the infection of P. sylvestris by the Woodgate Peridermium which Boyce (1957) believed to be E.

harknessii. However this paper does not report the presence of subcuticular hyphae, but instead describes an infection process similar to that of C. quercuum fusiforme (Miller et al. 1980); this makes Boyce's identification of the rust questionable.

The habit of early mycelium development in the subcuticular region is similar to what occurs in Venturia inaequalis (Cke.) Wint. (Nusbaum and Keitt 1938), although the mycelium of V.inaequalis remains restricted to the subcuticular region. Also unlike V. inaequalis, the subcuticular hyphae of E.harknessii produce typical rust haustoria, thus in this sense appearing similar to normal intercellular hyphae.

The subsequent extention of the hyphae through out the cortex would appear to involve a forcible intrusion between adjacent host cells. Such a process is also evident during infection by C. quercuum fusiforme (Gray et al. 1983); C. ribicola (Robb et al. 1975b) and G. juniperi-virginianae (Mims and Glidewell 1978). Such forcible intrusion would not appear to be peculiar to intercellular hyphae of monokaryotic infections, since the report on G. juniperi-virginianae dealt with the dikaryotic stage of this rust.

The haustorial mother cells of E. harknessii are characteristic of those described for other rust M- haustoria (Littlefield and Heath 1979) and show little or no morphological specialization. Indeed, structurally they appear identical to all other intercellular hyphal elements which have not formed haustoria. Thus they differ from haustorial mother cells sensu stricto, the latter being specialized terminal elements of

dikaryotic hyphae. Thus it has been suggested the term haustorial mother cells should be restricted to cells producing haustoria during the dikaryotic stage of a rust (Harder and Chong 1984). However the literal meaning of the term refers to any haustorial producing pseudocell and, accordingly, the use of the term in reference to monokaryotic infections is justified.

Due to the lack of structural specialization, and the common occurrence of intercalary mother cells in E. harknessii, the possibility cannot be discounted that all intercellular hyphal elements in this rust are potential haustorial mother cells. Whether this is common for most monokaryotic infections is uncertain. Harder and Chong (1984) reported that the M- haustoria of cereal rusts are only produced from terminal hyphal cells, but both C. quercuum fusiforme (Gray et al. 1983) and U. appendiculatus (Gold and Mendgen 1984b) produce M- haustoria from both terminal and intercalary hyphal cells.

Production of several haustoria per mother cell may be unique to E. harknessii, there being no other reports of such an occurrence in the literature. However there is a line drawing of G. juniperi-virginianae in its aecial host Pyrus malus L. (Nusbaum 1935, Fig 21) which seems to show two haustoria originating from opposite sides of a common hyphal element, though this event is not recorded in the text of this paper. This feature, which is common in the downy mildews, suggests that haustoria must play a significant role in the absorption of nutrients, as a good deal of energy must be expended in their production. However, the fact

that this phenomenon occurs in the downy mildews, a less specialized group of pathogens, does raise some questions as to its degree of specialization.

During and subsequent to host cell penetration by many other rusts, the haustorial mother cells of D- haustoria display a thickened convex appearance surrounding the base of the penetration peg and this is usually due to the thickening of the middle wall layer of the mother cell. In E. harknessii the haustorial mother cell appeared somewhat similar during the later stages of penetration peg development; this was due to an invagination of the inner wall layer. However, as only a few sections of this stage were obtained, it is difficult to know whether this is a consistent feature of penetration peg development in E. harknessii. If it is, then it must be ephemeral as it was not apparent in mother cells associated with more advanced stages of haustorial development.

Penetration peg production is not well understood in most pathogenic fungi, the process occurs over a short period of time, and serial sections are required to determine the true nature of their development. However in the few reports that appear to accurately describe the process in D- haustoria, the wall of the peg is extremely thin at the point of penetration. In M. lini (Littlefield and Bracker 1972) and U. phaseoli vignae (Heath and Heath 1975) the wall of the penetration peg appears to be continuous with only the inner wall layer of the haustorial mother cell, but Chong et al. (1981) noted that the middle and inner layers of the mother cell are continuous through the zone of

penetration in P. graminis tritici. In E. harknessii the inner wall layer of the haustorial mother cell was continuous through the zone of penetration, while the outer layer, which apparently surrounds the haustorial mother cell, was not obvious at the point of penetration. In C. ribicola a similar observation was made by Robb et al. (1975b) who noted that the capsular sheath surrounding the intercellular hyphae became obscure at the point of entry; they also observed a similar staining layer towards the apex of the penetration peg.

The outer wall layer of the haustorial mother cell appeared to break away and be pushed through the host cell wall in advance of the penetration peg, suggesting that it is more rigid than previously believed, at least in this region of the mother cell. This layer appears to remain continuous over the elongating penetration peg and incipient haustorium, suggesting that it is continually being synthesized. This outer layer is believed by many authors to have an adhesive function in intercellular hyphae, (e.g. Rijkenberg and Truter 1973) but it is not certain what its function would be around the developing penetration peg.

Littlefield and Bracker (1972) noted a dark-staining region of the host cell wall produced in advance of the penetration peg of M. lini. They suggested it was host cell wall altered by the enzymatic action of penetration. The argument can be made that the PACP positive area at the apex of the penetration peg of E. harknessii also represents altered host cell wall components or alternatively may represent the mingling of host and fungal

materials. However in E. harknessii it was apparent that a similar staining layer exists between the non-evaginated portion of the mother cell and host cell wall, so a similar staining region does pre-exist. What seemed to be the same layer was also continuous with the inner wall layer of the haustorial neck through the zone of penetration, as well as distal to the host cell wall in mature haustoria (Chapt. 2). For these reasons I believe that there is evidence of the involvement of two fungal wall layers in penetration peg development.

Most authors agree that penetration of the host cell wall is an enzyme moderated process, but it would appear from the distortion of the host cell wall that there is also mechanical pressure applied by the penetration peg of E. harknessii. This is also obvious in the penetration region of C. ribicola in pine callus tissue (Robb et al. 1975b) and the developing peg of the M-haustoria of P. poarum (Al-Khesraji and Lösel 1981). However in some young haustoria of E. harknessii, the juxtaposed host cell wall was not distorted, thus the process must be at least partly enzymatic. It is also evident that the wall layers of the penetration peg remained uniform in thickness during penetration. Some compression of the apex of the elongating peg would be expected if the peg was breaching the host wall by strictly mechanical means.

The mechanisms underlying growth of penetration pegs in E. harknessii are confusing and unclear. The peg appeared devoid of any membrane-bound vesicles similar to those found in actively

growing hyphal tips. Further, in one of the few reports on penetration peg development, Heath and Heath (1975) reported the occurrence of electron-dense granules in the penetration peg of U. phaseoli vignae, but similar inclusions were not evident in the penetration pegs of E. harknessii. In fact all of the penetration pegs examined lacked any of the features that one would normally expect to be associated with an active growth process.

Clearly haustorial development in E. harknessii requires additional study; there is still much that cannot yet be understood or explained.

It is probable that young, non-septate, anucleate haustora are non-functional, and it was evident that at this stage the extrahaustorial matrix (Chapt. 2) had not yet differentiated. The haustorium probably does not become functional until a nucleus has migrated into the expanded haustorial body and the extrahaustorial matrix differentiates. In both P. coronata (Chong 1981) and U. phaseoli vignae (Heath and Heath 1971) expansion of the D-haustorial body is synchronized with migration of mitochondria and nuclei from the haustorial mother cell. How similar the process is in E. harknessii has yet to be elucidated, but the general morphology of haustorial development, as demonstrated by light microscopy, is not dissimilar to that suggested for D-haustoria of M. lini (Littlefield 1972) and ultrastructural comparisons may find further similarities.

C H A P T E R 2

LIGHT AND ELECTRON MICROSCOPIC OBSERVATIONS ON THE HAUSTORIUM OF *ENDOCRONARTIUM HARKNESSII*

Introduction

Ultrastructural studies of rusts have generally concentrated on dikaryotic infections of cereals, and dicotyledonous hosts. Consequently, much is known about the D- haustoria of a number of rusts, and the degree of specialization (Bushnell 1972; Harder and Chong 1984; Littlefield and Heath 1979). Conversely M- haustoria have received much less attention, probably due to the fact that they are often associated with economically unimportant hosts.

In rusts associated with coniferous trees, with the exception of the genus Gymnosporangium, it is the monokaryotic mycelium that is damaging to the commercially important host. While some ultrastructural studies have been reported on the M- haustoria of Cronartium flaccidum (Longo 1982; Longo et al. 1982), C. quercuum fusiforme (Gray et al. 1982), C. ribicola (Robb et al. 1975b), Melampsora pinitorqua (Jonsson et al.; Longo and Naldini-Longo 1975) and Peridermium pini (Walles 1974), none has been reported for E. harknessii.

This study used light and electron microscopic techniques in an investigation of the cytological and histochemical nature of the haustorium of E. harknessii to gain a better understanding of this important pathogen.

RESULTS

Using electron microscopy, it is often difficult to determine the three dimensional structure of haustoria. However, using light microscopy, which provides a far greater depth of field, it was evident that the haustoria of E. harknessii are pleomorphic; the shape ranging from elongate and finger-like (Fig. 1), to globose (Fig. 2) to obpyriform (Fig. 3). All haustoria displayed a definite constriction at the point of penetration; this constituted a neck region (Fig. 2, arrow) which terminated in the expanded portion of the haustorium, the haustorial body. The haustorium was produced from an intercellular hyphal element, the haustorial mother cell (HMC)(Figs. 2 and 4), which was separated from the haustorial body by a septum in the haustorial neck region (Figs. 2 and 4).

The entire haustorium was surrounded by, and closely associated with, an invaginated portion of the host plasmalemma, the extrahaustorial membrane (EM)(Fig. 4). The EM closely followed the contours of the haustorium and was continuous with the remainder of the host plasma membrane (Fig. 11). The haustorium itself was uninucleate, and its protoplasm appeared similar to that of the intercellular hyphae with the exceptions that lipid bodies, though present in the haustorium, were not common, and mitochondria were, usually located along the periphery of the cell close to the plasmalemma (Fig. 4, arrow heads).

Legend

Figures 1-3 Light microscope photographs of haustoria.

Figure 1. Haustoria display a finger-like appearance. Nomarski interference microscopy. X1000.

Figure 2 A haustorium showing constricted septate(S) neck region and globose body. Nomarski interference microscopy. X1000.

Figure 3. A haustorium with an obpyriform shaped body. Phase contrast microscopy. X1600.

Figure 4. Transmission electron micrograph of a mature haustorium.

Figure 4. The haustorium displays a constricted, septate(s) neck region terminating in an expanded haustorial body which is surrounded by the extrahaustorial membrane (EM). The haustorium is uninucleate (N) and mitochondria (arrowheads) appear to be arranged around the periphery of the haustorial body. Glut/OsO_4. UA/PbC. X11000.

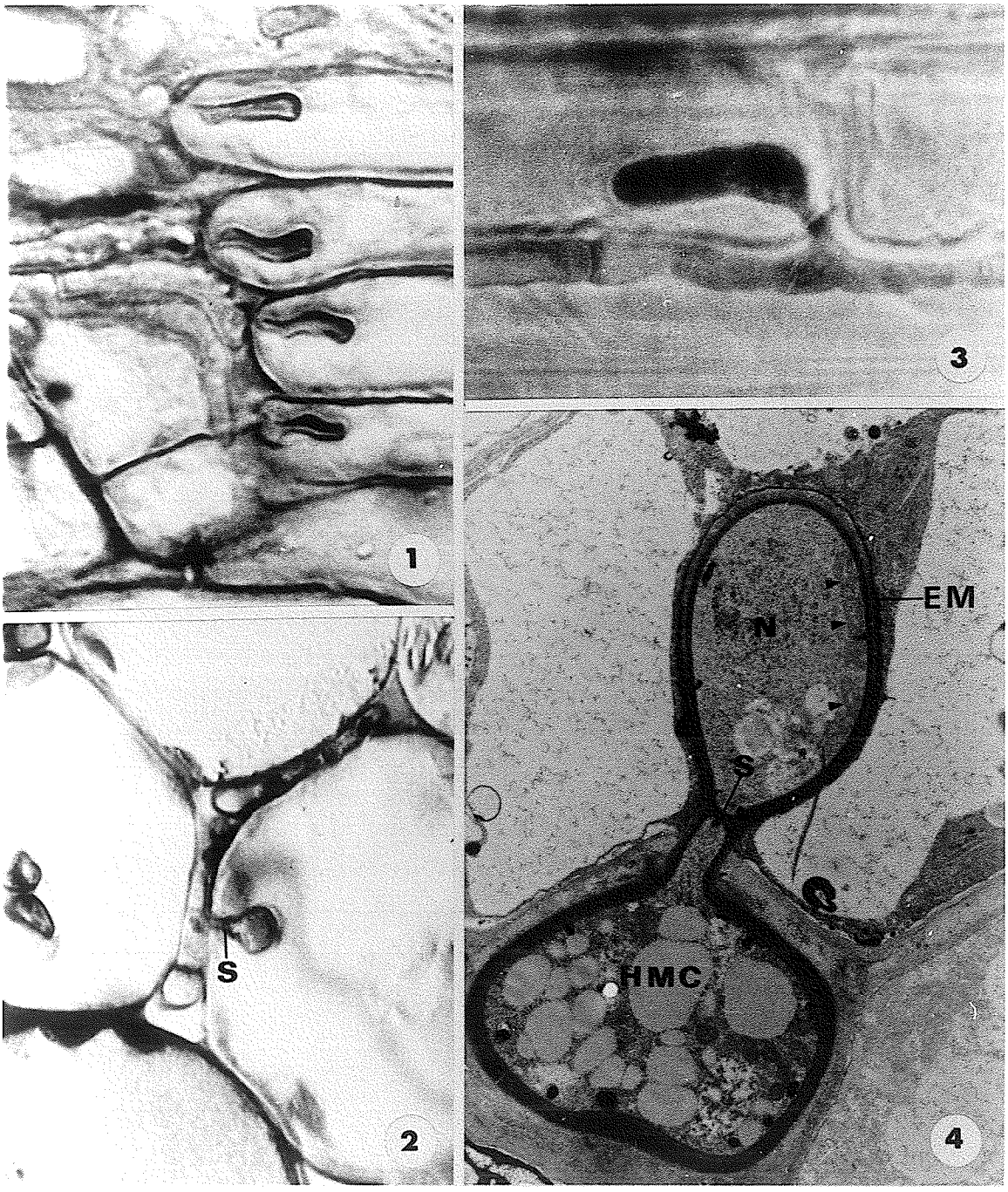
1
2
S
3
EM
N
S
HMC
4

The haustorial septum was typical of those described for the rust fungi (Littlefield and Heath 1979), and appeared trilamellar with the outer layers continuous with the haustorial walls and tapered somewhat towards the central pore (Figs. 5 and 6). The pore itself was typically plugged with a dark-staining substance of varying shape, e.g. from a pulley-wheel shape (Fig. 5, arrow) to apparently more reduced forms (Fig. 6, arrow).

The haustorial septum was very similar to that observed in intercellular hyphae. In the latter, however, it appeared that the central electron lucent layer (Fig. 7, arrow) was often bounded on either side by two further wall layers which were continuous with the hyphal walls (Figs. 7 and 7 inset); however this layer (WL1) was not always evident (Fig. 8), suggesting that this region may be difficult to preserve.

The pore apparatus of the intercellular hyphae was similar to that of the haustoria, and even displayed similar variations in shape (Figs. 7 and 8). Even though the septal plug of E. harknessii was similar to that reported for other rusts, it seemed to lack the surrounding membrane reported for C. quercuum (Khan and Kimbrough 1982). Such was not apparent with any staining procedure used and, as other membrane structures were preserved, it seems probable that one does not exist in this rust.

Histochemical tests suggested that the septal plug differs from the hyphal walls in composition. In contrast to the walls, the plugs did not stain after treatment with PACP (Fig. 9, arrow), and when treated with PA-TCH-SP (14 h in TCH) showed only a limited

Legend

Figures 5-10. Transmission electron micrographs of the fungal septum and pore apparatus.

Figure 5. A haustorial septal pore with a dark-staining pulley-wheel shaped plug (arrow). Glut/OsO_4 . UA/PbC. X52500.

Figure 6. A haustorial septal pore apparatus showing a more reduced plug (arrow). Glut/OsO_4. UA/PbC. X52500.

Figure 7. An intercellular hyphal septum exhibiting a multilayered appearance. The septum consists of a central electron-lucent layer (arrow) bounded on both sides by two wall layers (WL1, WL2), which are continuous with the hyphal wall. The hyphal element is separated from the host cell wall (CW) by an outer amorphous layer (AL). The inset shows the septal wall layers at increased magnification. Glut/OsO_4. UA/PbC X40000. Inset X80,000.

Figure 8. A hyphal septum showing no evidence of WL1. The septal pore apparatus is similar to that in the haustorium. Glut/OsO_4. UA/PbC. X60000.

Figure 9. A haustorial septal plug (arrow) showing no reaction to PACP staining. Glut/OsO_4. PACP. X90000.

Figure 10. A haustorial septal plug (arrow) showing only a slight reaction to Thiery staining. Glut/OsO_4. PA-TCH-SP. X90000.

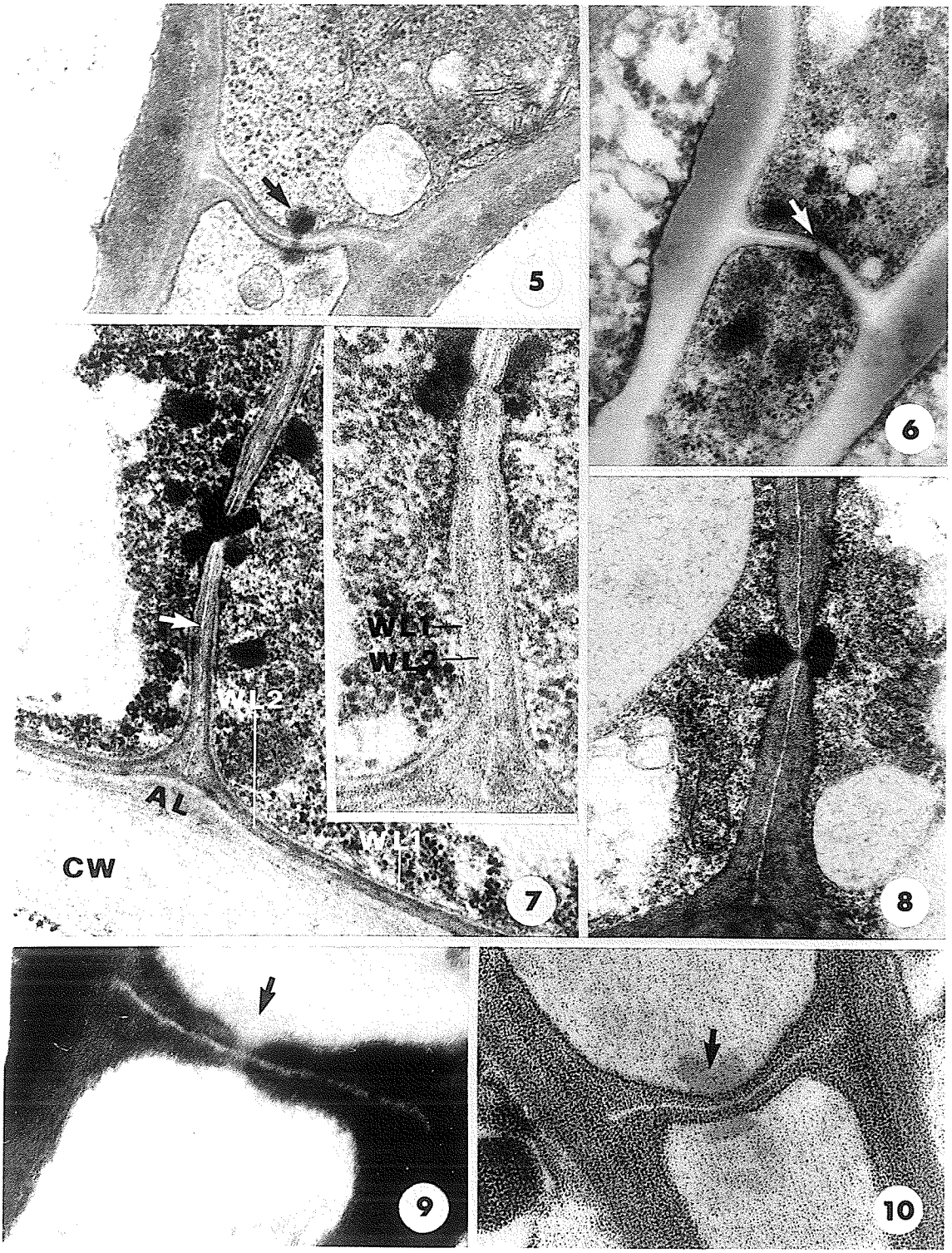
5
6
WL1
WL2
WL2
AL
CW
WL1
7
8
9
10

reaction similar to that shown by the background cytoplasm (Fig. 10, arrow). Negative results with both these tests suggest an absence of either a lipid or glycol moiety. Attempted protein extraction using the enzyme protease was not successful and failed to extract even known proteinaceous regions (e.g. chloroplasts), thus the possibility of the plug being composed of protein cannot be discounted.

When the haustorial neck was stained using conventional techniques (UA/PbC), it appeared to be composed of two distinct wall layers (WL2, WL4, Fig. 11) separated by a dark staining interlamelar region (Fig. 11, arrow). Wall layer 2 was continuous through the penetration zone with the corresponding region of the HMC, (Figs. 11, 12) and accordingly with WL2 of the intercellular hyphae (Fig. 7). It should be noted, however, that the innermost layer observed in the intercellular hyphae (WL1, Fig. 7) was not apparent in the haustorial neck (Fig. 11).

The outermost layer (WL4) also appeared to be continuous with the HMC but was much more diffuse at the neck base where it joined the HMC (Fig. 12, arrow), though in the more proximal portions of the neck this layer was discrete and easily distinguished from the host cell wall (Fig. 11, open arrow). Wall layer 4, as it continues over the intercellular hyphae, became less distinct and took on the appearance of an amorphous layer (AL). It appeared to merge with the host cell wall (Fig. 15), suggesting a possible mucilaginous nature. This AL also appeared to expand between the HMC and the host cell wall to provide direct contact between the

Legend

Figures 11-12. Transmission electron micrographs of the haustorial neck region and the adjoining haustorial mother cell (HMC).

Figure 11. Two wall layers (WL2, WL4) are apparent in the neck (HN), separated by an electron dense interlamellar region (arrow). The outer wall layer (WL4) is distinct from the collar through the zone of penetration distal to the HMC (open arrow). Glut/OsO_4.UA/PbC. X72000.

Figure 12. WL4 appears to merge with the host cell wall (CW) at the point of penetration (arrow) and becomes an amorphous layer (AL) over the HMC. WL2 appears continuous through the neck and HMC. Glut/OsO_4. UA/PbC. X72000.

Figures 13-14. Transmission electron micrographs the amorphous layer of intercellular hyphae.

Figure 13. The AL (arrow) appears to expand between the HMC and the CW to provide contact between the two cells. Glut/OsO_4. UA/PbC. X48000.

Figure 14. Expansion of the AL between intercellular hyphae and the host cells. Glut/OsO_4. UA/PbC. X17000.

two cells (Fig. 13, arrow). A similar situation occurred where hyphal elements were present in large intercellular spaces; there the AL formed an extensive matrix between the mycelium and host cell walls (Fig. 14).

The AL of the intercellular hyphae was only lightly stained with PA-TCH-SP (Fig. 16), in contrast to the adjacent WL2 which was moderately reactive to silver proteinate. The inner layer (WL1) was not visualized with PA-TCH-SP, though again, this may have resulted from poor preservation. Staining with PACP also resulted in the demonstration of two distinct regions being present in the hyphae, with the outer AL being densely stained in comparison to WL2, which showed a much reduced reaction (Fig. 17).

PA-TCH-SP and PACP staining were also used to clarify the structure of the haustorium. Staining with silver proteinate revealed three wall layers in the haustorial neck; the inner layer (WL2) was moderately reactive to silver proteinate (Fig. 21), as was the corresponding region in the HMC (Fig. 22) and intercellular hyphae (Fig. 16). This layer was continuous with the haustorial septum (Figs. 20 and 21) and was present in the more proximal portions of the haustorial body (Fig. 20) although, as will be demonstrated later, it was evident through the entire haustorial body. Even when present, WL2 formed a less significant portion of the haustorial body-wall than it did in the walls of the neck or HMC (compare Figs. 20 and 21). Wall layer 2 in the haustorial body was at least partly preserved in tissue fixed with glutaraldehyde only (Fig. 23), and was easily distinguished as being a separate

Legend

Figure 15-17. Histochemistry of intercellular hyphae.

Figure 15. The outer amorphous layer (AL) separating WL2 of the intercellular hyphae from the host-cell wall (CW) appears to merge with the latter. Glut/OsO_4. UA/PbC. X46500.

Figure 16. The AL displays only a slight reaction to Thiery staining while adjacent WL2 reacts more intensely. Glut/OsO_4. PA-TCH-SP. X46500.

Figure 17. The AL shows intense staining with PACP while WL2 displays a reduced reaction. Glut/OsO_4. PACP. X44000.

Figures 18-19. Thiery staining of the haustorial neck region after prolonged incubation in TCH.

Figure 18. 14 h incubation in TCH results in intense staining of WL2 and WL3. Wall layer 4 displays a lesser reaction to the stain and becomes less distinguishable at the base of the neck, (arrowheads). Glut/OsO_4.PA-TCH-SP. X46500.

Figure 19. Prolonged incubation (14 h) of unosmicated material in TCH results in intense staining of WL2 and WL3 but an absence of staining in WL4. Wall layer 4 shows reduced staining, and is possibly discontinuous from the AL of the HMC (arrows). Glut. PA-TCH-SP. X46500.

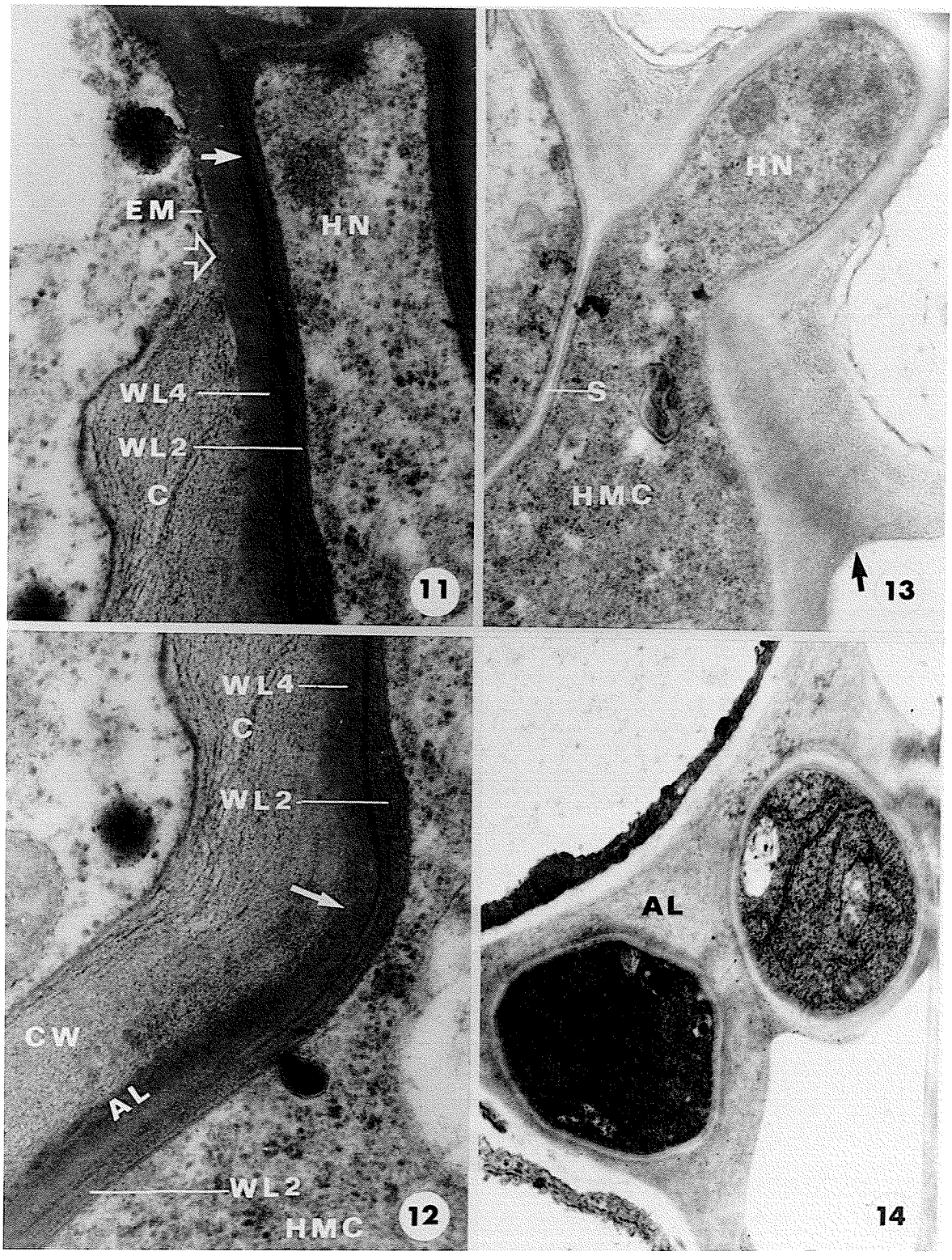
EM
HN
WL4
WL2
C
11
HN
S
HMC
13
WL4
C
WL2
CW
AL
WL2
HMC
12
AL
14

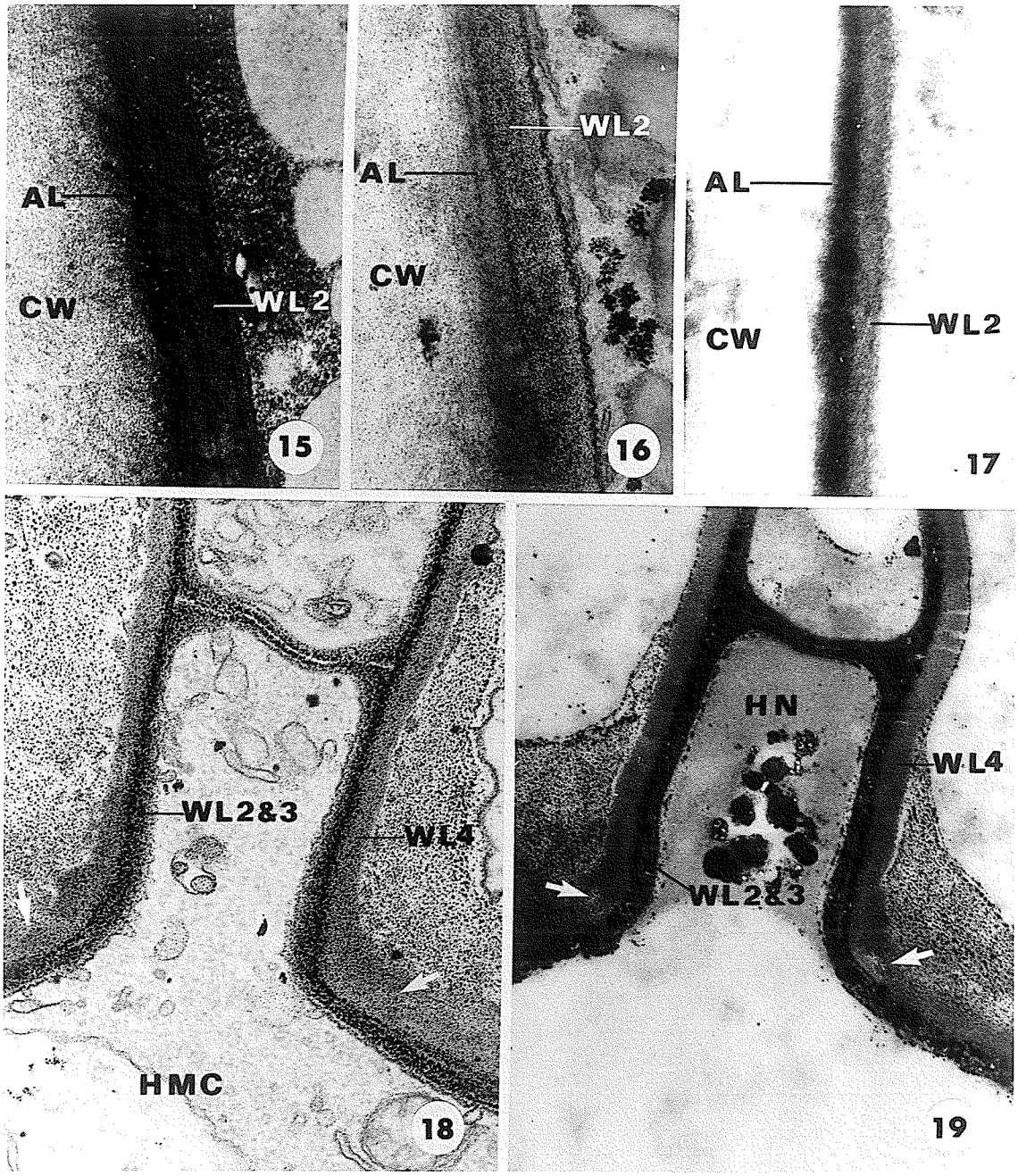
AL
CW
WL2
15
WL2
AL
CW
16
AL
CW
WL2
17
WL2&3
WL4
HMC
18
HN
WL4
WL2&3
19

region. As already noted, WL2 was observed in the more proximal portions of the haustorial body, and could be observed in cross section in what appeared to be a more distal section of the haustorial body on the basis of the width of the EHM (Fig. 23). However it was never observed at the terminal end of the haustorium (Fig. 24, arrow). Wall layer 2 of the haustorial body was morphologically similar to WL1 in the intercellular hyphae and shares with it the characteristic of being difficult to preserve. However, it is given a different designation due to its proximity to WL3 which is unique to the haustorium, and is equivalent to the interlamellar region (Fig. 11, arrow); WL2 of the neck region showing the same position relative to the middle wall layer (Fig. 21).

In comparison to WL2, the adjacent layer, WL3, was densely stained with silver proteinate. This layer continued over the entire haustorium (Fig. 25) and appeared to be present through the zone of penetration (Fig. 21). However WL3 seemed to unite or coalesce with WL2 in the region where the haustorial neck merged into the wall of the haustorial mother cell (Figs. 21, arrow, and 22). This coalescence was also seen in bleached, unstained sections (Fig. 26, arrow) where it was evident that WL3 either terminated, or was altered, where it met the HMC wall.

In PA-TCH-SP stained material WL3 also appeared to widen and intrude into the haustorial septum (Fig. 21, open arrow), although with this stain it was not clear whether it was continuous with the

septum. However in bleached sections continuity with the septum was evident (Figs. 26 and 27, arrowheads).

The outermost layer, WL4, was distinct from the two inner layers, and showed only a limited reaction to silver proteinate (Fig. 21). This differentiation of WL4 from the adjacent wall layers was even more evident when unosmicated tissue stained with PA-TCH-SP (Fig. 19) was compared to similarly stained osmicated material (Fig. 18). Both figures 18 and 19 represent material subjected to TCH for 14 hours prior to staining with silver proteinate. After such a period of incubation even more complex carbohydrates (e.g. glycoproteins) should have been bound, and caused an increase in staining intensity over tissue incubated for the time required to achieve maximal staining in simple polysaccharides (ca. 0.25 h in TCH). From Figure 18, it is obvious there was an overall increase in staining intensity, resulting in the differences between WL2 and WL3 being obscured. The outermost wall layer (WL4) also stained more intensely, but less so than the inner wall layers. In tissue fixed in Glut only (Fig. 19), the inner wall layers (WL2 and WL3) were again heavily stained although the stain deposits were aggregated; however the outermost layer (WL4) did not react with silver proteinate. Further, this PA-TCH-SP staining of glutaraldehyde-fixed tissue makes the discontinuity between WL4 and the AL of the mother cell more apparent (Fig. 19, arrows). In Glut/OsO_4 fixed-tissue stained as above, this region was diffuse and indistinct from the host cell-wall (Fig. 18, arrows).

Legend

Figures 20-22. Thiery staining of the haustorial neck and haustorial mother-cell wall-layers.

Figure 20. Three wall-layers are evident in the neck region and the proximal portion of the haustorial body. Wall layer 3 stains intensely and is continuous over the haustorial body and at least a portion of the septum. Wall layer 2 is present in both the neck and body but appears reduced in the latter. Glut/OsO_4. PA-TCH-SP. X60000.

Figure 21. Three wall layers are apparent in the neck, showing varying degrees of staining. Wall layer 2 is continuous with the HMC while WL4 shows similar staining characteristics but is broader and less regular in the HMC. The central layer, WL3, appears to merge with WL2 on the HMC (arrow). Glut/OsO_4. PA-TCH-SP. X60000.

Figure 22. The outer AL is expanded over the HMC and is only lightly stained when compared to WL2. There is no evidence of WL3 in the HMC. Glut/OsO_4.PA-TCH-SP. X6000.

Figure 23. Cross section of the haustorial body.

Figure 23. The inner wall layer (WL2) of the haustorial body is partially preserved in unosmicated material. The width of the EHM suggests the section is taken from a more distal portion of the body. Glut. UA/PbC. X72000.

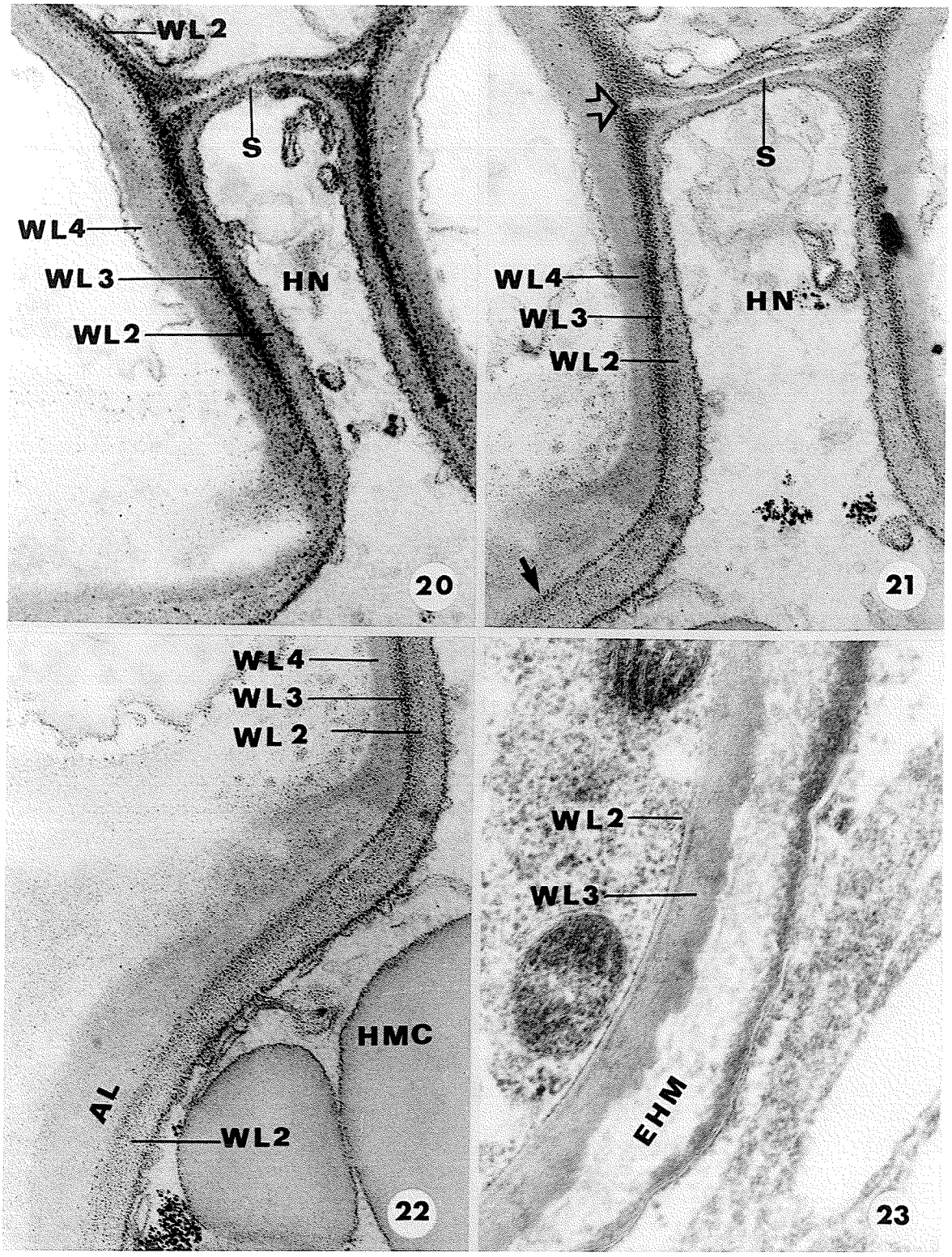
WL2
S
WL4
WL3
HN
WL2
20
S
WL4
WL3
HN
WL2
21
WL4
WL3
WL 2
HMC
AL
WL2
22
WL2
WL3
EHM
23

Legend

Figures 24–25. Thiery staining of the haustorial body.

Figure 24. The distal portion of the haustorial body (HB) shows no evidence of WL2 (arrow). The only obvious layer, WL3 is intensely stained. Glut/OsO_4. PA-TCH-SP. X46500.

Figure 25. WL3 which is intensely stained is continuous over the HB. Glut/OsO_4. PA-TCH-SP. X17000.

Figures 26–27. Bleached unstained sections of the haustorial neck region.

Figure 26. Three wall layers are apparent in the neck region. The middle layer (WL3) appears to protrude into the haustorial septum (arrowhead) and coalesce with the inner layer at the base of the neck (arrow). Glut/OsO_4 PA. X72000.

Figure 27. Lower magnification of the neck region showing three distinct wall layers corresponding to WL2, WL3, WL4. WL3 appears to be continuous with the middle layer of the septum. Glut/OsO_4.PA. X46500.

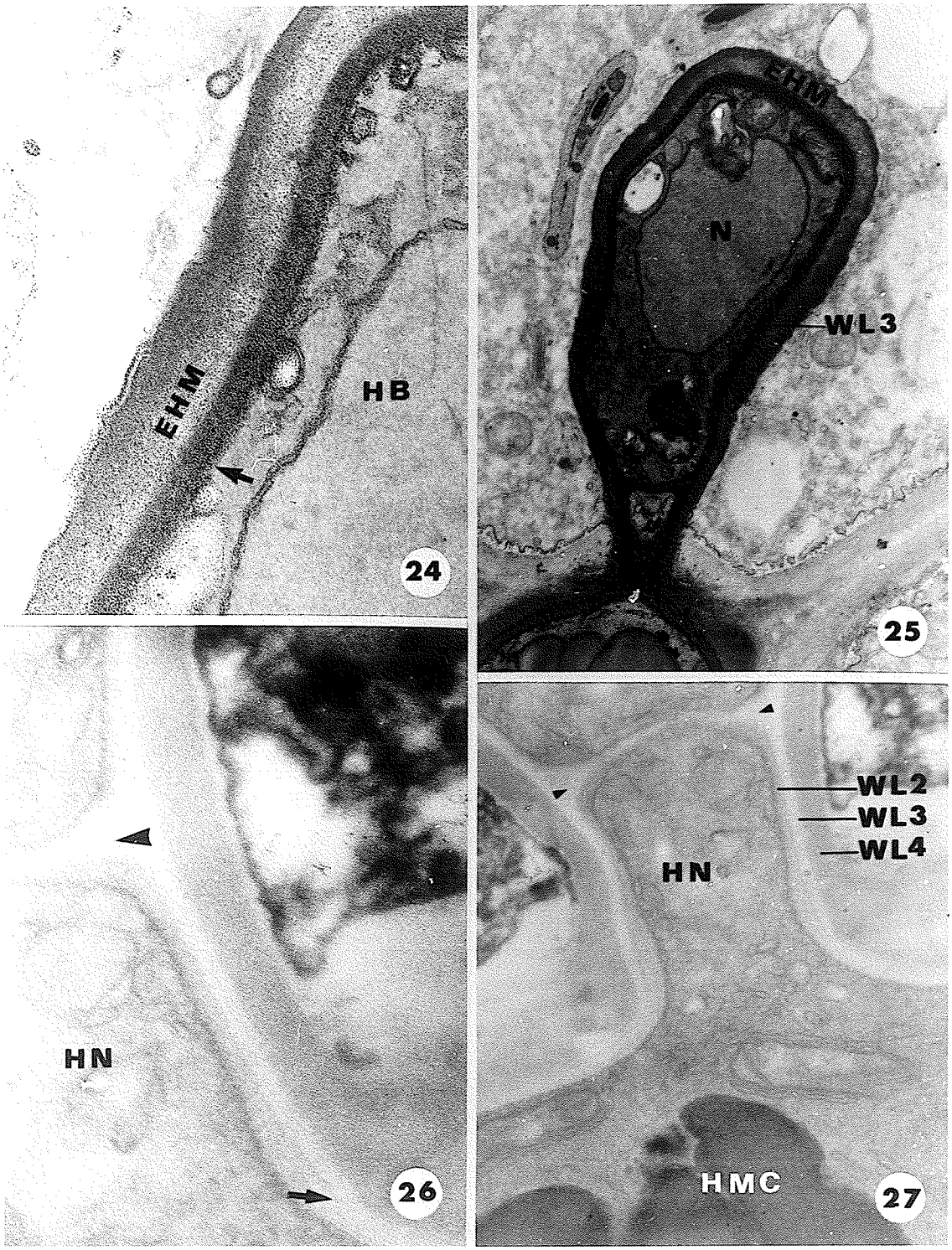
EHM
HB
24
EHM
N
WL3
25
HN
26
WL2
WL3
WL4
HN
HMC
27

When treated with PACP the outer wall layer of the haustorial neck (WL4) was densely stained; it appeared to terminate at the base of the neck and then merge laterally with the host cell wall material (Fig. 28, arrows). This abrupt termination of WL4 was more obvious in a tangential section (Fig. 29). Here WL4 appeared to terminate in a disc-like structure, which again suggests a merging with the host cell wall (Fig. 29, arrows). When stained with PACP, wall layer 3 stained less intensely than WL4 and appeared continuous across the septum (Fig. 28). Wall layer 2, in contrast to WL3, was strongly PACP positive in both the neck and haustorial body (Fig. 28).

Oxidation with periodic acid was not always a prior necessary step to staining with PTA. Direct staining with PTA in chromic acid resulted in the staining of the outer neck wall (WL4) and the inner wall layer (WL2) in both the neck and the haustorial body, though the middle layer (WL3) showed no evidence of staining (Fig. 30). The amorphous layer of the HMC also appeared intensely stained by this treatment (Fig. 31).

Oxidation with H_2O_2 provided contrasting results. Hydrogen peroxide bleaches OsO_4 from the specimens, but it does not specifically oxidize glycols (Hall 1978). None of the samples oxidized with H_2O_2 prior to staining with PTA showed any staining in the fungal walls of the haustorial neck, including WL4 (Fig. 32). There was also a reduction in the staining of the amorphous layer of the HMC (Fig. 33).

Legend

Figures 28-29. PACP staining of the haustorial neck (HN) region.

Figure 28. Wall layers 2 and 4 showing intense staining, WL4 appears to terminate at the base of the neck (arrows). WL3 in the haustorial neck and body shows a reduced level of staining. Glut/OsO_4. PACP. X46500.

Figure 29. Tangential section of the haustorial neck showing a disc-like region at the base of the neck (arrows). Glut/OsO_4. PACP. X46500.

Figures 30-31. Controls for PACP staining of the haustorial neck and HMC; no oxidation with periodic acid prior to staining with PTA in chromic acid (CP).

Figure 30. Wall layers 2 and 4 show reduced but positive staining, WL3 showing an absence of staining. Glut/OsO_4. CP. X32000.

Figure 31. The AL of the HMC shows positive but reduced staining. Glut/OsO_4. CP. X32000.

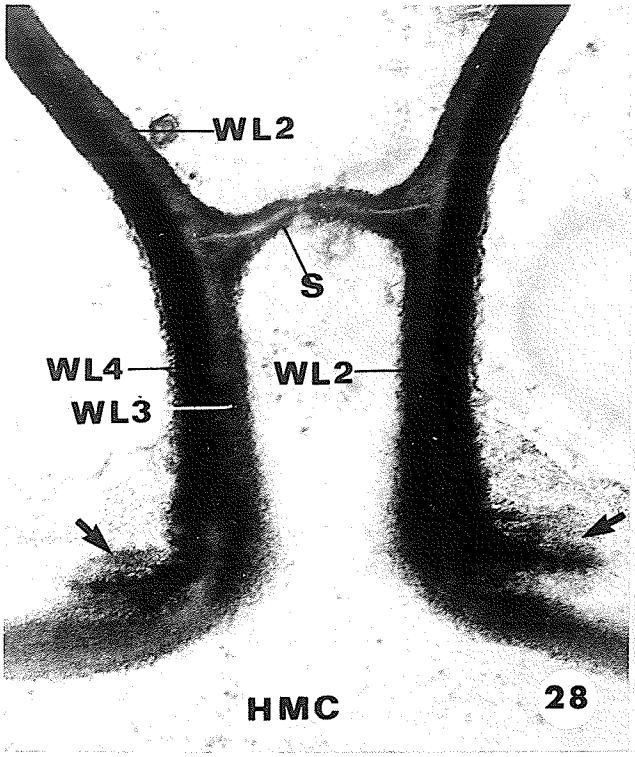
WL2
S
WL4
WL2
WL3
HMC
28

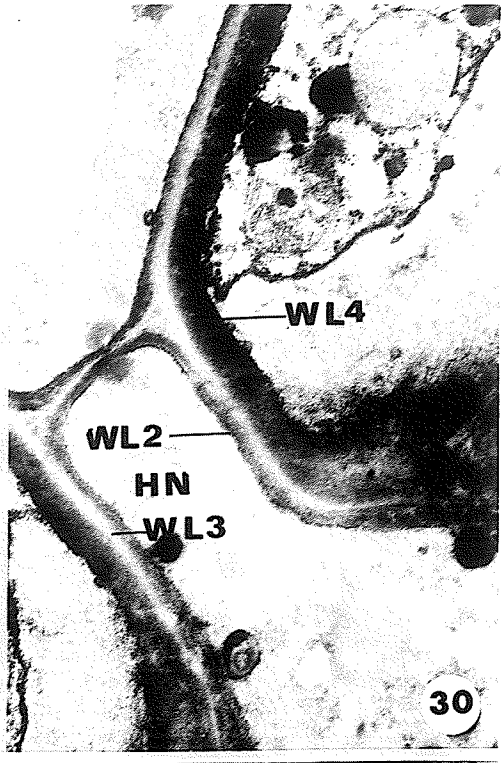
WL4
WL2
HN
WL3
30


29

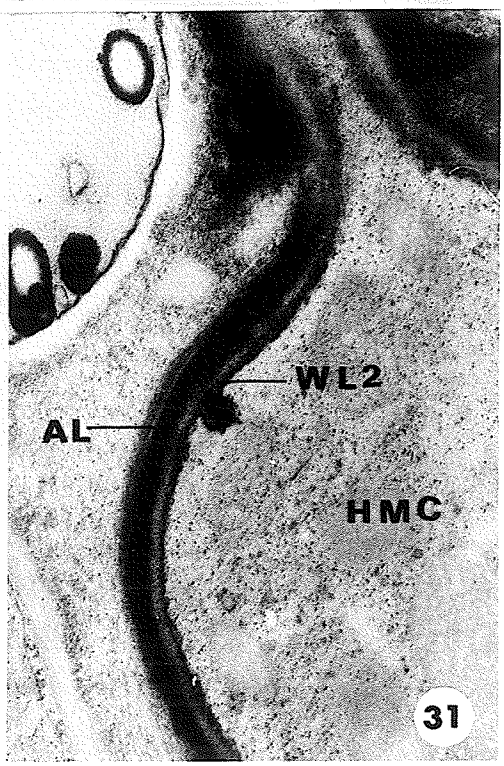
WL2
AL
HMC
31

When tissue fixed in glutaraldehyde only was subjected to PACP, wall layers 2 and 3 in the haustorial neck and body did not stain, while WL4 showed a reduced, but positive staining reaction (Figs. 34 and 35). The amorphous layer of the HMC also stained in a like manner to WL4 in the neck region (Fig. 35). Tissue fixed with Glut only, and stained with PACP also illustrated the discontinuity between WL4 in the haustorial neck and the AL of the mother cell and intercellular hyphae (Fig. 34, arrowheads) and thus showed WL4 was distinct from the other layers in the haustorial neck and from the host wall material.

Cellulase, a beta-[1, 4(1, 3)] glucanase, was also used to help determine the nature of the wall layers. Treating sections with cellulase prior to staining with PA-TCH-SP revealed that the enzyme removed the host-cell wall but left WL4 in the haustorial neck relatively unaffected (Fig. 36). In intercellular hyphae where the outer wall layer (AL) was less distinct, cellulase treatment again did not remove the fungal wall (Fig. 37), although both wall layers did appear to become more reactive to PA-TCH-SP after cellulase treatment, particularly WL2. Perhaps there was some alteration of the wall components such as the partial breakdown of the complex carbohydrates in WL2, thus creating more reactive sites.

At the distal end of the haustorium, positioned between the EM and the fungal wall, was a region of uncertain composition referred to as the extrahaustorial matrix (EHM). There has always been some question as to the authenticity of this region, which may simply be

Legend

Figures 32-33. Controls for PACP staining of the haustorium; oxidation with H_2O_2 prior to staining with PTA in chromic acid (H_2O_2 - CP).

Figure 32. Wall layers of the haustorial neck lack evidence of staining. Glut/OsO_4. H_2O_2 - CP. X60000.

Figure 33. Lower magnification of Fig. 32. Wall layers of the haustorial body appear to be relatively unstained. Glut/OsO_4. H_2O_2-CP. X9000.

Figures 34-35. PACP staining of unosmicated tissue in the haustorium.

Figure 34. Wall layers 2 and 3 in the haustorial neck appear unstained while WL4 shows positive but reduced staining. Glut. PACP. X60000.

Figure 35. Lower magnification of Fig. 34, WL3 of the haustorial body appearing unstained. The AL of the HMC appears positively stained. Glut. PACP. X12000.

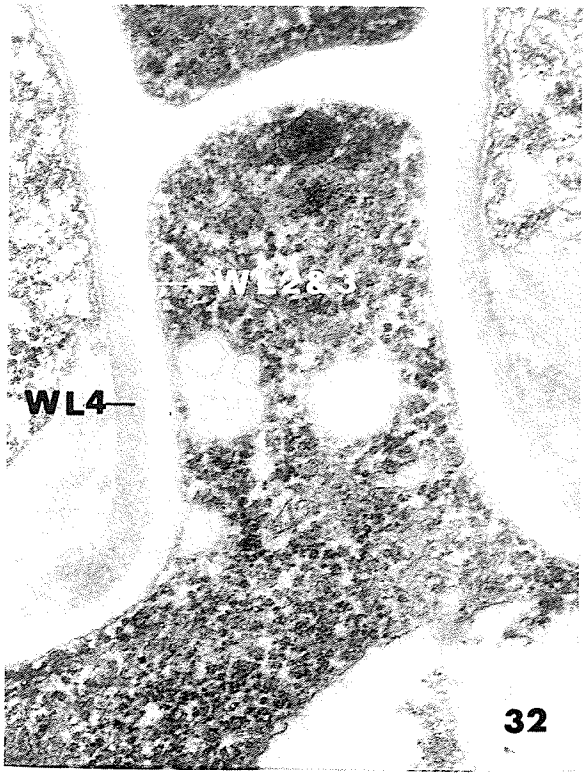

32

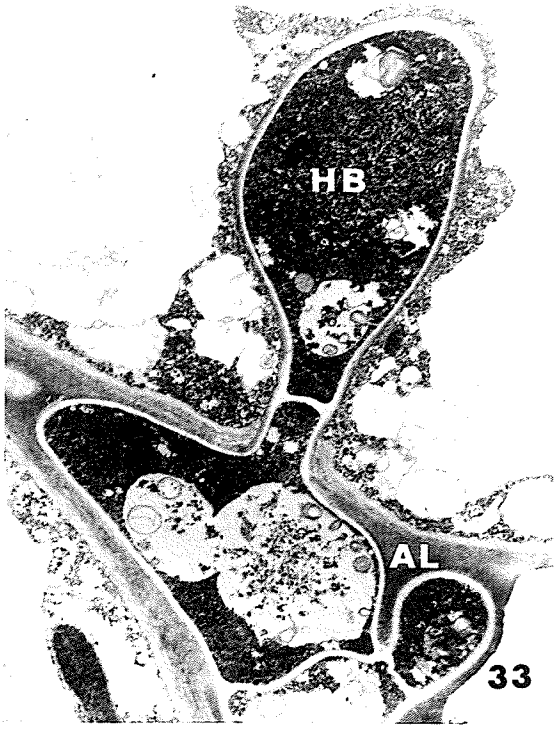

33

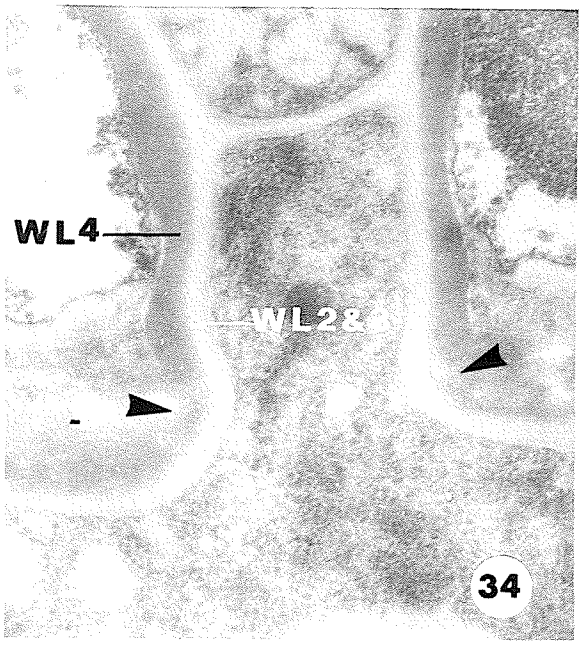

34

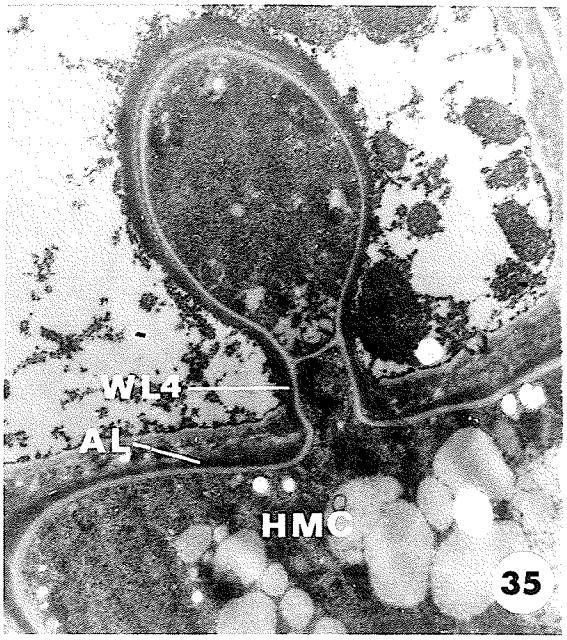

35

Legend

Figures 36-37. Fungal walls after treatment with cellulase

Figure 36. Host cell wall material is extracted while the outer wall layer of the haustorial neck (WL4) remains intact. Glut cellulase - OsO_4. UA/PbC. X29500.

Figure 37. Complete extraction of the cell wall but no evident extraction of either wall layer in the intercellular hyphae. Both the AL and WL2 show an increase in Thiery staining Glut-cellulase - OsO_4. PA-TCH-SP. X30000

Figure 38. Light microscopic photograph of unfixed haustorium.

Figure 38. Evidence of a region surrounding the distal portion of the haustorium (arrows) in fresh tissue, corresponding to the region occupied by the EHM. Phase contrast microscopy. X2000.

Figures 39-40. PACP staining of the haustorial body and the extrahaustorial matrix.

Figure 39. The EHM (region B) stains positively but in a fibrillar manner, as compared to the haustorial neck (region A). The extra haustorial membrane (EM) stains intensely while the remaining host plasmalemma (HP) is unstained. Glut/OsO_4. PACP. X17000.

Figure 40. The EHM and WL4 of the neck appear to merge in the lower portion of the haustorial body (arrow). The material in the EHM and the EM both stain intensely. Glut/OsO_4. PACP. X47500.

Figure 41. Control for PACP staining of the extra haustorial matrix, no oxidation in periodic acid prior to staining in PTA in chromic acid (CP).

Figure 41. Material in the EHM as well as the EM remain stained while WL3 shows only slight staining, although there is evidence of a dark-staining region adjacent to WL3 (arrowhead). Glut/OsO_4. CP. X40000.

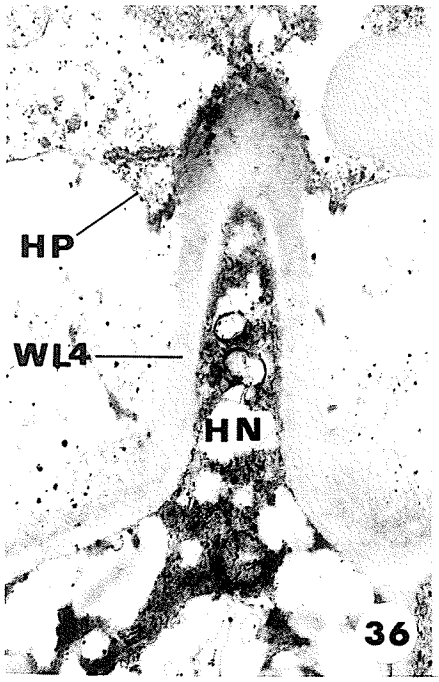
HP
WL4
HN
36

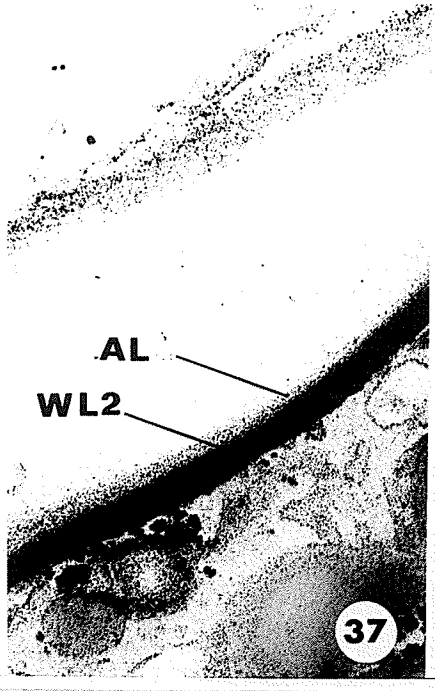
AL
WL2
37

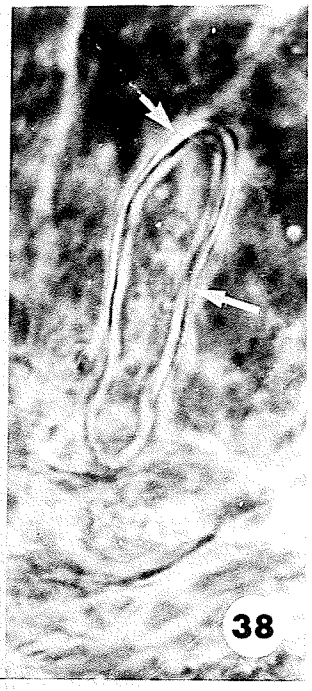
38

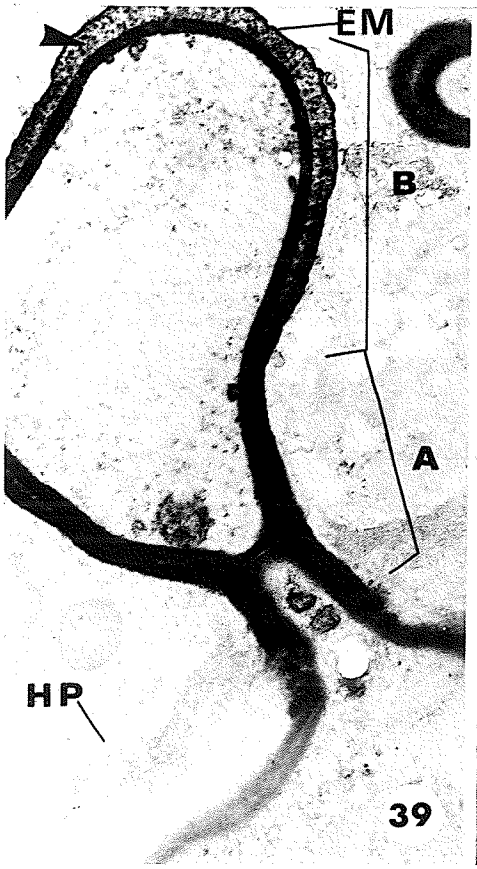
EM
B
A
HP
39

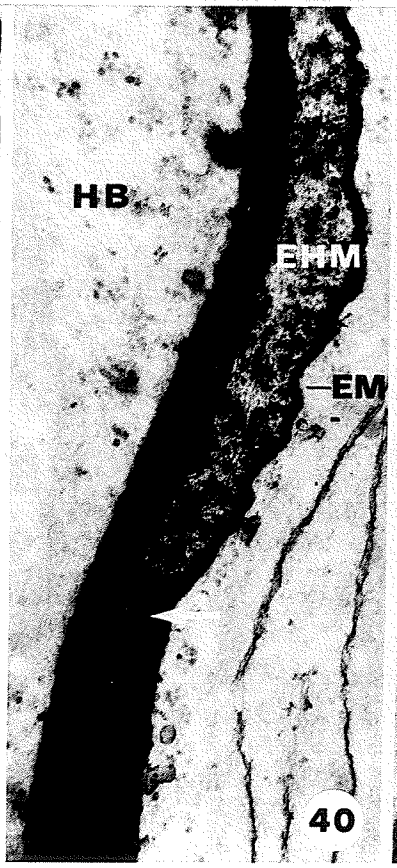
HB
EHM
EM
40

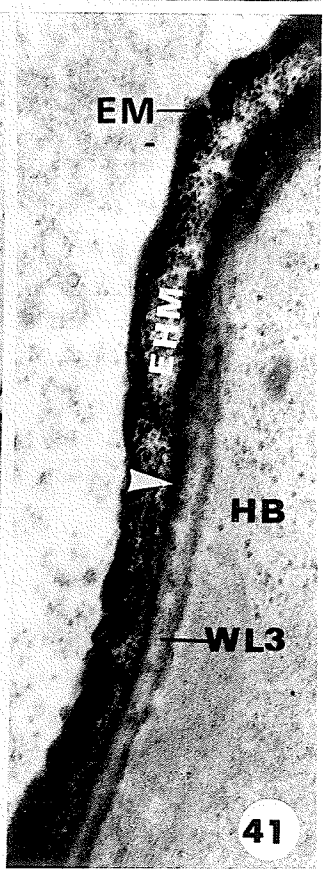
EM
FRM
HB
WL3
41

a fixation artifact. However, when haustoria present in fresh-frozen tissue sections were examined using phase contrast microscopy, a region corresponding to the EHM was observed (Fig. 38, arrows). The EHM seemed to reach its widest point at the distal end of the haustorium (Fig. 39, arrowhead) and tapered somewhat towards the neck. The contents of the EHM may be either homogeneous (Fig. 42) or heterogeneous (Fig. 43) in appearance when stained with UA/PbC, though this difference may be an artifact of fixation.

In the distal portions of the haustorial body the EHM occupied the same relative position to wall layers 2 and 3 as did WL4 in the proximal region of the haustorial body and neck. Indeed the EHM may well represent a modified extension of the outer neck layer (WL4). As previously noted, WL4 stained intensely with PACP to a point just beyond the septum (Figs. 39 region A, and 28). Then more distally, this region became less uniform and appeared to merge with, and become indistinguishable from, the EHM (Fig. 40 arrow and proximal portion of region B, Fig. 39). The material in the EHM, like that in WL4 was PACP positive in Glut/OsO_4 fixed tissue (Fig. 40), and also reacted positively without prior oxidation with periodic acid, although WL3 was only lightly stained (Fig. 41). When unosmicated sections were stained with PACP, the material in the EHM showed a reduced reaction (Fig. 44) much as it did in WL4 of the haustorial neck (Fig. 34). However, prior oxidation in H_2O_2 resulted in a lack of staining in the EHM (Fig. 45). With the exception of the latter treatment, PACP staining

Legend

Figures 42-43. Transmission electron micrographs of the extrahaustorial matrix.

Figure 42. The EHM appears to stain in a homogeneous fashion. Glut/OsO_4. UA/PbC. X40000.

Figure 43. The EHM appears to stain in a heterogeneous fashion. Glut/OsO_4. UA/PbC. X46000.

Figures 44-47. Cytochemistry of the extrahaustorial matrix.

Figure 44. PACP staining of unosmicated material results in a reduction of staining in the EHM and no staining of WL3. PACP positive material is evident juxtaposed with WL3 (arrowhead) and the EM (arrow). Glut. PACP. X46000.

Figure 45. Oxidation in H_2O_2 prior to staining in CP results in no evident staining of WL3 or the EHM. Glut/OsO_4. H_2O_2 - CP. X46000.

Figure 46. Material in the EHM reacts positively to Thiery staining after 0.2 h incubation in TCH. Glut/OsO_4. PA-TCH-SP. X46000.

Figure 47. Increasing the time of incubation in TCH to 14 h fails to produce a dramatic increase in Thiery staining of the EHM. Glut/OsO_4. PA-TCH-SP. X30000.

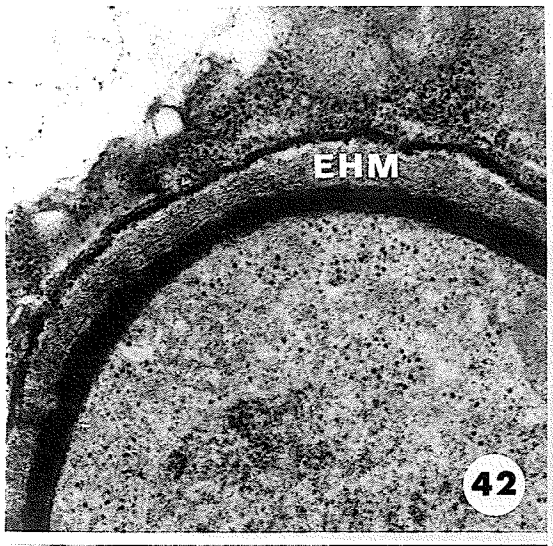
EHM
42

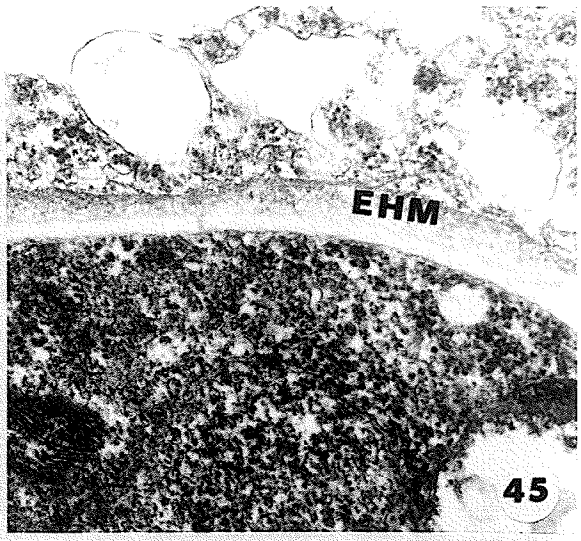
EHM
45

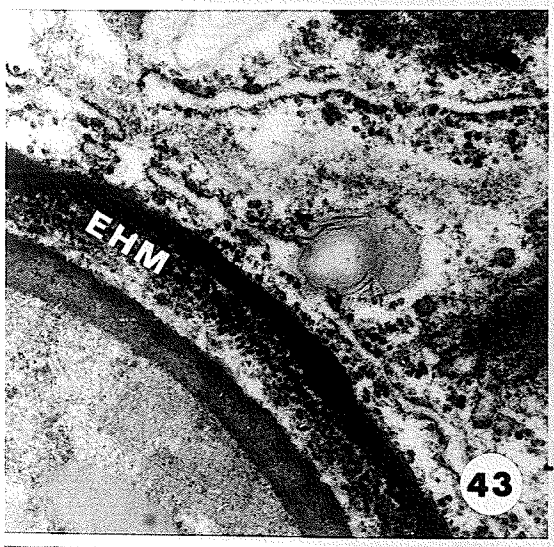
EHM
43

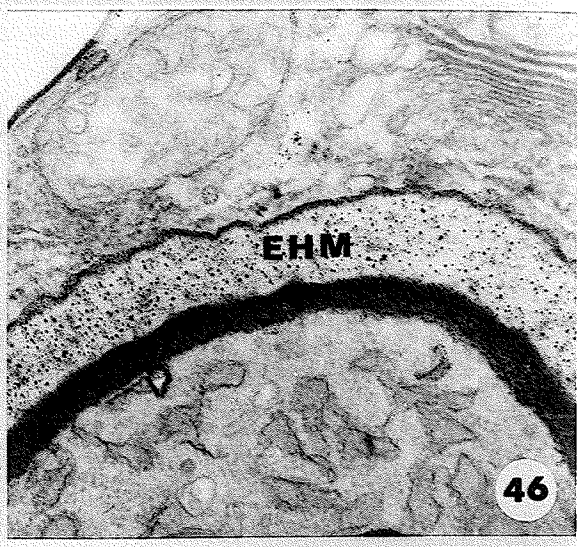
EHM
46

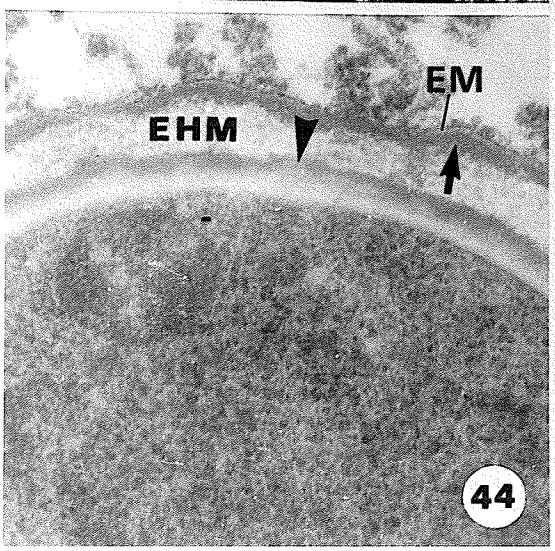
EHM
EM
44

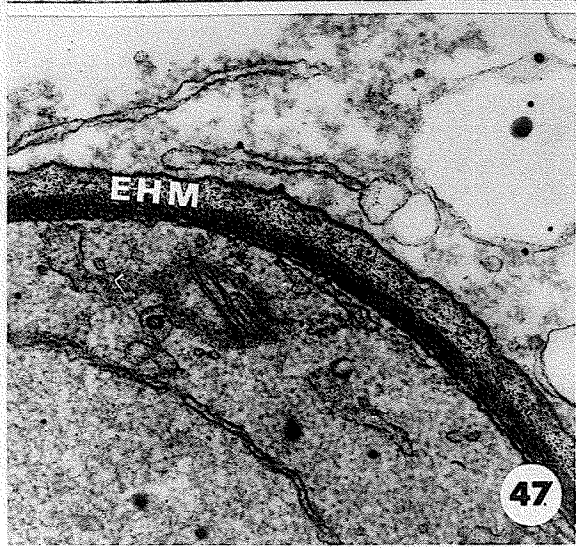
EHM
47

also suggested that a second wall layer was present in the distal portions of the haustorial body adjacent to WL3 (Figs. 41 and 44, arrowheads), and sometimes adjacent to the EM (Fig. 44, arrow) possibly representing remnants of WL4 of the haustorial neck.

The material of the EHM also reacted positively to PA-TCH-SP staining (Fig. 46), and increasing the time in TCH to 14 hours did not result in any noticeable increase in staining (Fig. 47). This would indicate that initially most of the reaction sites were neither complexed nor highly branched and were therefore bound after 0.25 hours in TCH. The presumptive polysaccharide in the EHM did not appear to be cellulose, as a decrease in PA-TCH-SP staining was not evident in cellulase-treated tissue (Fig. 48).

When tissue fixed in Glut only was subjected to PA-TCH-SP, a reduction in staining was evident in the EHM (Fig. 49). This decrease in stain intensity indicated that fatty acids were present in the EHM and were partly responsible for the positive reaction to silver proteinate. This was confirmed by the positive reaction of WL3 and the EHM to the Thiery reaction where periodic acid had been omitted from the procedure (Fig. 50); this latter treatment was found to be indicative of fatty acids (Chong et al. 1981).

Controls for the PA-TCH-SP reaction generally resulted in an absence of staining. No staining was evident in starch grains when periodic acid was omitted (Fig. 51), although lipid bodies and fungal wall (arrow) still showed a positive reaction (Fig. 52). Starch grains also failed to react when sodium borohydride was used to block aldehydes produced by periodic acid oxidation (Fig. 53,

Legend

Figures 48-50. Controls for Thiery staining of the EHM.

Figure 48. Cellulase treatment fails to reduce Thiery staining of the EHM. Glut - cellulase - OsO_4. PA-TCH-SP. X52000.

Figure 49. The EHM shows only a limited reaction when unosmicated material is subjected to Thiery staining. Glut. PA-TCH-SP. X46000.

Figure 50. The EHM as well as WL3 show a slight reaction to Thiery staining when periodic acid is excluded from the procedure. Glut/OsO_4. TCH-SP. X52000.

Figures 51-54. Controls for Thiery staining.

Figure 51. No staining is evident in starch gains without prior oxidation in periodic acid. Glut/OsO_4. TCH-SP. X40000.

Figure 52. Fungal walls (arrow) and lipid bodies (L) show a slight but positive reaction to Thiery staining without prior oxidation in periodic acid. Glut/OsO_4. TCH-SP. X48000.

Figure 53. Starch grains fail to stain after aldehyde blockage, although plastoglobuli stain intensely (arrowheads). Glut/OsO_4. PA - sodium borohydride - TCH-SP. X24000.

Figure 54. Elimination of TCH from the procedure results in a complete absence of staining in both lipid bodies (L) and the fungal wall (arrow) Glut/OsO_4. PA-SP. X29000.

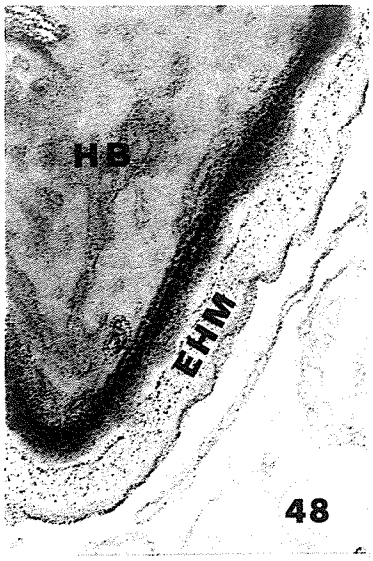
HB
EHM
48

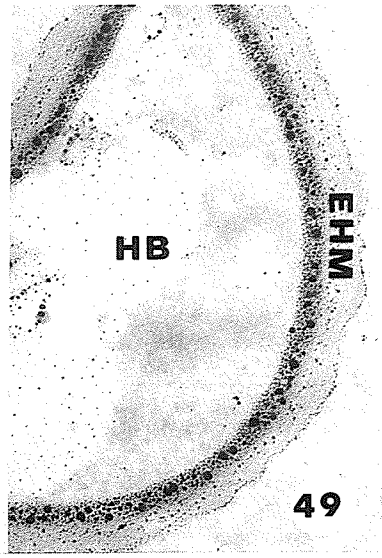
HB
EHM
49

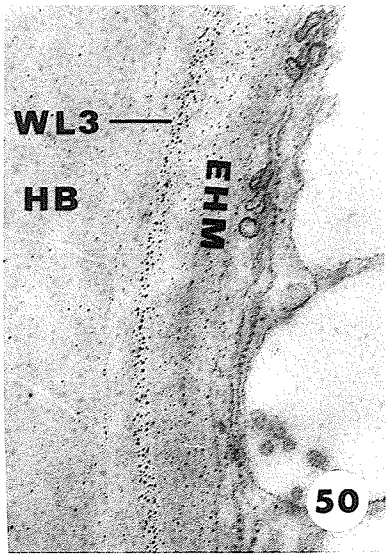
WL3
HB
EHM
50

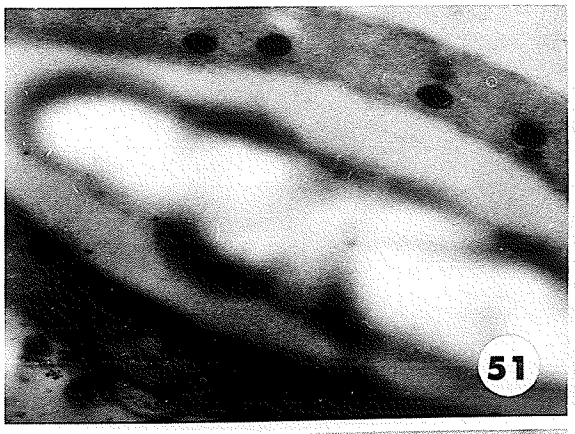
51

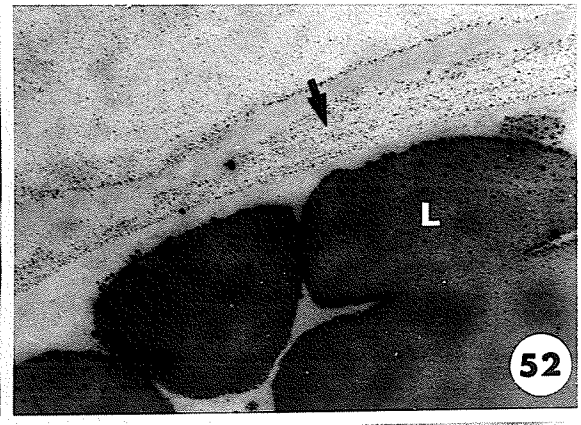
L
52

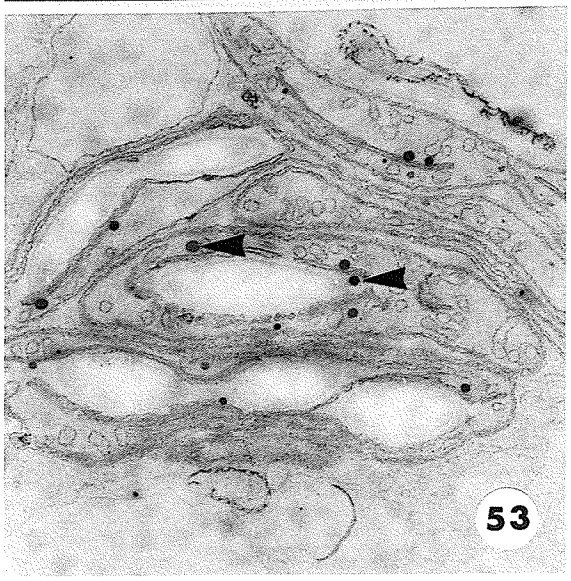
53

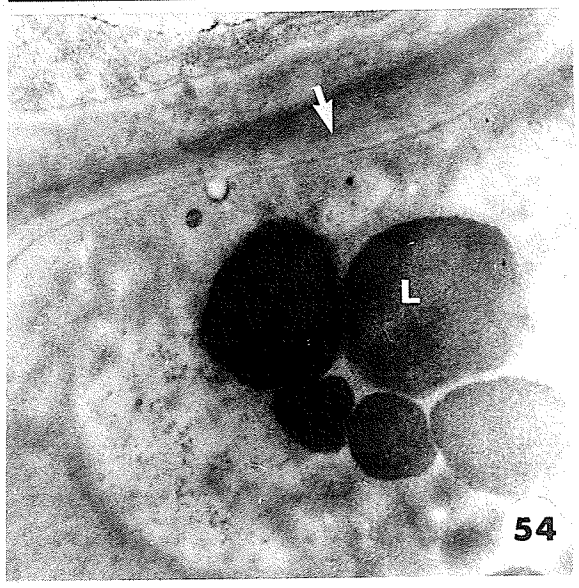
L
54

Legend

Figures 55-57. Gold-bound wheat germ lectin (WGL) binding to fungal walls.

Figure 55. WGL receptor sites are evident in the inner haustorial wall layers and septum (S) but not WL4. Glut. WGL - gold. UA. X47000.

Figure 56. WGL binding is evident in the inner walls and septum (S) of the intercellular hyphae but not in the outer AL. Glut. WGL - gold. UA. X47000.

Figure 57. WGL receptor sites are not evident in the EHM. Glut. WGL - gold. UA. X58000.

Figure 58. Hapten controls for wheat germ lectin binding to fungal walls.

Figure 58. Incubation in a chitin hydrolysate results in an absence of WGL-binding in WL3. Glut. Hapten - WGL - gold. UA. X58000.

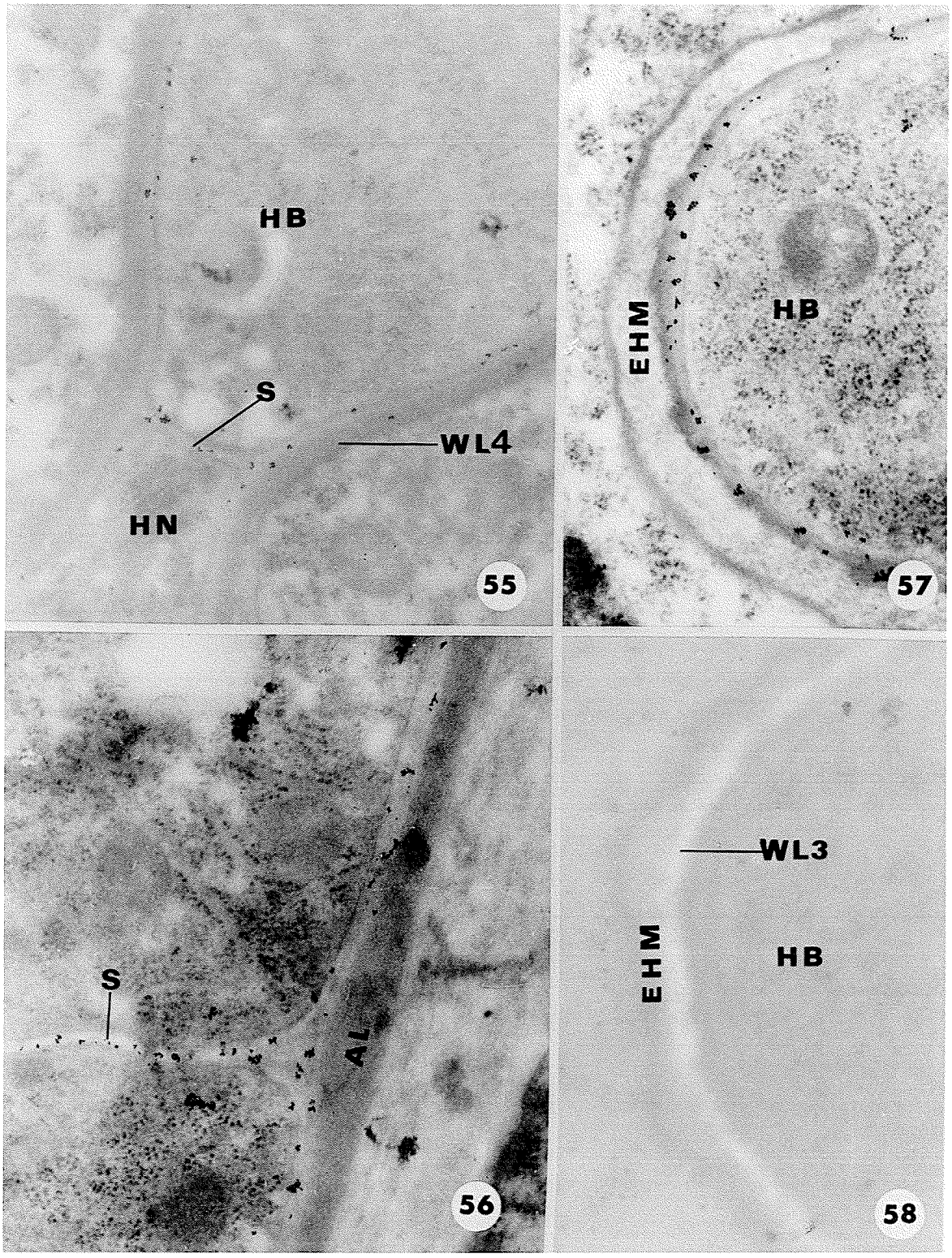
HB
S
WL4
HN
55
EHM
HB
57
S
AL
56
WL3
EHM
HB
58

arrow), although plastoglobuli in the chloroplasts stained after aldehyde blockage (Fig. 53, arrowheads). When TCH was eliminated from the procedure (i.e. PA-SP) there was also a total absence of silver staining in both lipids and fungal wall (Fig. 54, arrow); a similar lack of reactivity occurred when silver proteinate was eliminated (i.e. PA-TCH).

The controls suggested a specificity for polysaccharides and other glycosubstances with vicinal hydroxyl groups, although it was evident that some fatty acids react with the stain. However lipid solvent extraction is still required to confirm this.

Staining with PACP has been suggested as a selective stain for plant plasma membranes (Roland et al. 1972) and may demonstrate alterations in the plasmalemma of infected host cells (Littlefield and Bracker 1972). When so treated, the invaginated host plasmalemma (EM) was densely stained (Fig. 39); conversely the remainder of the host plasmalemma either remained unstained (Fig. 39) or, in some cases, was only lightly stained. This differing response to PACP may suggest a degree of specialization in the EM.

M- haustoria are not known to possess neck rings; the latter are postulated to prevent apoplastic flow along the neck wall (Heath 1976), and none are apparent in E. harknessii. However, if the haustorium is to serve as a highly specialized organ of nutrient absorption, a barrier to apoplastic transport must exist in the haustorium of this rust. Though the EM was loosely associated with the proximal portion of the neck, a tight junction between this membrane and the outer wall layer of the haustorial

neck was often observed near the haustorial septum (Fig. 59, arrow). As already noted, near the haustorial septum, WL4 appeared quite discrete, and perhaps this layer serves as a barrier to apoplastic transport in a manner analogous to a neck ring. This could occur provided that a tight association between the haustorial neck and the EM exists. In a further attempt to identify a functional neck-ring analogue, tissue was subjected to plasmolysis in a sucrose solution prior to fixation and infiltration. This resulted in a clear separation of the host cell plasmalemma from the host wall (Fig. 60, arrows), but the EM remained closely juxtaposed to the haustorium. It was evident that the EM was no longer directly attached to WL4 as depicted in Figure 59, but it is interesting to note that even after plasmolysis in sucrose solution, the association between the haustorium and the surrounding membrane still existed.

Some indirect evidence of the existence of this barrier to apoplastic transport is provided by the use of the fluorochrome SITS. It is believed this stain is transported via the apoplast, will label the plasma membrane, but will not enter the symplast (Maddy 1964), although it would also appear to stain fungal walls (Heath 1976). Therefore the fluorochrome should not stain haustoria unless they are open to the apoplast. Figure 61 shows a ruptured, infected host cell, exposed to SITS, within which is a strongly fluorescent haustorium (arrow). When intact cells were exposed to SITS, no fluorescence of the haustorium was observed (Fig. 62, arrow) though phase-contrast microscopy showed a haustorium to be present in the same cell (Fig. 63, arrow). The fluorochrome did,

Legend

Figures 59-60. Transmission electron micrographs of the association between the haustorial neck and the extrahaustorial membrane.

Figure 59. A tight junction is evident between WL4 and the EM (arrow). Glut/OsO_4. UA/PbC. X72000

Figure 60. Plasmolysis of the tissue prior to fixation results in a separation of the plasmalemma (arrows) from the host cell wall (CW). The EM however, remains associated with WL4 of the haustorial neck. Glut/OsO_4. UA/PbC. X32000.

Figures 61-63. Light microscopic photographs of fresh tissue incubated in SITS, showing a possible functional neck band.

Figure 61. The haustorium (arrow) contained within a ruptured host cell fluoresces brilliantly when exposed to SITS. Unfixed material. Fluorescence microscopy. X1000.

Figure 62. A haustorium (arrow) contained within an intact host cell fails to fluoresce in contrast to the HMC in the intercellular space. Unfixed material. Fluorescence microscopy. X1000.

Figure 63. Micrograph showing the position of the haustorium (arrow) in the intact cell shown in Fig. 62. Phase contrast microscopy. X1000.

Figures 64-65. Controls for aniline blue staining.

Figure 64. The haustorium fails to fluoresce after treatment with a Beta-1, 3 glucanase, prior to aniline blue staining. Unfixed material Fluorescence microscopy. X1000.

Figure 65. Micrograph showing the position of the haustorium from Fig. 64. Phase contrast microscopy. X1000.

Figures 66-67. Nile blue staining of unfixed fungal material.

Figure 66. Lipid bodies are evident in the intercellular hyphae (arrows) but there is no evidence of fluorescence in the haustorium. Unfixed material. Fluorescence microscopy. X1000.

Figure 67. Micrograph showing the position of the haustorium in fig. 66. Phase contrast microscopy. X1000.

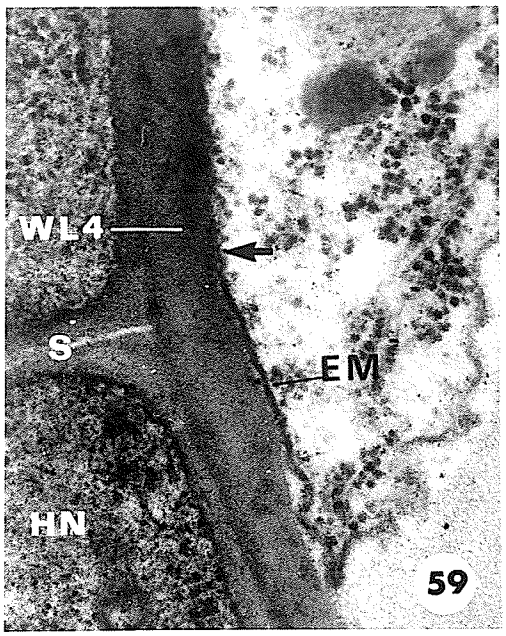
WL4
S
EM
HN
59

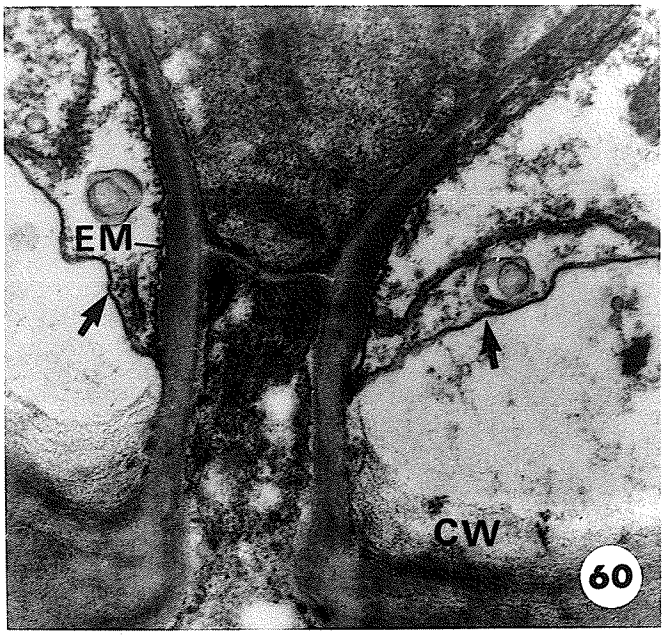
EM
CW
60

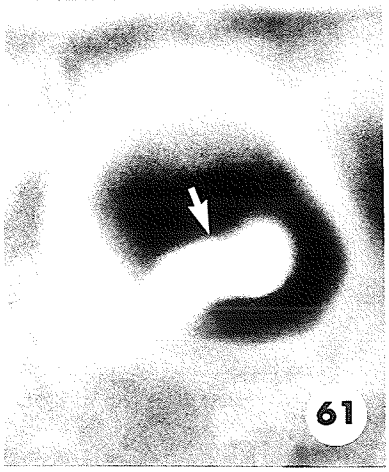
61

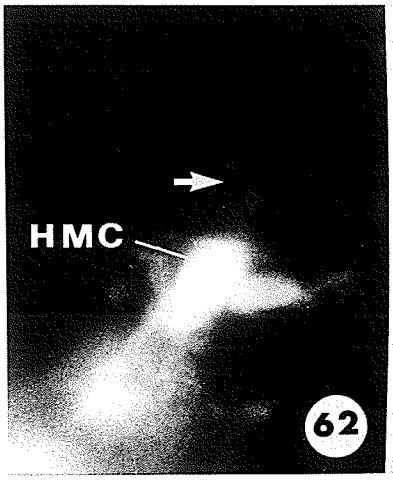
HMC
62


63

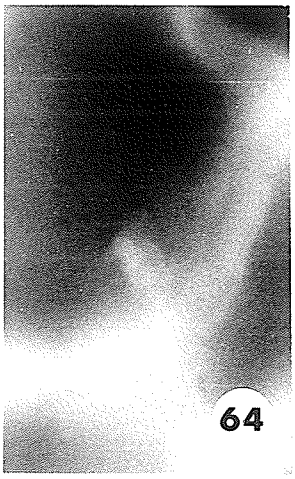
64


65

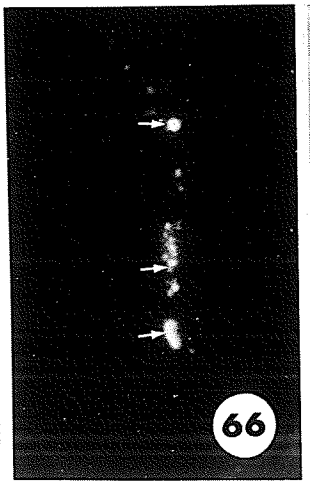
66

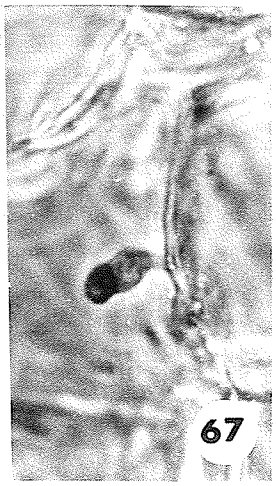
67

however, stain the mother cells located in the intercellular spaces (Fig. 62).

Wheat germ lectin (WGL) conjugated to colloidal gold is often used to detect the presence of chitin in fungal walls. Wheat-germ-lectin receptor sites were observed in the inner haustorial wall layers and septum, but not in WL4 (Fig. 55). Generally, receptor sites for WGL were not observed in the haustorial neck, but as the binding of WGL in this work was not consistent in all areas of the haustorium, no conclusion can be drawn regarding the presence of such sites in the neck. Wheat germ lectin was also bound to the inner walls and septa of the intercellular hyphae but not in the outer AL(Fig. 56). At the distal end of the haustorial body gold-bound WGL was observed in the fungal wall (WL3), but not in the EHM (Fig. 57). The results of this test did not distinguish between the two inner wall layers of either the haustorium or the intercellular hyphae, but it did support earlier evidence which suggested a specialized nature to the outer wall layer. Hapten controls resulted in the inhibition of WGL binding (Fig. 58) confirming the specificity for chitin or glycosubstances containing N-acetylglucosamine residues.

Fluorescence microscopy was also employed to investigate the nature of the haustorium of E. harknessii. However, to avoid possible complications from the use of chemical fixatives, fresh tissue was sectioned on a freezing microtome and then treated with the appropriate fluorochromes.

Sections treated with aniline blue, a fluorochrome believed to show some specificity for beta-1, 3 linkages (Fulcher and Wong 1980), showed a positive reaction in the distal portion of the haustorium (Fig. 68, arrow). It is this region of the haustorium which corresponds to the EHM (Fig. 38, arrows), and the positive reaction suggests beta-1, 3 glucans were present. Prior to staining with aniline blue, some sections were subjected to the PAS reaction to increase the fluorochrome's specificity (Smith and McCully 1978). This should have blocked any 1, 4 or 1-6 linked glucans that might have fluoresced with aniline blue, and a less intense but still positive reaction did occur in the distal haustorial body (Fig. 69, arrow). Some tissue was subjected to beta-1, 3 glucanase (lyticase), prior to staining with aniline blue, and fluorescence did not occur (Fig. 64), although mature haustoria were evident with phase contrast microscopy (Fig. 65).

When stained with calcofluor white, the entire haustorium as well as the intercellular hyphal elements fluoresced strongly (Fig. 70). This fluorochrome is known to react strongly with cell wall glucans of mixed linkage (Fulcher and Wong 1980), and was confirmed by staining epoxy embedded tissue with PAS reagent. This resulted in the haustorial wall staining red (Fig. 71), indicative of polysaccharides (O'Brien and McCully 1981). However, the region corresponding to the AL of the mother cell did not react to PAS reagent (Fig. 71, arrow) suggesting, as did PA-TCH-SP staining, that polysaccharides were not a major component of this wall layer.

Both the haustoria and intercellular hyphae reacted positively to ANS(Fig. 72), indicating protein presence (Fulcher and Wong 1980). This was confirmed by staining epoxy embedded sections in aniline blue black (Fig. 73, arrow), which is also a protein indicator (Jensen 1962).

An aqueous solution of Nile blue was also used to detect storage lipids. The results obtained with this stain indicated the presence of lipid bodies throughout the intercellular hyphae (Fig. 66, arrows). However, fluorescence was not evident where the haustorium was positioned (compare with Fig. 67, phase contrast micrograph indicating the position of the haustorium). On occasion, lipid bodies were also observed in the haustorium, but this was uncommon, and generally appeared to be associated with senescing haustoria.

Legend

Figures 68-73. Fluorescence and bright field microscopy of haustoria.

Figure 68. Aniline blue staining of fresh material results in the fluorescence of the distal portion of the haustorial body (arrow). Unfixed material. Fluorescence microscopy. X1200.

Figure 69. Treatment of fresh tissue with PAS reagent prior to staining with aniline blue results in a reduced but positive reaction in the distal portion of the haustorium. Unfixed material. Fluorescence microscopy. X1200.

Figure 70. Staining of fresh tissue with calcofluor white results in the fluorescence of the haustorium and intercellular hyphae. Unfixed material. Fluorescence microscopy. X1200.

Figure 71. PAS staining of epoxy-embedded tissue shows the haustorium and the inner walls of the HMC stain the characteristic red. The region corresponding to the AL remains unstained with this treatment. Bright field microscopy. X1500.

Figure 72. Staining of fresh material with ANS results in yellow fluorescence of the haustorium and intercellular hypha. Unfixed material. Fluorescence microscopy. X1200.

Figure 73. The haustorium (arrow) as well as the HMC reacts positively to aniline blue black in acetic acid. Bright field microscopy. X1500.

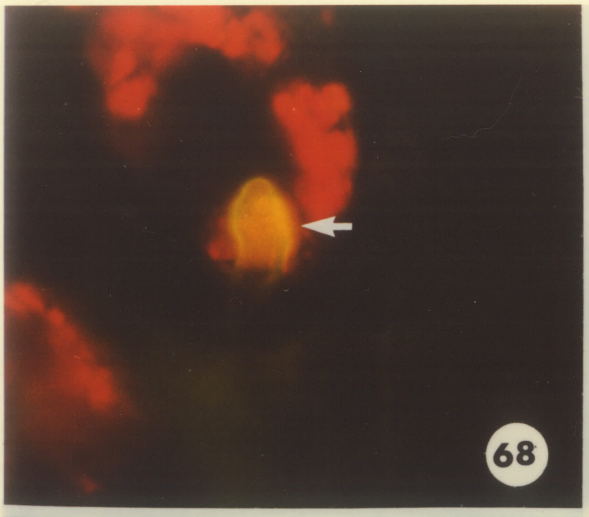
68

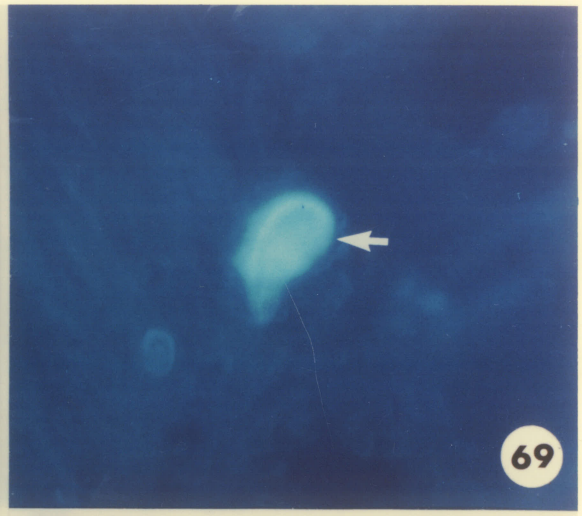
69

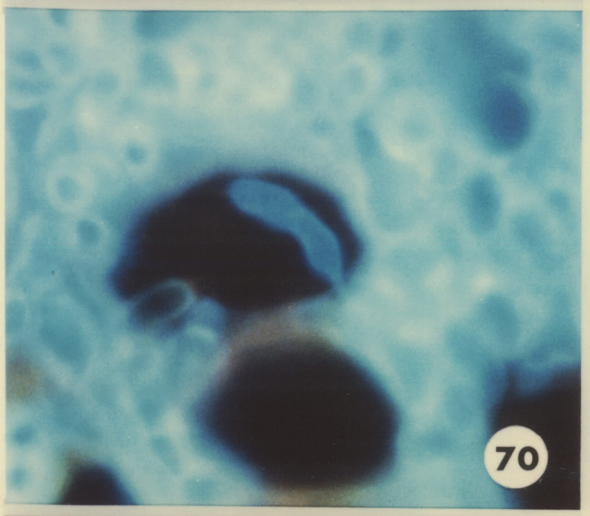
70

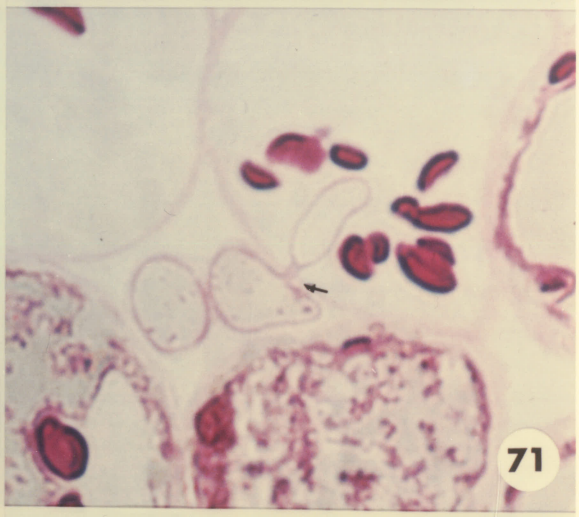
71

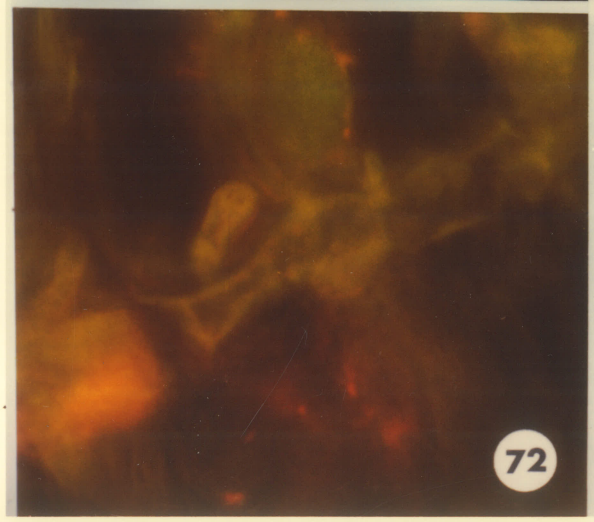
72

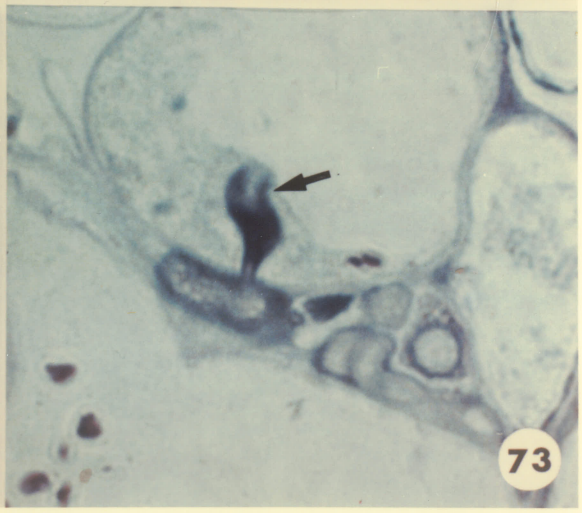
73

DISCUSSION

This is the first report on the ultrastructure of the haustorium of E. harknessii and, as such, provides preliminary information on the chemical nature and degree of specialization of this structure.

M-haustoria are generally believed to possess little of the structural specialization found in D- haustoria; indeed many authors consider them to be simply unaltered hyphae that terminate within host cells (e.g. Harder and Chong 1984). Neither the haustoria of E. harknessii, nor the monokaryotic hyphae which produced them, ever possessed more than a single nucleus; this is also true for most reports on M- haustoria. However, in possessing a constricted neck region and an expanded haustorial body, the haustoria of E. harknessii morphologically more closely approximate those reported for D- haustoria, than they do the typical descriptions of hypha-like M- haustoria. These apparently more morphologically specialized M- haustoria are similar to those of two other tree rusts, C. quercuum (Gray et al. 1982) and P. pini (Walles 1974), both of which are probably closely related to E. harknessii. However histochemical studies have not been reported on for C. quercuum or P. pini, and therefore their degree of similarity to E. harknessii cannot be fully determined.

The haustorial septum found in E. harknessii is typical of those described for the M- haustoria of other rusts. However in this rust it was always located in the haustorial neck near the

region of host cell penetration, while in other rusts such as Puccinia coronata avenae (Chong et al. 1981; Harder 1978), P. sorghi (Rijkenberg and Truter 1973), Uromyces appendiculatus (Gold and Mendgen 1984b), the M- haustoria possess septa occurring at any point in the intracellular body, resulting in a hypha-like appearance.

Similar to other M- haustoria that have been described, the structure of the septum and its pore apparatus resembled that found in intercellular hyphae, at least when test material was stained with UA/PbC; this is one reason why some authors believe M- haustoria are merely intracellular hyphae. However while certainly not conclusive, there is some histochemical evidence which suggests differences may exist between the haustorial septum of E. harknessii and those found in the hyphae. The haustorial septum possessed a silver proteinate positive wall layer continuous with the central electron lucent layer. This silver proteinate reactive component was not present in the hyphal septa examined, and may be evidence of a greater degree of specialization in the haustorial septa.

Amongst Uredinales and Ascomycetes, both the septal and pore apparatus appear fairly consistent. The pulley-wheel shaped plugs of E. harknessii are similar to those described in C. quercuum (Khan and Kimbrough 1982) and P. pini (Walles 1974). While Walles believed the septal plugs were Woronin bodies, the lack of any apparent bounding membrane surrounding the plugs in E. harknessii makes such an assumption questionable in this fungus; further,

Woronin bodies are considered to be unique to Ascomycetes (Bracker 1967). Walles also observed a granular ribosome-free area around the haustorial septum in P. pini which was not apparent in E. harknessii. However this latter region was organelle free as reported by Littlefield and Heath (1979).

Histochemical tests showed that the septal plugs were of uniform composition throughout the mycelium. Evidence obtained from PACP and PA-TCH-SP staining of both glutaraldehyde and glutaraldehyde/osmium tetroxide fixed material suggested that the plugs were neither carbohydrate nor lipid in composition. Chong (1981) demonstrated that the septal plugs of P. coronata avenae were proteinaceous, and possibly analogous to the p- protein found in sieve plates of higher plants. In this study, treatment with protease was unsuccessful, and no extraction was evident in either the host or fungal tissues. This probably resulted from poor infiltration of the hypocotyl tissues by the enzyme, although this was attempted on a number of occasions. However, since as noted above both PACP and PA-TCH-SP staining indicated an absence of carbohydrates and lipids in the plug, it is possibly composed of protein.

Conventional staining revealed that the intercellular hyphal walls of E. harknessii consist of up to three layers. Typically, ultrastructural studies have shown rust hyphae to be composed of only two layers; an amorphous outer layer, and a more defined inner wall. However Longo et al. (1982) reported that the intercellular hyphae of C. flaccidum possessed two discrete wall layers plus an

outer capsular sheath, the latter analogous to the amorphous layer. Subsequently Chong *et al*. (1985) using histochemical techniques showed that the hyphal wall of *P. graminis tritici* possessed four wall layers.

In *E. harknessii* the inner wall layer adjacent to the plasmalemma was not consistently observed, and more refined techniques such as freeze substitution may be necessary to determine the extent of this layer in the mycelium. It was also unclear whether this layer was restricted to the intercellular hyphae, as it was not observed in the haustoria. The adjacent middle layer, (WL2) which was always present, was moderately reactive to PA-TCH-SP staining, although prolonged periods of section incubation in TCH were required to achieve maximal staining; this suggests that the middle layer is composed of complex carbohydrates. The outermost layer of the intercellular hyphae was amorphous in appearance and merged imperceptibly with the host cell wall, possibly indicating a degree of functional integration as suggested by Coffey (1983). Some authors (Hardwick *et al*. 1971; Rijkenberg and Truter 1973; Walles 1974) have suggested that such a layer plays a role in the adhesion of hyphae to the host cell wall, while others (Welch and Martin 1974) feel it may function in nutrient uptake by intercellular hyphae. However, both the large number of haustoria produced by *E. harknessii* and their apparent specialized nature would suggest that nutrient uptake by the systemic mycelium is primarily through the haustorium, and the most probable function of the outer layer is one of adhesion.

The absence of PA-TCH-SP staining of the amorphous layer in unosmicated tissue indicated that polysaccharides with vicinal hydroxyl groups were not major components of this layer. The limited reaction to silver proteinate of this region when postfixed in osmium tetroxide would suggest fatty acids are responsible for PA-TCH-SP staining in this region. In contrast to the inner wall layer, this amorphous layer also lacked chitin. Chong et al. (1985) made a similar observation with respect to P. graminis tritici, although they noted binding of Con-A, indicating the presence of polysaccharides with alpha linked non-reducing terminal ends. The amorphous layer of E. harknessii reacted strongly to PACP staining; this has been reported for other rusts (e.g. Littlefield and Bracker 1972).

The use of the term wall layer to denote the outer amorphous layer may be contentious. However, although its composition is uncertain, most authors believe it is secreted by the fungus, and this study shows it differs from the other fungal wall layers. Moreover the results of the cellulase treatments indicated this layer was distinct from the host and, as it was continuous with the hyphae, the term wall layer has been used.

PA-TCH-SP staining provided strong evidence that three discrete wall layers existed in the haustorial neck; this was less evident in UA/PbC stained material. The three layers each displayed a different reaction to the combination of tests which were employed in this study.

The inner layer adjacent to the fungal plasmalemma was continuous with the haustorial mother-cell wall, and of similar thickness thereto throughout the region of penetration. This is typical of M- haustoria, and is reported as a feature distinguishing M- haustoria from D- haustoria (Littlefield and Heath 1979). However, the discovery in this study that there was an initial reduction in the thickness of this layer in the distal portion of the neck, which was then further reduced throughout the haustorial body, is not typical of earlier reports of M- haustoria. The adjacent middle layer stained much more intensely with silver proteinate than the inner layer after brief incubation in TCH. This suggests the middle layer was composed of simple polysaccharides, and the use of an aldehyde blocking agent which greatly reduced the staining, confirmed the presence of the carbohydrates, residual staining being due to the presence of fatty acids.

The inner wall layer required a longer exposure to TCH than did the middle layer for maximal staining to occur, and this indicates it contained complex carbohydrates. It also appeared to react more strongly with PACP in contrast to the very slight reaction of the middle layer with this stain, thus confirming the difference in composition between these layers.

This differential staining of the two inner wall layers of the haustorial neck contrasts to that reported for the M- haustoria of P. coronata avenae by Chong et al. (1981). They found that PA-TCH-SP treatment caused intense but apparently regular staining

of all fungal walls, including those of the haustorial neck; the fungal wall apparently consisted of a single layer. This latter situation may be more typical of M- haustoria in general than those of E. harknessii, although there is scant literature on which to base such an assumption. However, the fact that in E. harknessii there appeared to be differences in the staining of the two inner layers, and that the middle layer appeared to be unique to the haustorium of this rust, suggests that the haustorium of E. harknessii is a specialized structure and not merely an intracellular hyphal element.

After PA-TCH-SP staining of unosmicated tissue, it was not clear whether the outer wall layer of the haustorial neck was continuous with the analogous region of the intercellular hyphae. However from observations of early stages in haustorial development, there is evidence that this layer originated from the amorphous layer surrounding the haustorial mother cell (Chapt. 1). It was also evident from the use of PA-TCH-SP and PACP staining as well as gold-bound wheat-germ lectin, that these two regions are of similar composition in possessing lipids but not polysaccharides or chitin.

PACP staining of the neck region of haustoria has been reported proximal to the neck band in M. lini (Littlefield and Bracker 1972), and through the neck region of the oomycete Albugo candida (Woods and Gay 1983); the latter authors suggested this represented a specialized region of the neck which corresponded to a functional neck band. The intense and continuous staining of the

neck region of E. harknessii may indicate some similarity with the neck regions of these fungi. However, staining with PACP must be interpreted with caution as various authors have suggested the stain is specific for different compounds, further, Hall (1978) has pointed out that the mechanism of staining is poorly understood. Also Chong et al. (1981) reported that while both the neck wall of the D- haustorium of P. graminis tritici and middle layer of the haustorial mother cell stained uniformly with PACP, further tests showed the two regions differed in composition. The results of Chong et al. (1981) as well as those obtained in this study raise doubts as to the specificity of this stain.

The outer wall layer of both the neck and intercellular hyphae stained with equal intensity regardless of whether periodic acid oxidation preceded staining with PTA in chromic acid. This implies that the stain does not bind selectively to polysaccharides with vicinal hydroxyl groups. However if, prior to staining, the tissue was oxidized with hydrogen peroxide which removes osmium but does not specifically oxidize glucans, only ribosomes stained.

Regardless of the similarities in staining, the more well defined nature of the outer wall layer of the haustorial neck in E. harknessii contrasts with the amorphous appearance of that layer on the hyphae, and might indicate some functional differences. While the hyphal outer wall (AL) is considered to be fungal in origin (Littlefield and Heath 1979), the corresponding region of the haustorial neck is considered by some authors to be part of the extrahaustorial matrix, which they believe to be of host origin

(Gray et al. 1982; Robb et al. 1975b). An outer wall layer was evident in the D- haustorial necks of Puccinia helianthi (Coffey et al. 1972) and Uromyces phaseoli vignae (Heath and Heath 1971), and in both of these cases the authors considered this layer to be host derived. Heath (In Littlefield and Heath 1979) provided further evidence of a host origin of the outer layer in haustoria, when she reported that this region disperses when the bounding membrane fragments in certain incompatible reactions. However, in E. harknessii, this layer remained intact and attached to the other fungal wall layers when the surrounding host cell wall material was removed by cellulase.

While histochemical evidence suggests there are similarities between the outer haustorial neck wall and the extrahaustorial matrix, the presence of carbohydrates in this region, indicated by PA-TCH-SP staining of unosmicated tissue, shows some differences do exist between these regions. Although the extrahaustorial matrix of the rusts has been the subject of much speculation, the composition of this region is still uncertain as few diagnostic investigations of it have been undertaken. The results of this study indicated the presence of lipids, polysaccharides, and a PACP positive material, possibly glycoprotein, in the matrix of E. harknessii.

Chong et al. (1981), and Hickey and Coffey (1978) reported the presence of cellulose in the extra haustorial matrices of P. coronata avenae and Peronospora pisi, respectively, implying a host origin, but cellulose did not appear to be present in the

extrahaustorial matrix of E. harknessii. Chong et al. (1981) also demonstrated the presence of protein, but not lipid, in P. coronata avenae, and similar findings are reported by Rohringer et al. (1982) for P. graminis tritici. Conversely, the extrahaustorial matrix of E. harknessii showed some staining in TCH-SP controls, probably due to the presence of unsaturated fatty acids similar to those evident in wall 4 layer of the haustorial neck. Because protease treatment was not successful in this study, it is uncertain whether protein is a component of the extrahaustorial matrix, but the haustorial walls did show evidence of protein as indicated by ANS fluorescence.

The extrahaustorial matrix in most rust/host systems is generally believed to be of host origin. In the majority of those examined, only the innermost wall layer adjacent to the fungal plasmalemma in the haustorial body is considered to be fungal wall; the remaining portion between this and the extrahaustorial membrane being the matrix. However, Heath and Heath (1971) and Erlich and Erlich (1970) reported on the occurrence of a second, fibrillar, haustorial wall layer adjacent to the inner layer. In E. harknessii a similar zone positioned adjacent to the extrahaustorial membrane was often evident after PACP staining; this zone also resembled the zone of apposition described for Peronospora parasitica (Fr.) Tul., which is believed to be "an integral part of the haustorial wall" (Chou 1970).

Coffey et al. (1972) suggested that the extra-

haustorial matrix of Melampsora lini originated as a result of fragmentation of a fungal wall but, in a subsequent paper, Coffey et al. (1976) implied a host origin of this region. While difficult to prove, the evidence obtained in this study could be interpreted as demonstrating that the extrahaustorial matrix of E. harknessii is of fungal origin. Assuming that the outer wall of the intercellular hyphae and haustorial neck are produced by the rust, the similarity in staining of the neck and matrix would suggest a common origin. However, considering the nature of the extrahaustorial matrix and its probable function as the zone across which nutrients pass, it is likely that the host material also partially contributed to the development of the matrix.

The appearance of beta-1,3 glucans surrounding the haustorium of E. harknessii, as denoted by aniline blue fluorescence, appears to be unique. Such fluorescence has been reported by other workers (e.g. Coffey 1976), but was attributed to haustorial encasements which occur in incompatible host/rust interactions. In E. harknessii, this fluorescence appeared to be a common property of mature haustoria in a compatible reaction. Although aniline blue fluorescence must be interpreted with caution (Smith and McCulley 1978), the fact that it was evident after pretreatment with periodic acid-Schiffs reagent, and was eliminated after extraction with a beta- 1,3 glucanase, strongly suggested the presence of beta- 1,3 glucans. The appearance of this polymer in the matrix may represent an unsuccessful attempt by the host to wall off the haustorium as a non-specific response by plants to wounding (Currier 1957).

Hickey and Coffey (1978) using a beta- 1,3 glucanase reported the presence of beta- 1,3 glucans in the haustorial walls of Peronospora pisi. However they did not note the occurrence of this polymer in the extrahaustorial matrix. Beta glucans with 1,3 and 1,6 linkages are widespread among the fungi as wall components (Griffin 1981), though to date, I am not aware of beta- 1,3 glucans having been demonstrated in the rust fungi.

The possibility of a barrier to apoplastic transport existing in the neck region of rust M- haustoria has not been reported previously. Though the evidence is not conclusive, the fact that the plasmalemma surrounding the haustorium was frequently observed closely adhering to the outer wall layer of the haustorial neck is suggestive of such a barrier. A slight separation between the plasmalemma and haustorial neck was also evident in plasmolyzed tissue. However, the association between the extrahaustorial membrane and outer neck wall was not completely disrupted as would be expected if the two regions were not attached in any manner. In conventionally fixed tissue, the plasmalemma is not always directly attached to the haustorial neck; however, the fact that the outer wall layer always appeared compact and never fibrillar at its edges, may be due to the close attachment of the plasmalemma in vivo. Thus the outer neck wall layer may serve as a barrier between the extrahaustorial matrix and host apoplast.

The existence of such a barrier should not be unexpected in any specialized biotroph. Obvious barriers to apoplastic transport are present in the form of neck rings in D- haustoria of rusts

(Littlefield and Heath 1979), and neck bands in powdery mildews (Gil and Gay 1977). The latter consists of lobed portions of the haustorial wall that contact and adhere to the extrahaustorial membrane. Woods and Gay (1983) and Coffey (1983) provided evidence of a functional neck barrier in the Oomycete Albugo candida (Pers.) Kuntze, although the former authors suggested that this barrier may not be as tight as in other specialized parasites; this is possibly the case in E. harknessii. Woods and Gay also demonstrated that regional specialization occurred in the neck of A. candida, and were able to demonstrate that the extrahaustorial membrane, unlike the non-invaginated portion of the host plasmalemma, was deficient in ATPase activity. These two regions of the plasmalemma join at the point on the neck which is believed to represent the functional neck band. A similar situation was reported for U.appendiculatus appendiculatus and Erysiphe pisi DC. ex Saint Amans (Spencer-Phillips and Gay 1981).

The extrahaustorial membrane of E. harknessii has not been tested for ATPase activity. However the results obtained with PACP staining indicate that differences may exist between this membrane and other portions of the host plasmalemma. While it has been suggested this stain is selective for plasma membranes (Roland et al. 1972), it is readily apparent that it does stain other materials. However, in E. harknessii the extrahaustorial membrane was intensely stained with PACP in contrast to the more lightly stained or unstained, non-invaginated portions of the host plasmalemma.

The differential intensity in staining of the various regions of the host plasmalemma described in this study, has counterparts in other studies e.g., in M. lini (Littlefield and Bracker 1972) and the M- haustorium of P. coronata (Chong et al. 1981). In the former case, the neck ring appeared to be the point of transition between the differently staining regions, but in both these cases it was the extrahaustorial membrane portion of the plasmalemma that remained unstained. Such evidence suggests that the point of transition between the PACP stained and unstained sections of the plasmalemma in E. harknessii, may occur along a zone analogous to a functional neck band.

The results obtained with SITS were similar to those reported by Heath (1976), but not as dramatic. Fluorescence of intercellular hyphae was reduced, and required in excess of 12 hours for the stain to infiltrate the material. A similar problem existed in enzyme treatments resulting in poor infiltration, apparently due to the nature of the host material. The fact that intercellular hyphae fluoresced would suggest transport of the fluorochrome through the apoplast. The failure of haustoria in intact host cells to fluoresce, in spite of the concomitant fluorescense of the attached intercellular mycelium, would suggest a barrier to apoplastic transport existed between inter- and intracellular portions of the rust.

C H A P T E R 3

HOST RESPONSES IN COMPATIBLE AND INCOMPATIBLE REACTIONS

Introduction

In compatible host/rust interactions the initial invasion of the host cell by the D- haustorium generally results in little disruption of the protoplasm. However some recent studies, Harder et al. (1978) and Chong and Harder (1982) noted alterations to the host endoplasmic reticulum system, and provided evidence of a continuity between the haustorium and the host ER. Other workers such as Al-Khesraji and Lösel (1980) observed a definite association between haustoria and host nuclei, and suggested some alteration of the nucleus occurred in infected cells. Preferential association between haustoria and other host organelles has not been proven, although some do appear to undergo changes after infection has occurs.

Most of the typical host responses to invasion by D- haustoria have not been reported for monokaryotic infections. This may imply, as other workers have suggested, a less specialized nature of the host/parasite relationship. However it may also reflect the fact that relatively few studies have been carried out on this portion of the rust life cycle. This is particularly true for microcyclic or endocylic rusts such as E. harknessii; therefore one purpose of this study is to report on observable host responses in apparently susceptible tissue.

Rust resistance mechanisms have been thoroughly studied in cereals and some dicotyledonous plants. However relatively little research has been conducted on the histology of rust resistance

mechanisms in pines, with the possible exception of the light microscopic studies dealing with C. quercuum fusiforme.

Western gall rust is a major problem in tree nurseries and intensively managed plantations in North America. Long term control of this disease would best be achieved through host resistance. However, before this can be accomplished, it is necessary to acquire a better understanding of effective resistance. As western gall rust is believed to infect seedlings only through susceptible tissue, effective forms of resistance might act to prevent the spread of the rust into more mature tissue. Work with C. quercuum fusiforme (e.g. Gray 1982) showed that juvenile seedlings may display forms of resistance analogous to that in the infectable portions of more mature seedlings. This study attempts to recognize such possible resistance mechanisms to western gall rust that may exist in such juvenile tissue.

RESULTS

A. Compatible Reactions

Mature haustorial bodies of E harknessii usually had abundant host endoplasmic reticulum, with associated ribosomes in close juxtaposition (Fig. 1); however this appeared to represent a redistribution of the host ER system, rather than an absolute increase in amount within the penetrated host cell protoplast. This endoplasmic reticulum followed the contour of the haustorial body (Figs. 1 and 2); in some cases it appeared to completely surround the latter. The cytoplasm about the haustorial body usually appeared quite concentrated, and contained large numbers of vesicles (Figs. 2 and 3) which, unlike the endoplasmic reticulum, were not specifically closely associated with the extrahaustorial membrane. Golgi bodies were also observed close to the haustorial body (Figs. 3 and 4) suggesting the vesicles noted above have been Golgi derived, but there was no evidence that they contributed to the formation of the extrahaustorial matrix. PA-TCH-SP staining did not produce similar reactions in both the Golgi vesicles and the extrahaustorial matrix (Fig. 4, arrows) although these vesicles may produce and contribute material which was not reactive to Thiery staining.

The host ER system associated with the haustorial body was not particularly organized as was the case in D- haustoria of some rust-infected cereals (Harder and Chong 1984). However, there was some evidence of a direct connection between the extrahaustorial matrix and either the host ER or cytoplasmic vesicles (Fig. 5,

Legend

Figures 1-5. Transmission electron micrographs of the association between haustoria and the host endoplasmic reticulum system.

Figure 1. Host ER is evident juxtaposed to the haustorial body (HB). Glut/OsO_4. UA/PbC. X46500.

Figure 2. Host ER is evident surrounding and following the contours of the HB. The cytoplasm appears condensed in the vicinity of the haustorium. Glut/OsO_4. UA/PbC. X17000.

Figure 3. Golgi (G) as well as ER are apparent in close association with the HB. Glut/OsO_4.PA-TCH-SP. X17000.

Figure 4. Golgi vesicles (arrows) exhibit only a slight reaction to Thiery staining as compared to the EHM, after 20 h incubation in TCH. Glut/OsO_4. PA-TCH-SP. X46500.

Figure 5. The arrow indicates a possible direct connection between the EHM and either the host ER or a cytoplasmic vesicle. Glut/OsO_4. PA-TCH-SP. X102000.

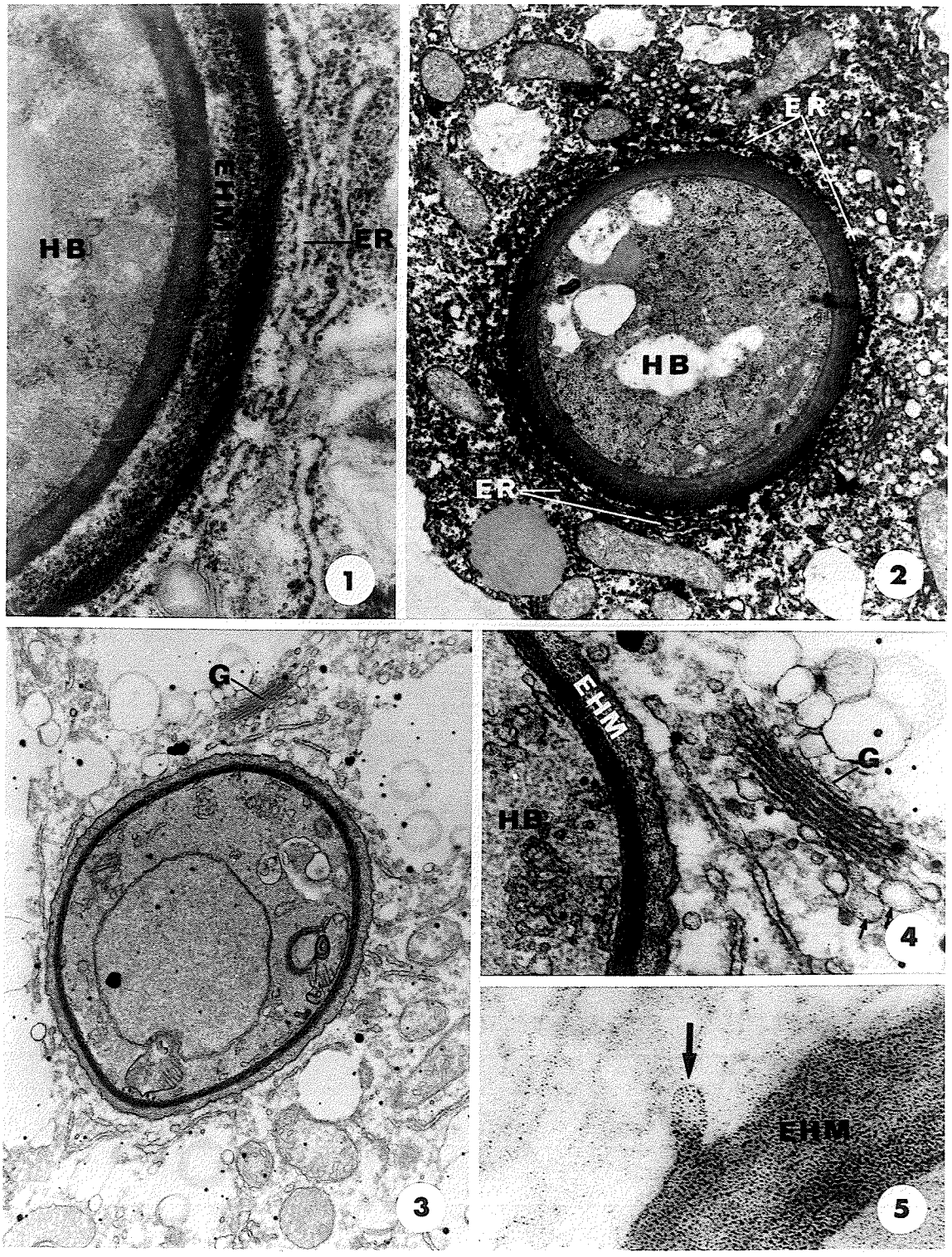
HB
EHM
ER
1
ER
HB
ER
2
G
3
EHM
HB
G
4
EHM
5

arrow), and an association between the extrahaustorial membrane about the haustorial neck and vesicles of uncertain origin (Figs. 6 and 7, arrows). These vesicles with darkly-stained contents were directly connected to the membrane. When cross sections through haustorial neck regions were examined, large numbers of vesicles were again seen in the host cytoplasm (Fig. 8), but there was not the same close association here with the host ER that was evident about the haustorial body (Fig. 7).

Often the haustorium was associated with the host cell nucleus. The nucleus was frequently indented by the haustorial body (Fig. 9) and, in extreme cases, the nucleus appeared to enfold the haustorium (Fig. 10). However, the host nucleus was not in direct contact with the extrahaustorial membrane, but merely appeared to follow its contours. Further, the protoplasm lying between the haustorium and the nucleus appeared normal, and there was no evidence that endoplasmic reticulum was continuous between the nucleus and the haustorium throughout the protoplasm in this area (Fig. 12). This type of association was easily seen in cleared specimens (Fig. 11) but light microscopy also revealed that such associations, although very common, did not occur in all infected cells.

Significant changes in chloroplast structure were induced as the fungus spread throughout the cortex. In uninfected cells chloroplasts were elliptical in outline, and possessed well developed grana and stroma thylakoids (Fig. 13); some plastoglobuli were present, but large starch grains were rarely evident. In

Legend

Figures 6-8. Transmission electron micrographs of host protoplasm in association with the haustorial neck.

Figure 6. A vesicle with dark-staining contents (arrow) appearing to be directly attached to the extrahaustorial membrane (EM) in the neck region. Glut/OsO_4. UA/PbC. X46500.

Figure 7. Host ER appears to follow the contours of the neck region but does not appear as closely associated with the neck as it is with the haustorial body. Vesicles with dark-staining contents appear to be associated with the haustorial neck (arrow). Glut/OsO_4. UA/PbC. X46500.

Figure 8. A cross section of the haustorial neck (HN), showing an association with numerous host cytoplasmic vesicles. Glut/OsO_4. UA/PbC. X29500.

Figures 9-12. Micrographs of the association between haustoria and host nuclei.

Figure 9. A host nucleus (N) closely associated with and indented by the haustorial body (HB). Glut/OsO_4. UA/PbC. X5700.

Figure 10. In some instances the host nucleus appears to enfold the haustorium. Glut/OsO_4. UA/PbC. X4500.

Figure 11. A phase contrast micrograph demonstrating the association of the haustorium with the host nucleus; in cleared host tissue. X800.

Figure 12. Although closely associated, the host nucleus is never in direct contact with the haustorium. The protoplasm between the two bodies shows no evidence of ER. Glut/OsO_4. UA/PbC. X16000.

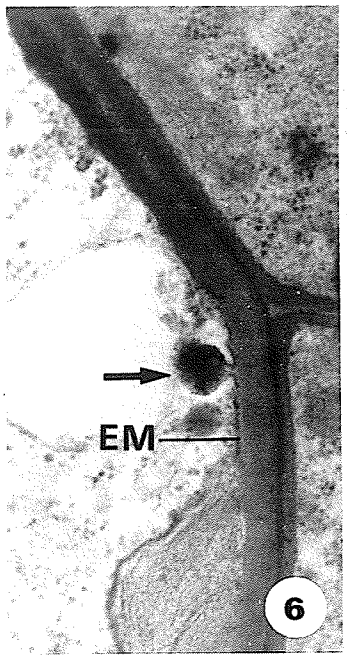
EM
6

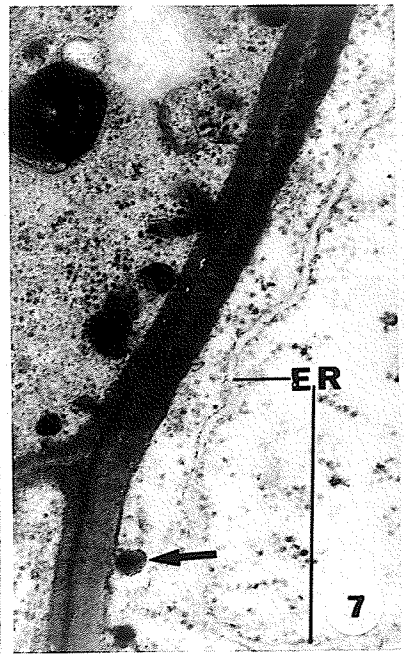
ER
7

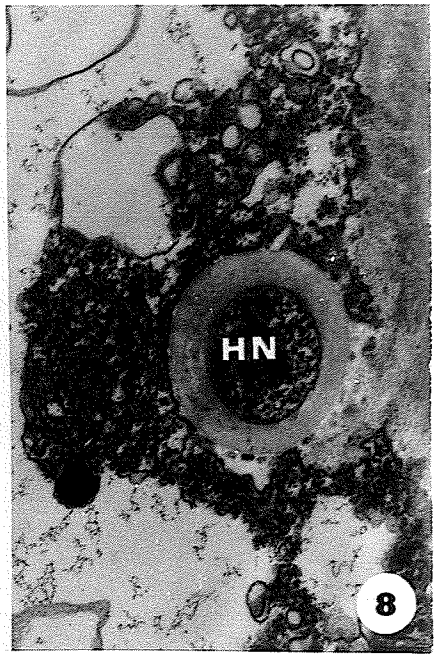
HN
8

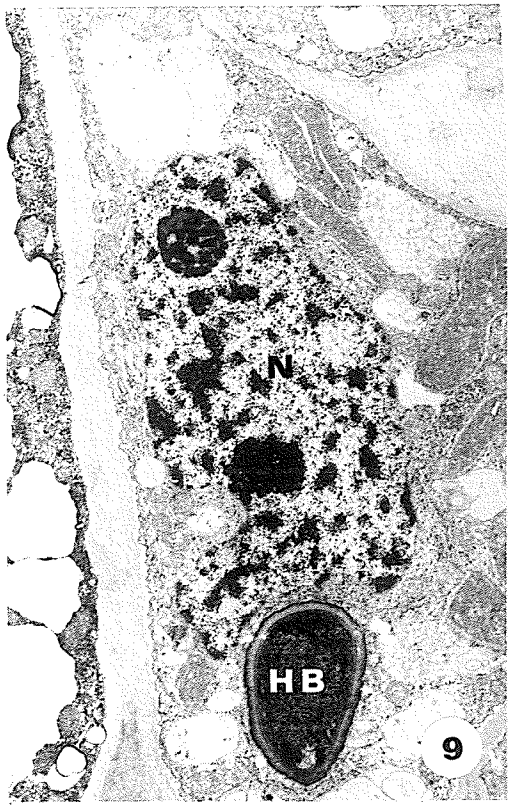
N
HB
9

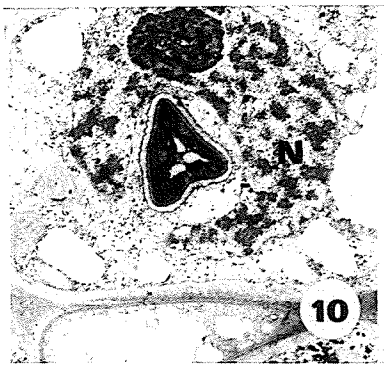
N
10

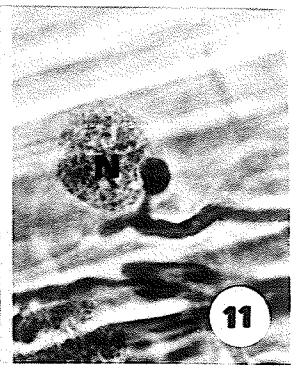
N
11

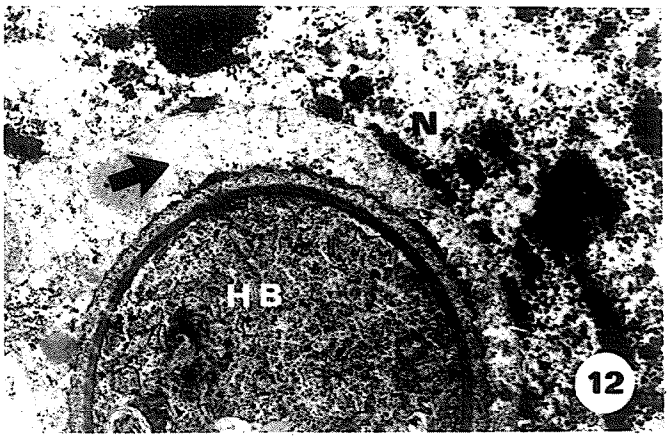
N
HB
12

recently infected tissues, chloroplasts remained quite unchanged (Fig. 14) relative to uninfected tissues, but this situation did not persist. As the infection became more advanced, large starch grains appeared in the chloroplasts, and the chloroplasts themselves became redistributed in close proximity to the haustorial body (Fig. 15). In even later stages, when the first signs of senescence were visible, the chloroplasts became swollen and contained abnormally large starch grains and disrupted thylakoids (Fig. 16). However, there was no evidence of any increase in size or frequency of plastoglobuli.

Collars were frequently observed at the base of the haustorium, at the point where the latter initially penetrated the host cell wall (Fig. 17, arrows). These type II collars according to the classification of Littlefield and Heath (1979), were always closely appressed to the outer wall layer of the haustorial neck (Fig. 18) and the host plasmalemma, while continuous over the collar and haustorial neck, was only rarely found intervening between these two regions. However, in E. harknessii, in the few instances when the upper portion of the collar was separated from the haustorium by the plasmalemma, the latter was only slightly invaginated between these two regions (Fig. 19, arrows).

Collars were continuous with, and usually indistinguishable from, the host cell wall. Some collars showed evidence of cellulose-like fibrils (Fig. 18) suggesting that collar formation may have been partially due to host cell wall invagination at the time of penetration by the developing haustorium; such an inward

Legend

Figures 13-16. Transmission electron micrographs of chloroplast morphology in infected host cells.

Figure 13. Control: chloroplast in uninfected host cell displaying well developed grana and stroma thylakoids. Glut/OsO_4. UA/PbC. X17000.

Figure 14. The chloroplasts in a recently infected cell appearing similar to that in the control. Glut/OsO_4. UA/PbC. X6700.

Figure 15. A more advanced infection in which the chloroplasts appear in close proximity to the haustorium and contain large starch grains (arrows). Glut/OsO_4. PA-TCH-SP. X17000.

Figure 16. A late stage of infection; the chloroplasts appear swollen, contain large starch grains (arrows) and show some evidence of thylakoid disruption. Glut/OsO_4. UA/PbC. X8900.

13

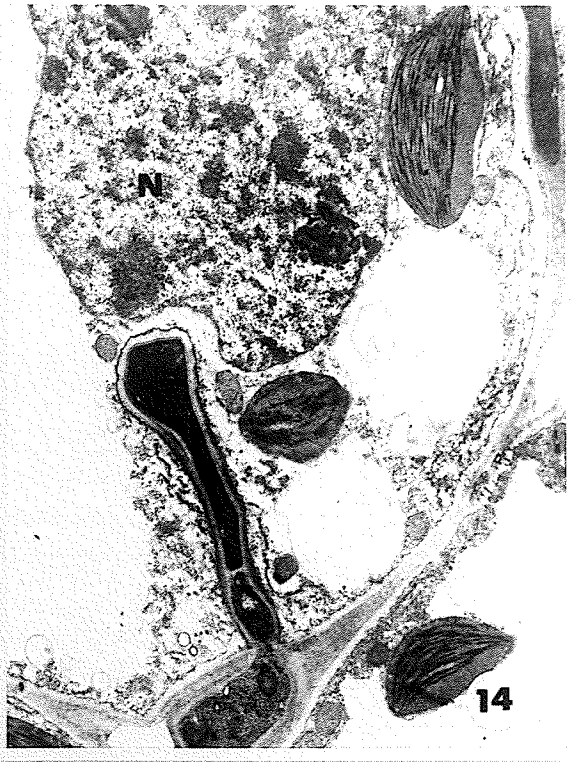

14

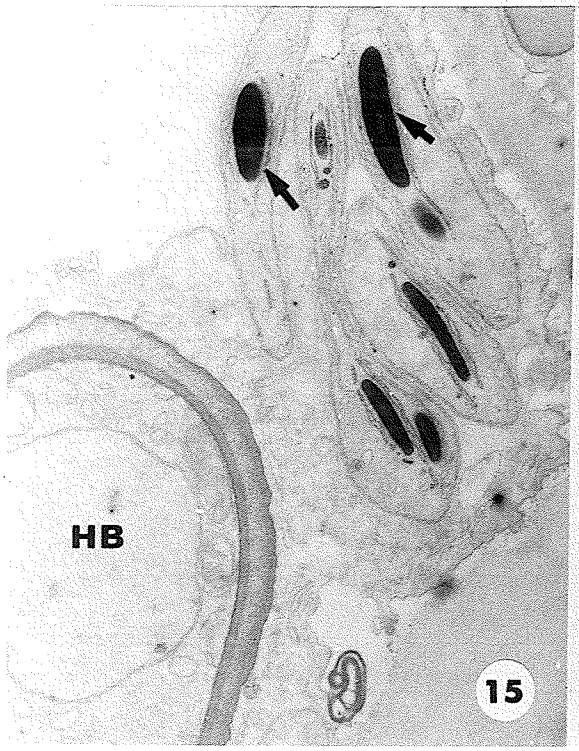

15

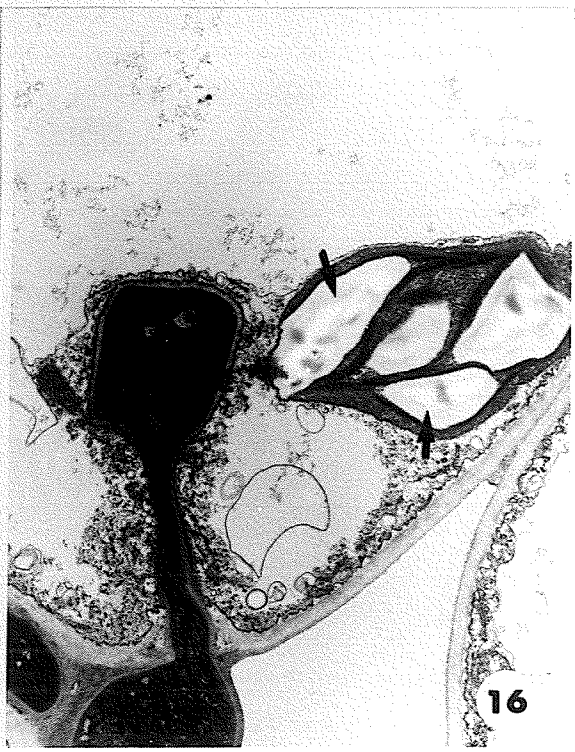

16

displacement of the host cell wall was sometimes seen at the point of contact of the haustorial mother cell with the host cell wall (Fig. 20). This alone could not account for the formation of larger collars; even stretching and thinning of the host wall coupled with cell wall displacement could not account for the collar mass seen in situations similar to that represented in Fig. 21. Rarely, remnants of what appeared to have been collars of excessive length were observed extending beyond the haustorial neck, with their termini lying adjacent but not appressed to the haustorial body (Fig. 22, arrow). These may have represented collars that had originally encased young developing haustoria, but which had finally been breached by them. It would be impossible for such collars to be produced solely as a result of host cell wall displacement; they must have been partly, if not solely, produced by the host cell as the haustorium elongated.

Collars generally appeared fibrillar in structure, although there was evidence of some membranous material contained within (Figs. 19 and 25, arrowheads). Electron lucent regions were not evident within them, and as electron lucence is believed to suggest the presence of callose (Heslop-Harrison 1966) it is likely this polysaccharide was not present. Examination of fresh material employing fluorescence microscopy after staining with aniline blue, also did not demonstrate callose in the penetration zone. Indeed the fact that both collars and cell walls were intensely stained with PA-TCH-SP after 14 hours incubation in TCH (Fig. 23) and were both lightly stained after 0.2 h incubation (Fig. 24) suggesting that they have a common origin.

Legend

Figures 17-22. Transmission electron micrographs of collars in E. harknessii infections.

Figure 17. A typical collar (arrows) in evidence at the point of infection. Glut/OsO_4. UA/PbC. X8000.

Figure 18. Collars appear closely appressed to the outer wall layer of the haustorial neck (HN). The collar (C) which is bounded on one side by the host plasmalemma (HP) appears to contain cellulose fibrils and is continuous with host cell wall (CW). Glut/OsO_4. UA/PbC. X46500.

Figure 19. In some instances the upper portion of the collar is separated from the haustorial neck by the HP (arrows). There is also some indication of membranous contents in the collar (arrowheads). Glut/OsO_4. UA/PbC. X17000.

Figure 20. A tangential section showing inward displacement of the CW is evident at the point of contact with the HMC. Glut/OsO_4. UA/PbC. X25000.

Figure 21. An abnormally long collar associated with a necrotic haustorium. Glut/OsO_4. UA/PbC. X17000.

Figure 22. A remnant of what might have been an encasement or a collar of excessive length, appearing to be associated with but not appressed to, the haustorium (arrow). This may indicate a forcible breaching of the presumed encasement or collar by the haustorium. Glut/OsO_4. UA/PbC. X6700.

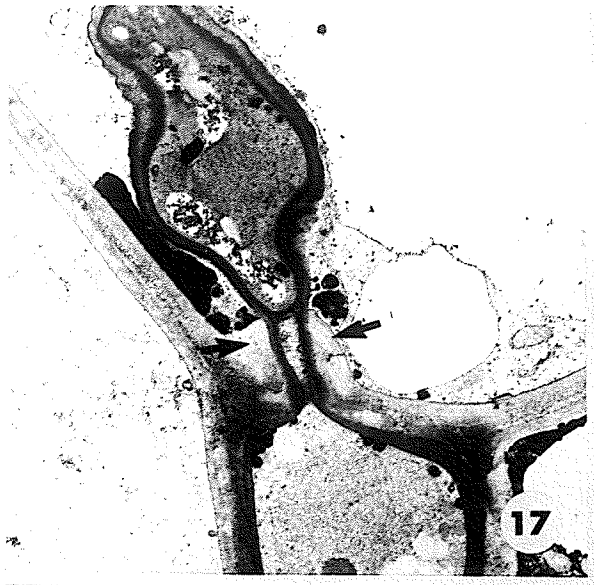
17

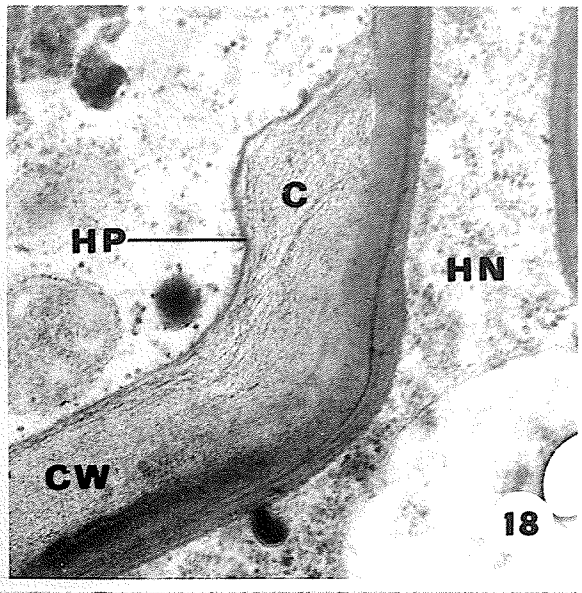
C
HP
HN
CW
18

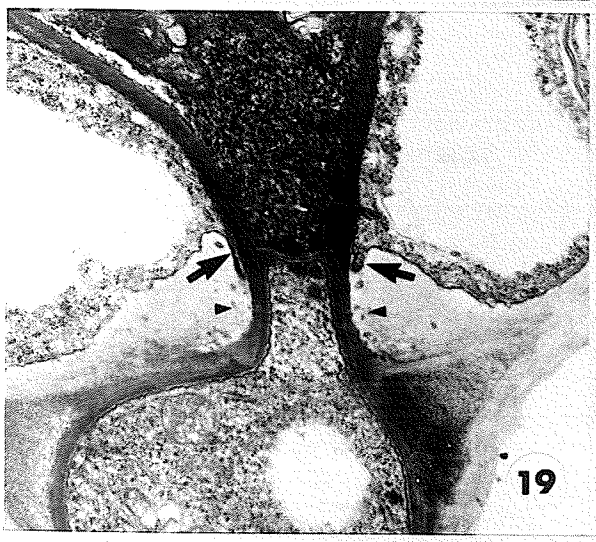
19

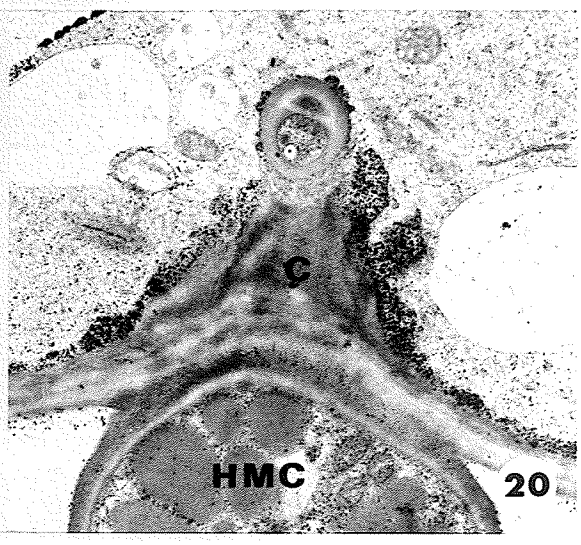
C
HMC
20

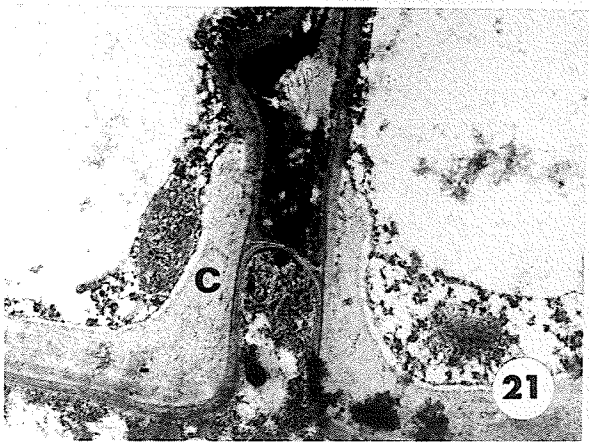
C
21


22

How are collars produced? The common belief is that type II collars develop on the host cell walls either prior to successful penetration by the penetration peg, or directly on the latter as it emerges from the host cell wall, with the haustorium subsequently growing through the collar (Littlefield and Heath 1979). It is possible, however, that type II collars may also be produced after the haustoria develop. Figures 25 and 26 are two of a single set of serial sections obtained through a region of penetration which possibly illustrate collar development. Figure 25 represents a near median section through this region, and shows vesicles and osmiophilic bodies (arrows) closely associated with both the collar and invaginated plasmalemma of the haustorial neck. A more lateral section (Fig. 26) shows similar bodies and vesicles (arrows) associated with the edge of the collar; such inclusions were only evident in the cell in close proximity to the collar, and not at other points along the host wall. In a few cells, similar vesicles which stained intensely with the PA-TCH-SP procedure, were observed associated with the plasmalemma about the collar and at the base of the haustorial neck, (Fig. 24, arrows). However, such vesicles were also evident at other points along the host cell wall, not just in the vicinity of the collar, and it is therefore unclear whether they were contributing to the development of the collar.

Legend

Figures 23-24. Thiery staining of collars.

Figure 23. Incubation of sections in TCH for 14 h results in intense staining of both the collar (C) and the host cell wall (CW). Glut/OsO_4. PA-TCH-SP. X17000.

Figure 24. Incubation of sections in TCH for 0.2 h results in only a slight reaction in both the CW and collar. Vesicles (arrows) associated with the collar and haustorial neck stain intensely with this treatment. Glut/OsO_4. PA-TCH-SP. X46500.

Figures 25-26. Serial sections through a developing collar

Figure 25. A near median section showing vesicles and osmiophilic bodies (arrows) closely associated with the collar and haustorial neck. The collar also appears to contain some membranous material close to the haustorial neck (arrowheads). Glut/OsO_4. UA/PbC., X17000.

Figure 26. A lateral section through the outer edge of the collar showing cytoplasmic vesicles and osmiophilic bodies (arrows) associated with the collar. Glut/OsO_4. UA/PbC. X17000.

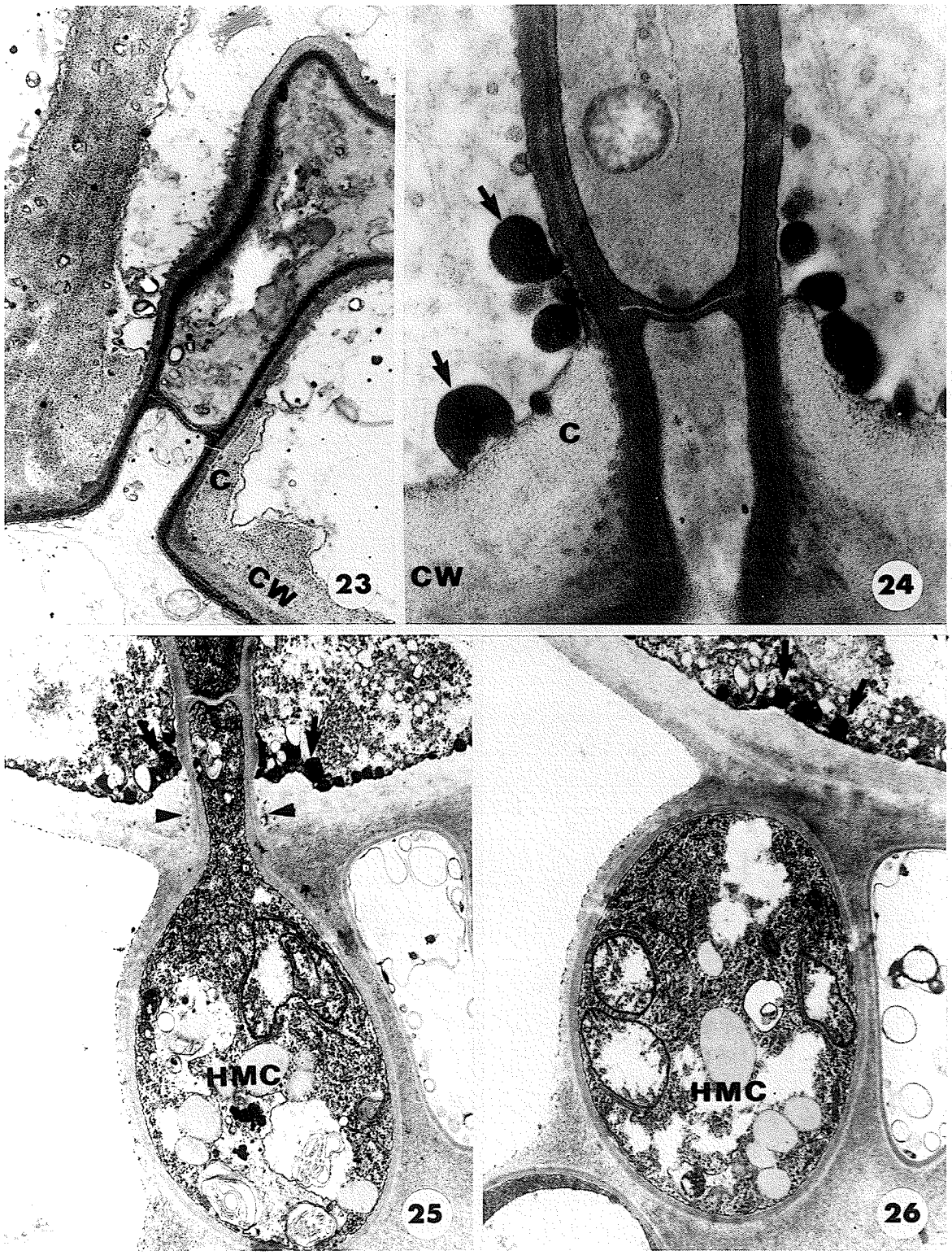
C
CW
23
C
CW
24
HMC
25
HMC
26

B. Incompatible Reactions

Since known resistant lines of P. contorta and P banksiana were not available for this study, Japanese black pine, P. thunbergii, which is believed to be resistant to western gall rust (Hiratsuka and Maruyama 1983) was employed to study presumptive resistant mechanisms which might occur in juvenile seedlings.

Macroscopic evidence of infection was not seen until 9-12 days after inoculation. Initially infection appeared as a well-defined necrotic streak on the hypocotyl (Fig. 1) which was identical to that seen in early infections of susceptible pines. By day 20, the streak was still localized, but displayed what appeared to be early indications of periderm formation (Fig. 2, arrow). Subsequently, extensive periderm formation was evident on the surface of the inoculated hypocotyl. (Fig. 3).

Previously these pines had not shown signs of susceptibility, and it was therefore assumed a hypersensitive response would be a common occurrence. Accordingly, some cleared specimens showed evidence of a dark-staining region surrounding the haustoria in the epidermal cells (Fig. 8), and when some fresh tissue was stained with aniline blue and examined by fluorescence microscopy, the entire haustorium fluoresced indicating encasement by callose (Fig. 4). It is assumed specimens exhibiting such types of response to infection were reacting in a hypersensitive manner.

Seedlings exhibiting early periderm formation showed no evidence of mycelium in the cortex when examined by light

Legend

Figures 1-3 Phenotypic reactions of juvenile seedlings of *P. thunbergii* to *E. harknessii*.

Figure 1. Necrotic streak evident on the hypocotyl 9-12 days after inoculation (arrow). X12.

Figure 2. Localized necrosis showing some evidence of early periderm formation, 20 days after inoculation (arrow). X10.

Figure 3. Extensive periderm formation on the hypocotyl, 30 days after inoculation. X10.

Figures 4-7. Light microscope photographs of resistant reactions in hypocotyls of *P. thunbergii*.

Figure 4. A haustorium infecting an epidermal cell, showing yellow fluorescence of the haustorial body and neck after staining with aniline blue (arrow). Unfixed tissue. Fluorescence microscopy. X1000.

Figure 5. An epoxy thin section-showing restriction of the mycelium to the cortex 5 weeks after inoculation; infected cells appear necrotic. Bright field microscopy. X300.

Figure 6. Evidence of periderm formation in the cortex of an infected hypocotyl. The developing periderm exhibit a high degree of autofluorescence. Fluorescence microscopy. X650.

Figure 7. Hand section through the cortex of an infected hypocotyl showing a high degree of necrosis of host cells and haustoria; stained with calcofluor white and acridine orange. Fluorescence microscopy. X1000.


1


2


3

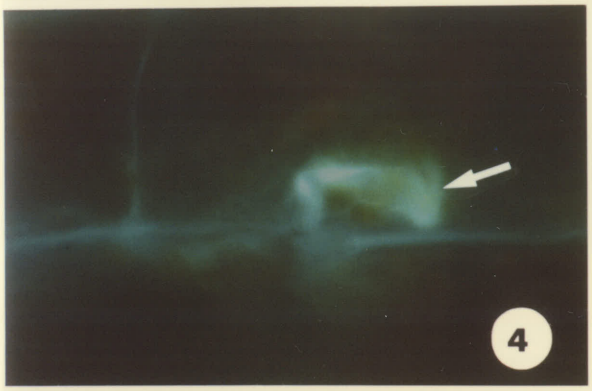
4

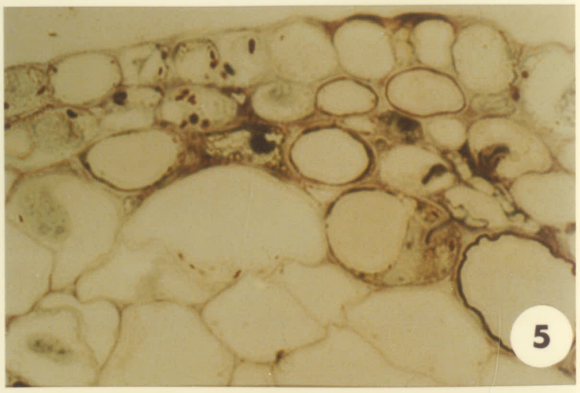
5

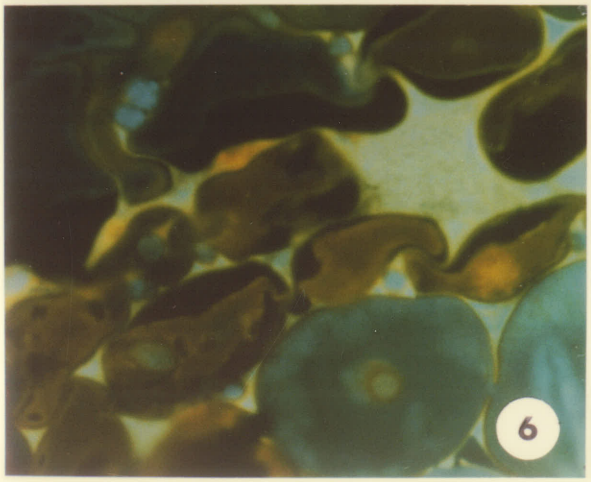
6

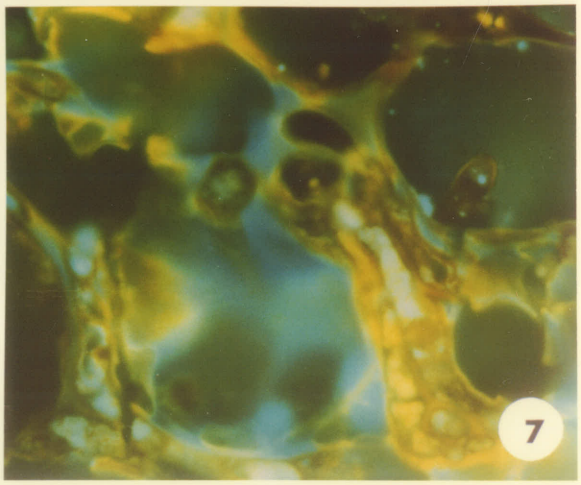
7

microscopy (Fig. 9). However ultrathin sections through similar regions showed they contained both necrotic intercellular mycelium and intracellular haustoria (Fig. 10); apparently the mycelium could neither survive within, nor progress beyond, this area. This may represent an extension of the hypersensitive reaction noted in the epidermal cells, or it may represent a discrete second hypersensitive response. Since host families with defined resistance reactions have not yet been identified or produced, the apparent epidermal cell hypersensitivity cannot yet be correlated with early periderm formation i.e. do they represent two stages in a single reaction, or two discrete reactions? Thus at present each seedling must be regarded as unique, with only one possible stage of its response being identified.

In the majority of cleared, inoculated seedlings examined there was extensive development of mycelium in the epidermis (Fig. 11). This precludes the possibility of a general hypersensitive or immune response based in the epidermal cells. Light microscopic examination of thin sections obtained from some infected seedlings clearly showed that hyphae had extended intercellularly into the cortex and, from these, haustoria had been produced (Fig. 12, arrow). And, while ultrastructural examination of similar material confirmed the results obtained by light microscopy as to fungal spread, it also revealed that many of the haustoria and infected cells were necrotic (Fig. 13). Further, it was also apparent that such necrotic haustoria had been fully developed prior to onset of degeneration; in contrast, a number of necrotic host cells were regularly observed which contained an apparently healthy haustorium

Legend

Figures 8-12. Host responses in early stages of infection of the hypocotyl.

Figure 8. A cleared specimen exhibiting necrosis of a haustorium (arrow) in an epidermal cell. Phase contrast microscopy. X650.

Figure 9. An epopxy thin-section showing early periderm development (arrow) in an infected portion of the hypocotyl. Bright field microscopy. X650.

Figure 10. Transmission electron micrograph showing intercellular hyphae (IH) and haustoria (arrow) contained within the periderm, as shown in Fig. 9. Glut/OsO_4. UA/PbC. X8100.

Figure 11. Extensive development of the mycelium is evident in the epidermis of a hypocotyl, cleared 5-7 days after inoculation. Phase contrast microscopy. X650.

Figure 12. An epoxy thin-section showing the extention of the mycelium into the cortex, and subsequent production of haustoria (arrowhead), several weeks after inoculation. Subcuticular hyphae are also in evidence (arrows). Bright field microscopy. X650.

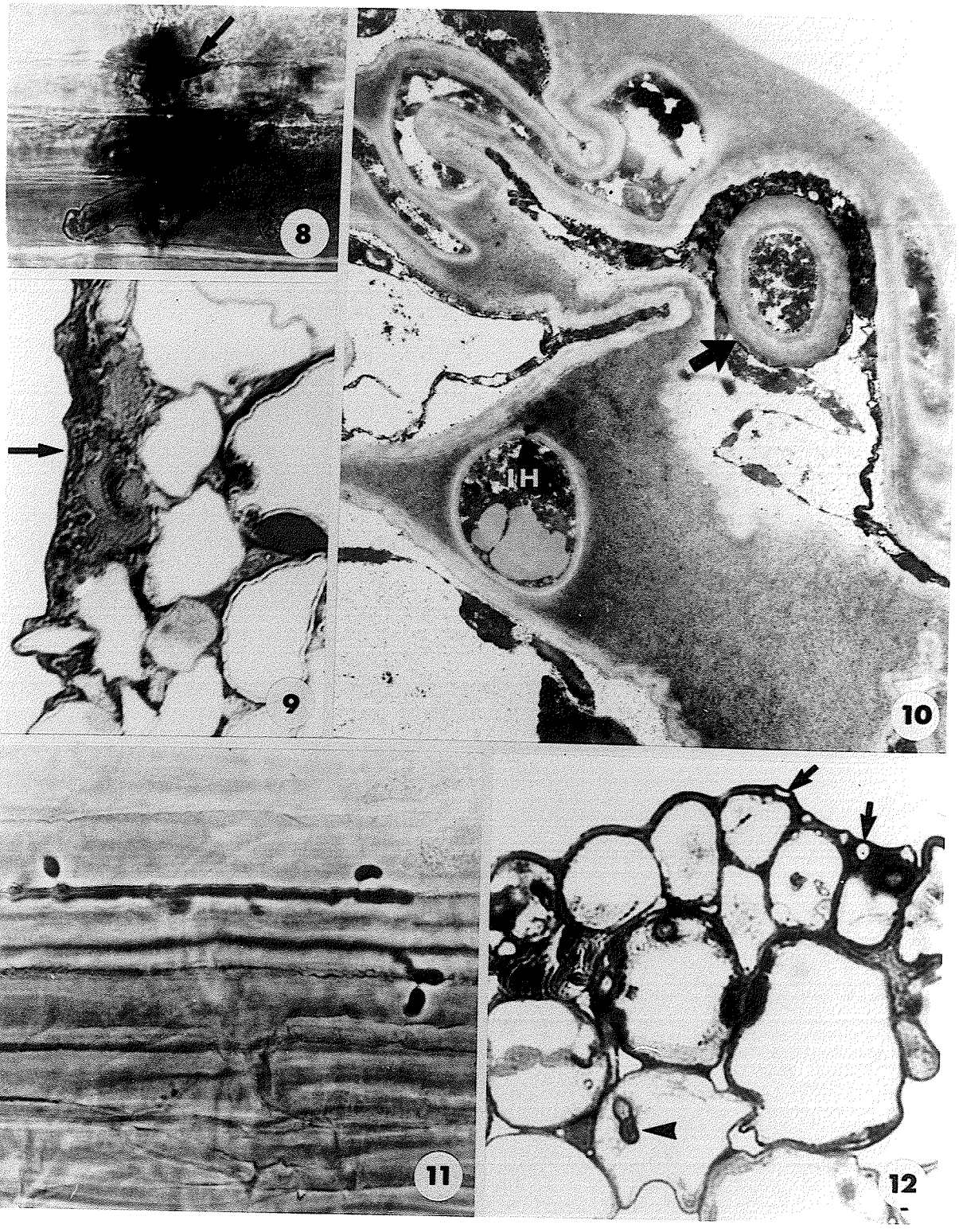
8
9
H
10
11
12

(Fig. 14). These observations collectively suggest that necrosis did not occur in advance of mycelial spread, but resulted from invasion of the cortex and production of the haustoria. However, progress through the cortex appeared to be relatively slow, and the mycelium was often still confined to the cortex five weeks after inoculation (Fig. 5).

In the later stages of infection, areas of the cortex became hypertrophic, but there was also evidence of periderm formation (Fig. 15, arrow). Such regions exhibited a high degree of autofluorescence (Fig. 6), perhaps indicative of suberin deposition which could serve as a barrier to further mycelial spread, thus restricting the mycelium to the cortex (e.g. Fig. 16, arrows).

Ultrastructural examination of cortical sections revealed that many infected cells contained an electron dense substance which often filled the entire vacuole (Fig. 17), and also encased the haustoria. Hand sections taken through this region, stained with calcofluor and acridine orange for fluorescence microscopy, showed no evidence of healthy mycelium, but there was a correspondingly high degree of host cell necrosis (Fig. 7).

When examined by light microscopy, sections taken from a few seedlings revealed haustoria in the vascular tissue (Fig. 18) and yet, macroscopically, these seedlings appeared identical to those described earlier which, at the ultrastructural level, showed obvious resistant responses. When examined ultrastructurally, it was clear that many of the cells of these vascular-invaded seedlings had developed some features of an apparently compatible

Legend

Figures 13-17. Resistant reactions in the cortex of infected hypocotyls 3 to 5 weeks after inoculation.

Figure 13. Transmission electron micrograph showing a necrotic cortical cell and haustorium (H). Glut/OsO_4. UA/PbC. X17000.

Figure 14. Transmission electron micrograph of a necrotic host cell containing an apparently healthy haustorium. Glut/OsO_4. UA/PbC. X8100.

Figure 15. An epoxy thin section showing hypertrophy of the cortical cells and development of periderm (arrow). Bright field microscopy. X650.

Figure 16. An epoxy thin section showing developing periderm (arrowheads). The mycelium is only observed outside this region (arrows). Bright field microscopy. X250.

Figure 17. A transmission electron micrograph of an infected cortical cell. The vacuole (VA) of the cell contains an electron-dense substance. Glut/OsO_4. UA/PbC. X8800.

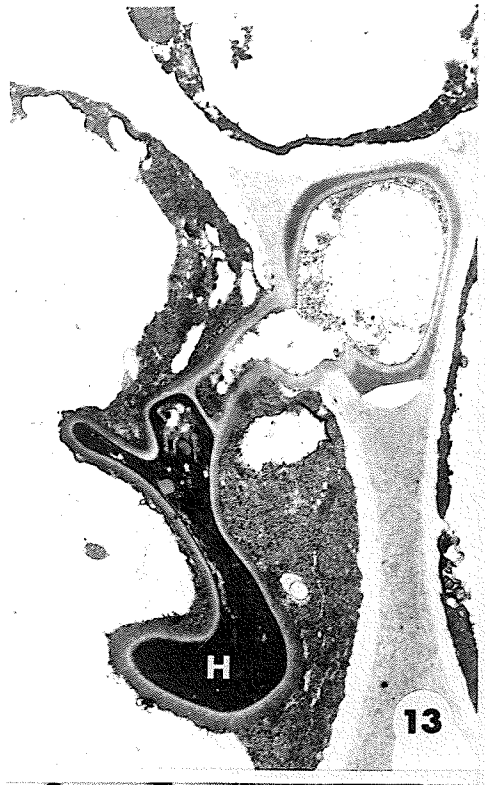
H
13

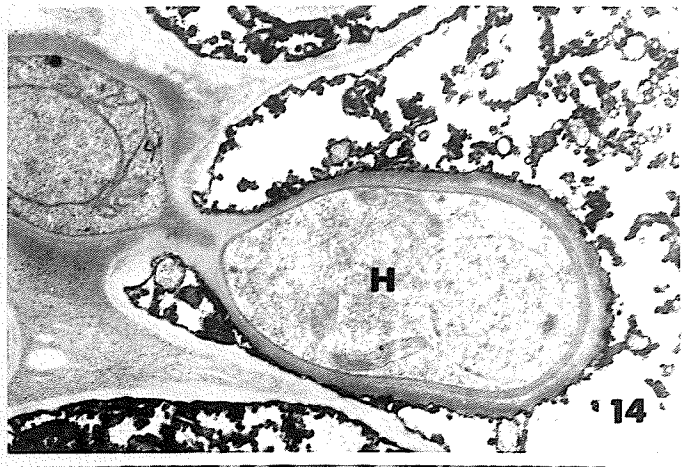
H
14

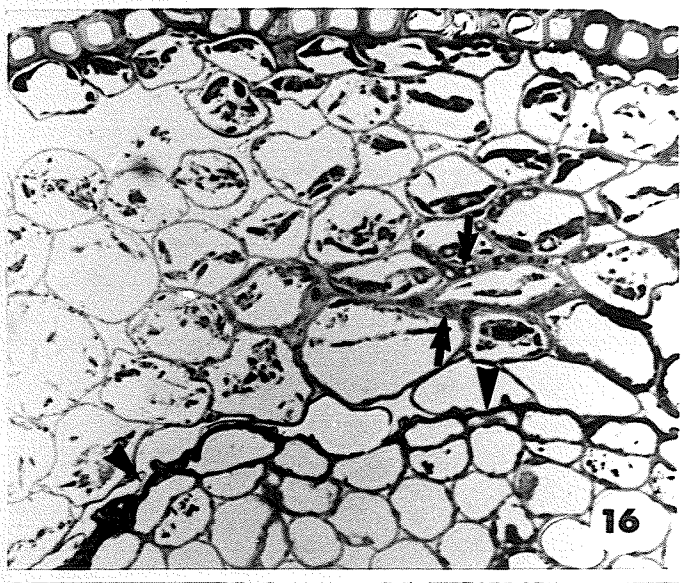
16


15

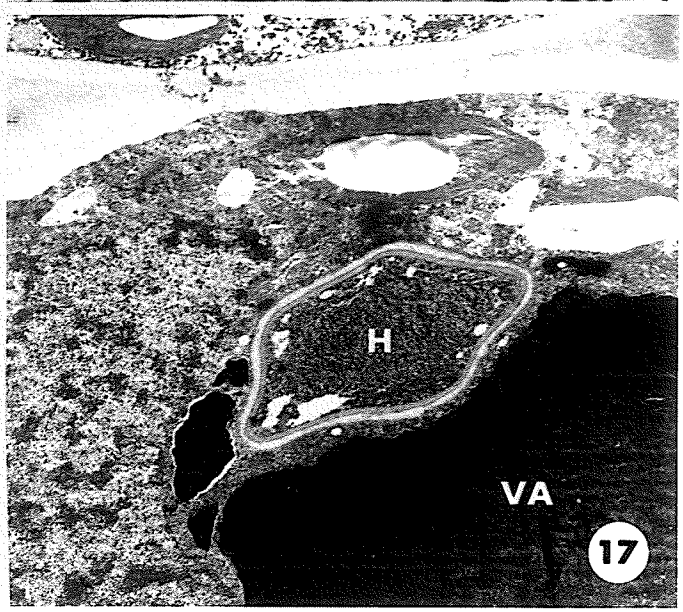
H
VA
17

relationship with the haustorium (Fig. 19), e.g., the positioning of the host cell endoplasmic reticulum relative to the haustorial body, the close proximity of the slightly indented host cell nucleus, etc. However, a significant number of the more internal infected cells contained large numbers of small vacuoles within the cytoplasm (Fig. 20); such were not normally found in healthy host cells. It was also noted that some infected cells lying external to the stele, and thus presumably invaded before the phloem cells, exhibited a complete breakdown of cell membranes (Fig. 21): it is possible the occurrence of the many vacuoles noted in Fig. 20 is an early indication of cell membrane breakdown; the haustorium appeared healthy, but was presumably non-functional.

The seedlings described above may have been exhibiting a degree of tolerance to infection by E. harknessii, since they showed no evidence of gall formation, either internally or externally, at the time of fixation; they may have been physiologically non-reactive to western gall rust. This suggestion must be treated with caution since a few seedings of P. thunbergii inoculated at the same time as those discussed above did have slight stem swellings which later developed into galls. Thus the suggested tolerance may simply be a latent infection which is slow to induce typical symptoms.

Legend

Figures 18-21. Reactions to infection in the vascular tissue of P. thunbergii.

Figure 18. An epoxy section showing extensive infection in the vascular tissue. Bright field microscopy. X650.

Figure 19. Transmission electron micrograph demonstrating the initial compatibility of the haustorium (H) with the vascular tissue. Glut/OsO_4. UA/PbC. X9000.

Figure 20. Transmission electron micrograph of a later stage of infection, showing the appearance of numerous cytoplasmic vesicles (V). Glut/OsO_4. UA/PbC. X9000.

Figure 21. Transmission electron micrograph of an advanced stage of infection. The host cell exhibits a complete breakdown of cell membranes. Glut/OsO_4. UA/PbC. X17000.

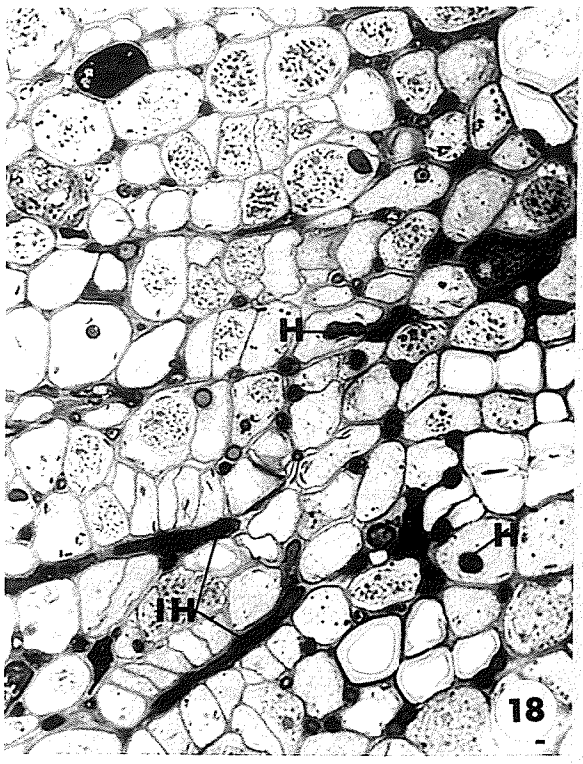
H
H
H
18

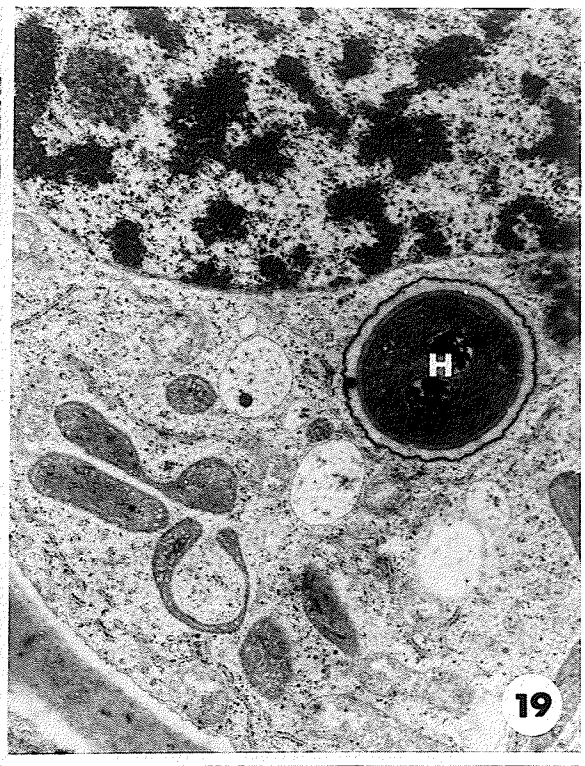
H
19

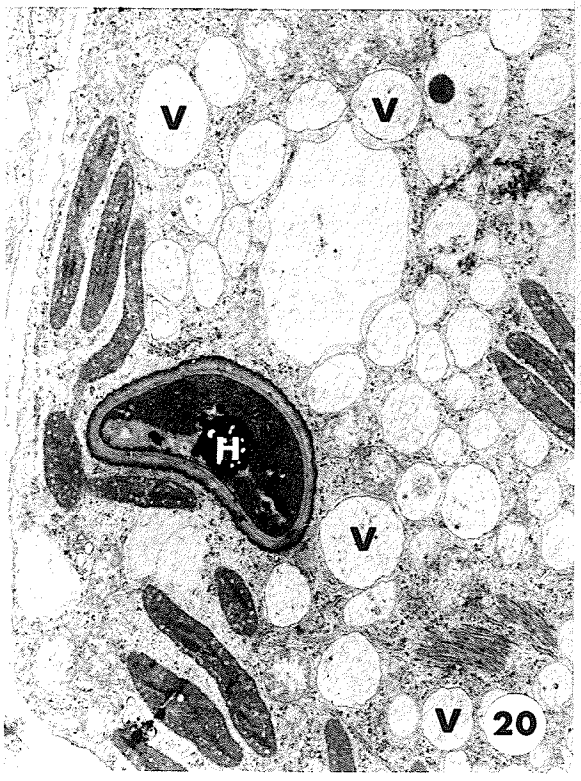
V
V
H
V
V
20

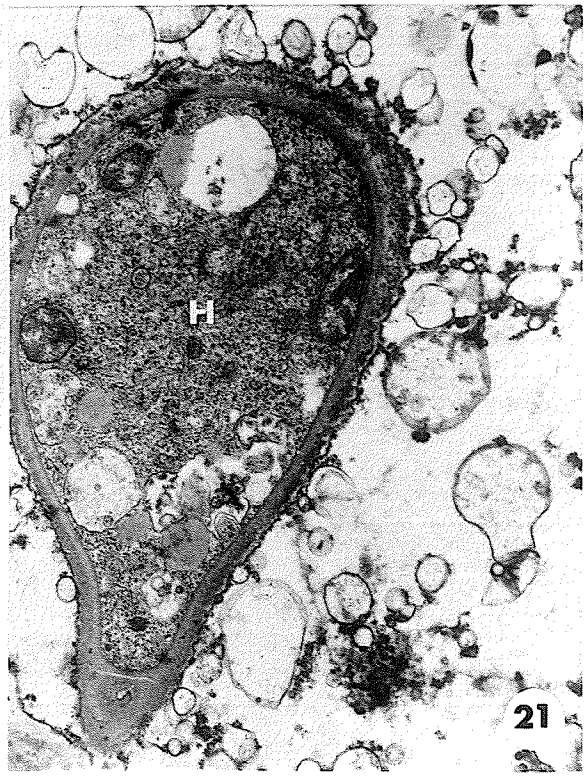
H
21

DISCUSSION

Commonly, rust fungi exhibit a high degree of compatibility with their hosts, usually reflected in the physical relationship between the host and parasite in features observable at the ultrastructural level.

Little host cell disruption occurred in the early stages of infection in the compatible interaction between hard pines and E. harknessii. However, one of the most obvious responses by the host cell was the apparent association of its endoplasmic reticulum with the invasive haustorium; this association was similar to that reported for most infections by M- or D- haustoria (Littlefield and Heath 1979; Harder and Chong 1984). Harder et al. (1978) and Heath and Heath (1971) suggested that this association is not static, but changes with the maturation stage of the haustorium. Initially, the endoplasmic reticulum was only found associated with the haustorial neck; D- haustoria of P. graminis tritici show a pronounced association with host ER in this region (Harder et al. 1978). However, as the haustorium matured the ER associated with the neck region became much less evident and, as this occurred, ER complexes developed about the haustorial body itself.

While host cell responses to the early developmental stages of an invasive haustorium have not yet been determined for E. harknessii, it is clear there was no close association of endoplasmic reticulum with the necks of mature haustoria. However, a possible direct association of cytoplasmic vescicles with the neck region was evident, but not as pronounced as in P. coronata (Chong and Harder

1982); the latter authors suggested that such an association was involved in collar formation.

Close association between the host endoplasmic reticulum and the haustorial body was evident in this study; although as noted earlier this is characteristic of most rust infections, in E. harknessii this association was neither as elaborate nor pronounced as demonstrated for some cereal rusts (Harder and Chong 1984). There was also evidence here of a direct connection between the extrahaustorial matrix and either associated endoplasmic reticulum or cytoplasmic vesicles, although such connections were rarely seen. Earlier reports of continuity between the endoplasmic reticulum and the extrahaustorial membrane have been restricted to P. graminis tritici (Harder et al. 1978) and P. coronata avenae (Chong et al. 1981). Unfortunately, in E. harknessii there was no evidence of any similarity between the material of the extrahaustorial matrix and the surrounding endoplasmic reticulum as was noted in D- haustorial infections of U. phaseoli (Heath and Heath 1971); this would have been added proof of a continuity between the two regions.

The occurrence of Golgi bodies near the haustorium was probably due to their chance distribution within the host cytoplasm, and not the result of any specific host response. Although Gold and Mendgen (1984b) observed Golgi bodies near the entry and exit points of intracellular hyphae in U. appendiculatus appendiculatis infections, neither in their report nor in E. harknessii was there an evidence of an increase in abundance of

Golgi bodies. Although cytoplasmic vesicles were in evidence about the haustorial body of E. harknessii, there was nothing to suggest these were derived from Golgi. In fact, Littlefield and Heath (1979) and Chong and Harder (1982) all suggest that despite it's normal intermediary role, the Golgi probably are not involved in any of the reported associations between endoplasmic reticulum and haustoria. None of the results obtained in this study would contradict that view.

The relationship between the host nuclei and the haustoria found in western gall rust infections was typical of earlier reports for other rusts. Nor did this study uncover any pronounced degree of specialization similar to the proliferation of tubules between the D- haustoria of P. coronata avenae, and host nuclei (Chong and Harder 1982). However, in compatible western gall rust interactions, as with other rusts, there was never any direct contact between the haustorium and the nucleus; the latter always remained a fairly uniform distance from the haustorium. Al-Khesraji and Lösel (1981) reported the host nucleus changed in size and form in cells infected by P. poarum but they, as well as Heath and Heath (1971), felt this host nucleus-haustorium association might only be important during certain stages of development. If this association is indeed ephemeral, as suggested, it is possible that the presence of tubules or endoplasmic reticulum between these two bodies, as noted by Chong and Harder (1982), would only be evident at certain developmental stages, and for short time periods; it is therefore possible they were present in E. harknessii but simply not recorded. A

transient nature of the host nucleus-haustorium association would also help explain why light microscopic observations of infected hypocotyls did not demonstrate this association in a number of the cells penetrated by E. harknessii haustoria.

Chloroplast clumping and their increased proximity to haustoria are common occurrences in rust infections, and were observed in this study. However, the apparent increase in starch deposition in the chloroplasts of E. harknessii infected cells is in direct contrast to the observations of Mlodzianowski and Siwecki (1976) who observed starch breakdown and the occurrence of glycogen in the chloroplasts of cells bearing D- haustoria of M. pinitorqua. Coffey and Allen (1983) also observed the presence of glycogen in chloroplasts in an incompatible reaction to flax rust, but they also suggested that infection could stimulate starch production in chloroplasts. As our knowledge of the ultrastructure of juvenile pine tissue is very incomplete, it is uncertain whether the changes observed in infected cells of P. banksiana and P. contorta are typical of normal or accelerated senescence. However, Heath (1974) noted that changes observed in the chloroplast structure of cells of rust-infected cowpea initially resembled those of normal senescence. The later stages she observed showed chloroplast alterations reminiscent of those induced by ethylene production during fruit ripening. Thus it is clear rust infection can induce major changes in the chloroplasts though it would appear that these changes are not uniform.

The collars produced during infection by E. harknessii are typical of the fibrillar type II collars noted in other reports of M-haustoria (e.g. Al-Khesraji and Lösel 1981; Walles 1974). In certain studies of M- haustoria (Al-Khesraji and Lösel 1981) and D-haustoria (Hardwick et al. 1971; Heath and Heath 1971), callose was implicated as a component of the collars. However, ultrastructural examination of E. harknessii haustoria did not detect any electron opaque regions such as those seen in other studies, and thought to be suggestive of callose (Heslop-Harrison 1966). Instead, collars observed during this study appeared to be composed of materials similar to those comprising the host cell wall. Further, staining with aniline blue followed by fluorescence microscopy did not demonstrate callose as it had elsewhere (Al-Khesraji and Lösel 1981; Hardwick et al. 1971). While this may simply indicate collars need not be of common origination, it is important to remember that in previous studies the tissue employed had been fixed in glutaraldehyde, which has been shown to induce callose formation in plant cells (Hughes and Gunning 1980).

The association of vesicles with collars, as reported herein, may be suggest a mechanism of collar production; however, as they were infrequently encountered, they may simply have been artifacts. It was not possible to determine whether the osmiophilic bodies were analogous to the PA-TCH-SP stained vesicles also viewed in association with the collar. This stain is also believed to visualize some fatty acids, but such vesicles, stained or otherwise, were not evident in the appropriate controls (Materials and Methods). If the vesicle contents were fatty acids rather than

carbohydrates, it is likely they were not involved in collar development; they may have been lipids displaced from cellular membranes as seen in water-stressed plants (Poljakoff-Mayber 1981). Chong and Harder (1982) noted cytoplasmic vesicles associated with collars in cells infected by P. coronata avenae, and suggested that these and the closely associated endoplasmic reticulum were responsible for the development of collars about D- haustoria. But a similar association of endoplasmic reticulum was not evident in western gall rust infections, and there is little information in other reports as to how type II collars are produced.

It is commonly believed that type II collars are deposited either on the host cell wall during rust penetration, or directly upon the haustorium initial as it emerges through the wall into the cell (Harder 1978; Walles 1974). However, while penetration peg formation as described in Chapter One indicated an inward displacement of the host cell wall, there was no evidence of collar material deposition prior to successful breaching of the wall. This suggests that some smaller collars may be produced by the invagination of the host cell wall as proposed by Rijo and Sargent (1974). With few exceptions, the more massive collars were not breached, but an increase in sample size might prove otherwise. Haustorial development occurred relatively quickly, as suggested by the lack of intermediate stages (Chapter 1), and it seems unlikely that collars produced by most cells in an otherwise compatible reaction would develop quickly enough to encase developing healthy haustoria. The larger collars were only observed in association with necrotic- appearing haustoria, and may be produced in response

to the presence of the dead haustorium (Littlefield and Heath 1979).

What constitutes mechanisms of resistance to E. harknessii is unclear. It was hoped that seedlings of the exotic pine P. thunbergii would display examples of defined resistance sequences which could have been related to the progeny of field resistant native stock. Unfortunately, while several possibly important resistance mechanisms to infection by E. harknessii were expressed in the juvenile seedlings of Japanese black pine, the available seeds of this host were not derived from well defined families showing characteristic expressions of resistance similar to isogenic cereal lines. Thus, at present, each seedling of this host examined must be regarded individually, and one cannot determine whether the resistance mechanisms observed in the early stages of infection of P. thunbergii are part of a continuum with those observed in later stages of infection on other seedlings.

In the reactions of P. thunbergii to western gall rust reported in this study, necrosis appeared to play an important role in juvenile resistance, evinced by the fact that host cell necrosis preceded haustorial death on many occasions. However in this study host cell necrosis only appeared to keep pace with the advance of the mycelium, implying haustorial penetration is a necessary prerequisite to induction of the necrotic reaction. This contrasts with the observations of Robb et al. (1975a) and Miller et al. (1976) who noted instances of host cell necrosis in advance of host cell penetration in their respective studies of C. ribicola and C.

quercuum fusiforme. Gray and Amerson (1983) were able to show a correlation between necrosis and juvenile resistance in P. taeda to C. quercuum fusiforme, but they found that it was the speed with which necrosis developed, and not the degree of development, that was important in determining incompatibility in that system.

Ultrastructural evidence obtained in this study showed that intercellular hyphae were not directly affected by host cell necrosis. This appears to be common in rust resistant reactions (Heath 1982), and as both haustoria and intercellular hyphae were observed well into the cortex of P. thunbergii, it would appear host cell necrosis only partially accounts for resistance to E. harknessii in this host.

In many seedlings, necrosis was not evident in infected epidermal cells, and it was assumed necrosis would not occur until the mycelium entered the cortex. However, in a few of the seedlings examined shortly after inoculation, necrotic appearing haustoria were noted in a few localized epidermal cells; some haustoria also appeared to be encapsulated in callose. It is not known whether this is indicative of a hypersensitive reaction with subsequent failure of mycelial penetration of the cortex. However, many inoculated seedlings never showed any macroscopic evidence of infection, and this may be related to a localized epidermal response such as described above. Miller et al. (1976) noted that a number of slash pine seedlings failed to show any evidence of infection after inoculation with C. quercuum fusiforme, and they suggested that the basidiospore germlings had failed to penetrate

the cuticle; however, no evidence was presented to support this hypothesis.

Periderm development within the cortex, in advance of the mycelium, would probably be regarded as one of the most effective barriers to infection in trees. To establish a successful infection, the rust must progress into the vascular tissues where cambial stimulation results in the formation of relatively long-lived woody-galls on which sporulation occurs (True 1938). Accordingly, in tree stem rusts, infections of the cortex are not indicators of susceptibility.

Although the results of this study can only be considered as preliminary, it would appear necrosis in the cortex only serves to reduce the rate of mycelial spread, thus allowing sufficient time for periderm production. The walls of peridermal cells were heavily suberized, suberin being an effective barrier to microbial penetration (Kolattukudy 1985). Wound periderm formation, a non-specific plant response to injury (Esau 1977), was also evident in rust infected seedlings of P. thunbergii possibly contributing to restriction of E. harknessii development. However, it is not clear whether this response occurred quickly enough to successfully wall-off the infected area in P. thunbergii, although there is evidence that responses similar to wound periderm formation limit the spread of wood-rotting organisms (Shigo 1984). However, previous reports dealing with rust resistance in pines usually noted the presence of necrotic parenchyma tissue, not wound

periderm, forming the reaction zones which restrict infection (Jewell et al. 1982; Jewell and Spiers 1980; Miller et al. 1976).

There was also some evidence of haustorial encapsulation in E. harknessii infected P. thunbergii, and such a mechanism has been suggested as contributing to resistance of P. sylvestris to M. pinitorqua (Jonsson et al. 1978). Walles (1974) also observed haustorial encapsulation with Peridermium pini in P. sylvestris, but he did not equate this with resistance. Littlefield and Heath (1979) suggested that collar-derived encapsulations are produced as reactions to the presence of dead or moribund haustoria, and are not the cause of haustorial death. It is possible this would explain the presence of encasements in response to E. harknessii, since encased non-necrotic haustoria were never observed. However it is also possible that, along with necrosis, they might serve to slow the spread of the rust mycelium, although there is no evidence to confirm this.

BIBLIOGRAPHY

Aist, J.R. 1976. Papillae and related wound plugs of plant cells. Ann. Rev. Phytopathol. 14: 145-163.

Allen, R.F. 1930. A cytological study of heterothallism in Puccinia graminis. J. Agric. Res. 40: 585-614.

Allen, R.F. 1932a. A cytological study of heterothallism in Puccinia triticina. J. Agric. Res. 44: 733-754.

Allen, R.F. 1932b. A cytological study of heterothallism in Puccinia coronata. J. Agric. Res. 45: 513-541.

Allen, R.F. 1934. A cytological study of heterothallism in Puccinia sorghi. J. Agric. Res. 49: 1047-1068.

Allen, R.F. 1935. A cytological study of Puccinia malvacearum from the sporidium to the teliospore. J. Agric. Res. 51: 801-818.

Al-Khesraji, T.O., and D.M. Lösel. 1980. Intracellular structures of Puccinia poarum on its alternate hosts. Trans. Br. mycol. Soc. 75: 397-411.

_____. 1981. The fine structures of haustoria, intracellular hyphae and intercellular hyphae of Puccinia poarum. Physiol. Plant Pathol. 19: 301-311.

Anderson, G.W. and D.W. French. 1965. Differentiation of Cronartium quercuum and Cronartium colesporioides on the basis of aeciospore germ tubes. Phytopathology, 55: 171-173.

Arthur, J.C. 1934. Manual of the rusts in United States and Canada. Purdue Research Foundation, Lafayette, Ind.

Borland J., and C.W. Mims. 1980. An ultrastructural comparison of the aecial and telial haustorium of the autoecious rust Puccinia podophylli. Mycologia, 72: 767-774.

Boyce, J.S. 1957. The fungus causing western gall rust and Woodgate rust of pines. Forest Sci. 3: 225-234.

Boyer, M.G. 1964. Studies on white pine phenols in relation to blister rust. Can. J. Bot. 42: 979-987.

Boyer, M.G. and P.K. Isaac. 1964. Some observations on white pine blister rust as compared by light and electron microscopy. Can. J. Bot. 42: 1305-1309.

Bracker, C.E. 1967. Ultrastructure of fungi. Ann. Rev. Phytopathol. 5: 343-374.

Bracker, C.E., and L.J. Littlefield. 1973. Structural concepts of host-pathogen interfaces. In Fungal Pathogenicity and the Plant's Response. Edited by R.J.W. Byrde and C.V.Cutting. Academic Press, London. pp. 159-318.

Bushnell, W.R. 1972. Physiology of fungal haustoria. Ann. Rev. Phytopathol. 10: 151-176.

Chong, J. 1981. Ontogeny of mono- and dikaryotic haustoria of Puccinia coronata avenae. Ultrastructure, cytochemistry and electron-probe x-ray analysis. Doctoral thesis, University of Manitoba, Winnipeg, Manitoba.

Chong, J., and D.E. Harder. 1982. Ultrastructure of haustorium development in Puccinia coronata avenae: some host responses. Phytopathology, 72: 1527-1533.

Chong, J., D.E. Harder, and R. Rohringer. 1981. Ontogeny of mono- and dikaryotic rust haustoria: cytochemical and ultrastructural studies. Phytopathology, 71: 975-983.

_____. 1985. Cytochemical studies on Puccinia graminis f. sp. tritici in a compatible wheat host. I. Walls of intercellular hyphal cells and haustorium mother cells. Can. J. Bot. 63: 1713-1724.

Chou, C.K. 1970. An electron-microscope study of host penetration and early stages of haustorium formation of Peronospora parasitica (Fr.) Tul. on cabbage cotyledons. Anns. of Botany, 34: 189-204.

Christenson, J.A. 1968. A cytological comparison of germinating aeciospores in the Cronartium coleosporioides complex. Mycologia, 60: 1169-1177.

Clinton, G.P., and F.A. McCormick. 1919. Infection experiments of Pinus strobus with Cronartium ribicola. Report of the Botanist for years 1917-18, Conn. Agr. Exp. Sta. Bull 214. pp. 428-459.

Coffey, M.D. 1976. Flax rust resistance involving the K gene: an ultrastructural survey. Can. J. Bot. 54: 1443-1457.

_____. 1983. Cytochemical specialization at the haustorial interface of a biotrophic parasite, Albugo candida. Can. J. Bot. 61: 2004-2014.

Coffey, M.D. and F.H.E. Allen. 1983. A quantitative histological and ultrastructural analysis of interactions between the flax rust and near -isogenic host lines varying in their degree of incompatibility. Can.J.Bot. 61: 1831-1850.

Coffey, M.D., B.A. Palevitz, and P.J. Allen. 1972. The fine structure of two rust fungi Puccinia helianthi and Melampsora lini. Can. J. Bot. 50: 231-240.

Colley, R.H. 1918. Parasitism, morphology and cytology of Cronartium ribicola. J. Agric. Res. 15: 619-660.

Craig, A.S. 1974. Sodium borohydride as an aldehyde blocking reagent for electron microscope histochemistry. Histochemistry 42: 141-144.

Cummins, G.B. 1959. Illustrated Genera of Rust Fungi. Burgess, Minneapolis.

Cummins, G.B. 1962. Supplement to Arthur's manual of the rusts in United States and Canada. Hafner Publishing Co., New York.

Currier, H.B. 1957. Callose substances in plant cells. Am. J. Bot. 44: 478-488.

DeBary, A. 1863. Recherches sur le devélopment de quelques champignons parasites. Ann. Sc. Nat. Bot. IV 20; 5-148.

Dodge, B.O. 1922. Studies in the genus Gymnosporangium IV. Distribution of the mycelium and subcuticular origin of the telium in G. clavipes. Am. J. Bot. 9: 354-365.

Erlich, M.A., and H.G. Erlich. 1970. Electron microscope radioautography of ^{14}C transfer from rust uredospores to wheat host cells. Phytopathology, 60: 1850-1851.

Esau, K. 1977. Anatomy of seed plants. John Wiley and Sons, New York.

Favoli, M.A., and M. Marte. 1973. Electron microscope autoradiography of rust-affected bean leaves labelled with tritiated glycine. Phytopathol. Z. 76: 343-347.

Feder, N., and T.P. O'Brien. 1968. Plant micro technique: some principles and new methods. Am.J.Bot. 55: 123-142.

Feder, N., and M.K. Wolf. 1965. Studies on nucleic acid metachromasy. II. Metachromatic and orthochromatic staining by toluidine blue of nucleic acids in tissue sections. J. Cell. Bio. 27: 327-336.

Fisher, D.B. 1968. Protein staining for ribboned epon sections for light microscopy. Histochemie, 16: 92-96.

Fromme, F.D. 1916. Facultative heteroecism (?) of Peridermium harknessii and Cronartium quercus. Phytopathology, 6; 411-412.

Fulcher, R.G., and R. Wong. 1980. Inside cereals - a fluorescence microchemical view. In Cereals for Food and Beverages. Recent Progress in Cereal Chemistry. Edited by G.E. Inglett and L. Munch. Academic Press, New York. pp. 1-26.

Gerhardt, P., R.G.E. Murray, R.N. Costilow, W.A. Wood, N.R. Kriel, and G.B. Phillips. 1981. Manual of methods for general bacteriology. American Society for Microbiology, Washington, D.C.

Gil, F. and J.L. Gay. 1977. Ultrastructural and physiological properties of the host interfacial components of haustoria of Erysiphe pisi in vivo and in vitro. Physiol. Plant Pathol. 10: 1-12.

Glidewell, D.C. and C.W. Mims. 1979. Ultrastructure of the haustorial apparatus in the rust fungus Kunkelia nitens. Bot. Gaz. 140: 148-152.

Gold, R.E. 1983. Activation and pattern of teliospore germination in Uromyces appendiculatus var. appendiculatus and basidiospore infection of Phaseolus vulgaris. Doctoral dissertation. Universitat Konstanz, Konstanz, Federal Republic of Germany.

Gold, R.E., and L.J. Littlefield. 1979. Light and scanning electron microscopy of telial, pycnial and aecial stages of Melampsora lini. Can. J. Bot. 57: 629-638.

Gold, R.E., L.J. Littlefield and C.D. Statler. 1979. Ultrastructure of the pycnial and aecial stages of Puccinia recondita. Can. J. Bot. 57: 74-86.

Gold, R.E., and K. Mendgen. 1984a. Cytology of basidiospore germination, penetration, and early colonization of Phaseolus vulgaris by Uromyces appendiculatus var. appendiculatus. Can. J. Bot. 62: 1989-2002.

_____. 1984b. Vegetative development of Uromyces appendiculatus var. appendiculatus in Phaseolus vulgaris. Can. J. Bot. 62: 2003-2010.

Goldstein, I.J., S. Hammerstrom and G. Sunblad. 1975. Precipitation and carbohydrate-binding specificity studies on wheat germ agglutinin. Biochem. Biophys. Acta. 405: 53-61.

Gray, D.J. 1982. Ultrastructure and histology of the fusiform rust fungus. Doctoral thesis, North Carolina State University, Raleigh, N.C.

Gray, D.J., and H.V. Amerson. 1983. In vitro resistance of Pinus taeda to Cronartium quercuum f.sp.fusiforme. Ultrastructure and histology. Phytopathology, 73: 1492-1499.

Gray, D.J., H.V. Amerson and C.G. Van Dyke. 1982. An ultrastructural comparison of monokaryotic and dikaryotic haustoria formed by the fusiform rust fungus Cronartium quercuum f.sp.fusiforme. Can. J. Bot. 60: 2914-2922.

_____. 1983. Ultrastructure of the infection and early colonization of Pinus taeda by Cronartium quercuum formae speciales fusiforme. Mycologia, 75: 117-130.

Griffin, D.H. 1981. Fungal physiology. John Wiley and Sons, New York.

Grove, N., and C.E. Bracker. 1970. Protoplasmic organization of hyphal tips among fungi: Vesicles and Spitzenkorper. J. Bacteriol. 104: 989-1009.

Hall, J.L. 1978. Electron microscopy and cytochemistry of plant cells. Elsevier/North Holland Biomedical Press, Amsterdam.

Harder, D.E. 1978. Comparative ultrastructure of the haustoria in uredial and pycnial infections of Puccinia coronata avenae. Can. J. Bot. 56: 214-224.

Harder, D.E., and J. Chong. 1984. Structure and physiology of haustoria. In The Cereal Rusts. Edited by W.R. Bushnell and A.P. Roelfs Eds. Academic Press, New York. pp. 431-476.

Harder, D.E., and K. Mendgen. 1982. Filipin-sterol complexes in bean rust and oat crown rust-fungal/plant interactions. Freeze-etch electron microscopy. Protoplasma, 112: 46-54.

Harder, D.E., R. Rohringer, D.J. Samborski, W.K. Kim, and J. Chong. 1978. Electron microscopy of susceptible and resistant near isogenic (sr6/Sr6) lines of wheat infected by Puccinia graminis tritic: I. The host pathogen interface in the compatible (Sr6/P6) interaction. Can. J. Bot. 56: 2955-2966.

Harder, D.E., D.J. Samborski, R. Rohringer, S.R. Rimmer, W.K. Kim and J. Chong. 1979. Electron microscopy of susceptible and resistant near-isogenic (sr6/Sr6) lines of wheat infected by Puccinia graminis tritici: III. ultrastructure of incompatible interactions. Can. J. Bot. 57: 2626-2634.

Hardwick, N.V., A.D. Greenwood and R.K.S. Wood. 1971. The fine structure of the haustorium of Uromyces appendiculatus in Phaseolus vulgaris. Can. J. Bot. 49: 383-390.

Harkness, H.W. 1884. New species of California fungi. Bull. California Acad. Sci. 1: 29-47. 1884.

Hayat, M.A. 1981. Principles and techniques of electron microscopy. Biological applications Vol. 1. University Park Press, Baltimore.

Heath, M.C. 1971. Hautorial sheath formation in cowpea immune to rust infection. Phytopathology, 61: 383-388.

_____. 1972. Ultrastructure of host and non-host reactions to cowpea rust. Phytopathology 62: 27-38.

_____. 1974. Chloroplast ultrastructure and ethylene production of senescing and rust infected cowpea leaves. Can. J. Bot. 52: 2591-2597.

_____. 1976. Ultrastructural and functional similarity of the haustorial neckband of rust fungi and the casparian strip of vascular plants. Can. J. Bot. 54: 2484-2489.

_____. 1980. Reactions of nonsuscepts to fungal pathogens. Ann. Rev. Phytopathol. 18: 211-236.

_____. 1982. Host defense mechanisms. In The Rust Fungi. Edited by K.J. Scott and A.K. Chakravorty. Academic Press, New York. pp. 223-245.

Heath, M.C., and M.R. Bonde. 1983. Ultrastructural observations of the rust fungus Physopella zeae in Zea mays. Can. J. Bot. 61: 2231-2242.

Heath, M.C., and I.B. Heath. 1971. Ultrastructure of an immune and a susceptible reaction of cowpea leaves to rust infection. Physiol. Plant Pathol. 1: 277-287.

Heath, M.C., and I.B. Heath. 1975. Ultrastructural changes associated with the haustorial mother cell septum during haustorium formation in Uromyces phaseoli var. vignae. Protoplasma, 84: 297-314.

Hedgecock, G.G. 1912. Notes on some western Uredineae which attack forest trees. Mycologia, 4: 131-147.

Heslop-Harrison, J. 1966. Cytoplasmic continuities during spore formation in flowering plants. Endeavour, 25: 65-72.

Heslop-Harrison, J., and Y. Heslop-Harrison. 1982. The growth of grass pollen tube: I. Characteristics of the polysaccharide particles ("P-particles") associated with apical growth. Protoplasma, 112: 71-80.

Hickey, E.L., and M.D. Coffey. 1978. A cytochemical investigation of the host-parasite interface in Pisum sativum infected by the Downy Mildew fungus Peronospora pisi. Protoplasma, 97: 201-220.

Hiratsuka, Y. 1969. Endocronartium, a new genus for autoecious pine stem rusts. Can. J. Bot. 47: 1493-1495.

Hiratsuka, Y., and P.J. Maruyama. 1983. Resistant reactions of two Asian pines to western gall rust, Endocronartium harknessii. Phytopathology, 73: 835 (abstr.).

Hiratsuka, Y., W. Morf, and J.M. Powell. 1966. Cytology of the aeciospores and aeciospore germ tubes of Peridermium harknessii and P. stalactiforme of the Cornartium coleosporioides complex. Can. J. Bot. 44: 1639-1643.

Hiratsuka, Y., and J.M. Powell. 1976. Pine stem rusts of Canada. Environment Canada, Can. For. Serv., North For. Res. Cent., For. Tech. Rep. No. 4, Edmonton, Alberta.

Hoff, R.J., and G.I. McDonald 1971. Resistance to Cronartium ribicola in Pinus monticola short shoot fungicidal reaction. Can.J.Bot. 49: 1235-1239.

_____. 1972. Resistance of Pinus armandii to Cronartium ribicola. Can.J.For.Res. 2: 303-307.

Horisberger, M., and R.J. Rosset. 1977. Colloidal gold, useful marker for transmission and scanning electron microscopy. J. Histochem. Cytochem. 25: 295-305.

Hughes, J., and M.E. McCully. 1975. The use of an optical brightener in the study of plant structure. Stain Technology, 50: 319-329.

Hughes, J.E., and B.E.S. Gunning. 1980. Gluteraldehyde-induced deposition of callose. Can. J. Bot. 58: 250-258.

Hutchinson, W.G. 1935. Resistance of Pinus sylvestris to a gall forming Peridermium. Phytopathology, 25: 819-843.

Jackson, H.S. 1932. Present evolutionary tendencies and the origin of life cycles in the Uredinales. Mem. Torrey Bot. Club 18: 1-108.

Jensen, W.A. 1962. Botanical histochemistry. Principles and Practices. W. Freeman & Co., San Francisco.

Jewell, F.F., D.C. Jewell and C.H. Walkinshaw. 1982. Histopathology of anatomical mechanisms for resistance to fusiforme rust in slash pine. In Resistance to Diseases and Pests in Forest Trees. Edited by H.M. Heybroek, B.R.S. Stephan, and K. von Weissenberg. Proceedings of the Third International Workshop on the Genetics of Host-Parasite Interactions in Forestry. Wageningen, The Netherlands. Centre for Agricultural Publishing and Documentation, Wageningen. pp. 110-118.

Jewell, F.F., and G.A. Snow. 1972. Anatomical resistance to gall rust infection in slash pine. Plant Dis. Rep. 56: 531-534.

Jewell, F.F., and D.C. Speirs. 1976. Histopathology of one-and two-year old resisted infections by Cronartium fusiforme in slash pine. Phytopathology, 66: 741-748.

Jonsson, A., M. Holmvall and B. Walles. 1978. Ultrastructural studies of resistance mechanisms in Pinus sylvestris L. against Melampsora pinitorqua (Braun) Rostr. (pine twisting rust). Stud. For. Suec. 145: 1-28.

Karling, J.S. 932. Studies in the Chytridiales. VII. The organization of the chytrid thallus. Am. J. Bot. 19: 41-74.

Khan, S. R., and J.W. Kimbrough. 1982. The fine structure of septa and haustoria of Cronartium quercuum formae speciales fusiforme on Quercus rubra. Mycologia, 74: 809-819.

Kinloch, B.B., and J.L. Littlefield. 1977. White pine blister rust: hypersensitive resistance in sugar pine. Can..J. Bot. 55: 1148-1155.

Kohno, M., H. Ishizaki and H. Kunoh. 1976. Cytological studies on rust fungi. V. Intracellular hyphae of Gymnosporangium haraeanum Sydow in cells of Japanese pear leaves. Ann. Phytopathology Soc. Japan, 42: 419-423.

_____. 1977. Cytological studies on rust fungi. VI. Fine structures of infection process of Kuehneola japonica (Diet.) Diet. Mycopathologia, 61: 35-41.

Kolattukudy, P.E. 1984. Biochemistry and function of cutin and suberin. Can. J. Bot. 62: 2918-2933.

Littlefield, L.J. 1972. Development of haustoria of Melampsora lini. Can. J. Bot. 50: 1701-1703.

Littlefield, L.J., and C.E. Bracker. 1972. Ultrastructural specialization at the host- pathogen interface in rust-infected flax. Protoplasma, 74: 271-305.

Littlefield, L.J., and M.C. Heath. 1979. Ultrastructure of Rust Fungi. Academic Press, New York.

Longo, N. 1982. Ultrastructural observations on the septal pore in Cronartium flaccidum (Alb. et Schw.) Wint. Also in relation to the taxonomy of the Uredinales. Carylogia, 35: 425-441.

Longo, N., and B. Naldini. 1972. Osservazioni sull'ultrastruttura dell'austorio di Melampsora pinitorqua (A.Br.) Rostr. in cellule di Populus tremula. Carylogia, 25: 383-401.

Longo, N., and B. Naldini-Longo. 1975. Observations of the fine structure of the haustorium of Melampsora pinitorqua (A.Br.) Rostr. in cells of Pinus pinea L. Caryologia, 28: 389-405.

Longo, N., F. Moriondo and B. Longo. 1982. Ultrastructural observations on the host-pathogen interface in infections of Cronartium flaccidum. Caryologia, 35: 307-326

Lorbeer, J.W. 1955. Several aspects of the pathology of Peridermium harknessii. J.P. Moore, M.Sc.Thesis. University of Washington, Seattle, Wash.

Maddy, A.H. 1964. The fluorescent label for the outer components of the plasma membrane. Biochem. Biophys. Acta 88: 390-399.

McDonald, G.I., and R.J. Hoff. 1970. Resistance to Cronartium ribicola in Pinus monticola; Early shedding of infected needles. U.S. Dep. Agric. For. Serv. Res. Note INI - 124.

McKenzie, M.A. 1942. Experimental autoecism and other biological studies of a gall-forming Peridermium on northern hard pines. Phyopathology, 32: 785-798.

Meinecke, E.P. 1916. Peridermium harknessii and Cronartium quercuum. Phytopathology, 6: 225-240.

_____. 1920. Facultative heteroecism in Peridermium cerebrum and Peridermium harknessii. Phytopathology, 10: 279-297.

_____. 1929. Experiments with repeating pine rusts. Phytopathology, 19: 327-342.

Mendgen, K. 1975. Ultrastructural demonstration of different peroxidase activities during the bean rust infection process. Physiol. Plant Pathol. 6: 275-282.

_____. 1977. Reduced lycine uptake by bean rust haustoria in a resistant reaction. Naturwisschaften 64: 438.

Mendgen, K., and R. Heitefuss. 1975. Microautoradiographic studies on host-parasite interactions. I. The infection of Phaseolus vulgaris with tritium-labelled urediospores of Uromyces phaseoli. Arch. Microbiology, 105: 193-199.

Miller, T, E.B. Cowling, H.R. Powers, and T.E. Blalock. 1976. Types of resistance and compatability in slash pine seedlings infected by Cronartium fusiforme. Phytopathology, 66: 1229-1235.

Miller, T., R.F. Patton and H.R. Powers, Jr. 1980. Mode of infection and early colonization of slash pine seedlings by Cronartium quercuum f. sp. fusiforme. Phytopathology, 70; 1206-1208.

Mims, C.W., and D.C. Glidewell. 1978. Some ultrastructural observations on the host-pathogen relationship within the telial gall of the rust fungus Gymnosporangium juniperi-virginianae. Bot. Gaz. 139: 11-17.

Mlodzianowski, F. and R. Siwecki. 1975. Ultrastructural changes in chloroplasts of Populus tremula L. leaves affected by the fungus Melampsora pinitorqua (Braun) Rostr. Phys. Plant Pathol. 6: 1-3.

Moore, R.T. and J.H. McAlear. 1961. Fine structure of mycota. 8. On the aecidial stage of Uromyces cladii. Phytopathol. Z. 82: 207-215.

Nagahasi, G., R.T. Leonard, and W.W. Thomson. 1978. Purification of plasma membranes from roots of barley. Specificity of the phosphotungstic acid-chromic acid stain. Plant Physiol. 61: 993-999.

Nelson, D.L. 1970. The ecology and pathology of pine gall rust in California. Doctoral thesis, University of California, Berkeley.

Nusbaum, C.J. 1935. A cytological study of the resistance of apple varieties to Gymnosporangium juniperi virginianae. J. Agric. Res. 51: 573-596.

Nusbaum, C.J., and G.W. Keitt. 1938. A cytological study of host parasite relations of Venturia inaequalis on apple leaves. J. Agric. Res. 56: 595-618.

O'Brien, T.P., N. Feder and M.E. McCully. 1964. Staining of plant cell walls by Toluidine blue O. Protoplasma, 59: 366-373.

O'Brien, T.P., and M.E. McCully. 1981. The study of plant structure principles and selected methods. Termarcphi Pty Ltd. Melbourne, Australia.

Onoe, T., T. Tani, and N. Naito. 1973. The uptake of labeled nucleosides by Puccinia coronata grown on susceptible leaves. Rep. Tottori Mycol. Inst. 10: 303-312.

Orvical, J. 1969. Infrastructure des sucoirs et relations hote-parasite dans des stades e'cidiens d'uredinales C.R. Hebd. Seances Acad. Sci. Ser. D.269: 1973-1975.

Pady, S.M. 1935a. Aeciospore infection in Gymnoconia interstitialis by penetration of the cuticle. Phytopathology, 25: 453-474.

_____. 1935b. The role of intracellular mycelium in systemic infections of Rubus with the orange-rust. Mycologia, 27: 618-637.

Patton, R.F., and D.W. Johnson. 1970. Mode of penetration of needles of eastern white pine by Cronartium ribicola. Phytopathology, 60: 977-982.

Pease, D.C. 1966. Polysaccharides associated with the exterior surface of epithelial cells-kidney, intestine, brain. Anat. Rec. 154: 400.

_____. 1970. Phosphotungstic acid as a specific stain for complex carbohydrates. J. Histochem. Cytochem. 18: 455.

Poljakoff-Mayber, A. 1981. Ultrastructural consequences of drought. In The Physiology and Biochemistry of Drought Resistance in Plants. Edited by L.G. Paleq and D. Aspinall. Academic Press, New York. pp. 389-403.

Prusky, D., A. Dinoor and B. Jacoby. 1980. The sequence of death of haustoria and host cells during the hypersensitive reaction of oat to crown rust. Phys. Plant. Pathol. 17: 33-40.

Rambourg, M.A. 1967. Detection des glycoproteines en microscopie electronique: coloration de la surface cellulaire et de 1'appareil de golgi par un melange acid chromique phosphotungstique. C.R. Hebd. Seances Acad. Sci., Ser. D 265: 1426-1428.

Rambourg, M.A., W. Hernandez, and C.P. Leblond. 1969. Detection of complex carbohydrates in the Golgi apparatus of rat cells. J. Cell Biol. 40: 395-414.

Reed, H.S. and C.H. Grabill. 1915. The cedar rust disease of apples caused by Gymnosporangium juniperi-virginianae Schw. Va. Agric. Exp. Stn. Tech. Bull. 9: 1-106.

Rijkenberg, F.H.J., and S.J. Truter. 1973. Haustoria and intracellular hyphae in the rusts. Phytopathology, 63: 281-286.

Rijo, L., and J.A. Sargent. 1974. The fine structure of the coffee leaf rust Hemileia vastatrix. Can. J. Bot. 52: 1363-1367.

Robb, J., A.E. Harvey, and M. Shaw, 1975a. Ultrastructure of tissue cultures of Pinus monticola infected by Cronartium ribicola. I. Penetration host changes. Physiol. Plant Pathol. 5: 1-8.

_____. 1975b. Ultrastructure of tissue cultures of Pinus monticola infected by Cronartium ribicola. II. Penetration and prepenetration. Physiol. Plant Pathol. 5: 9-18.

Robinson, W. 1913. XI. On some relations between Puccinia malvacearum Mont. and the tissues of its host plant (Althaea rosea). Manchester Mem. 57: 1-24.

Rohringer, R., J. Chong, W.K. Kim, and D.E. Harder. 1982. Cytochemistry of the host/parasite interface and the use of gold markers in cereal/rust interactions. In Active Defence Mechanism in Plants. Edited by R. K.S. Wood. Plenum, New York.

Roland, J.C., C.A. Lembi, and D.J. Moore. 1972. Phosphotungstic acid-chromic acid as a selective electron-dense stain for plasma membranes of plant cells. Stain Technol. 47: 195-200.

Sato, T., K. Katsuya, and S. Sato. 1980. Host range, teliospore germination and infection process of Uromyces aloes. Trans. Mycol. Soc. Japan 21: 273-282.

Shipton, W.A., and J.F. Brown. 1962. A whole-leaf clearing and staining technique to demonstrate host-pathogen relationship of wheat stem rust. Phytopathology, 52: 1313.

Shigo, A.L. 1984. Compartmentalization: A conceptual framework for understanding how trees grow and defend themselves. Ann. Rev. Phytopathol. 22: 189-214.

Smith, M.M., and M.E. McCully. 1978. A critical evaluation of the specificity of aniline blue induced fluorescence. Protoplasma, 95: 229-254.

Spencer-Phillips, P.T.N., and J.L. Gay. 1981. Domains of ATPase in plasma membranes and transport through infected plant cells. New Phytol. 89: 393-400.

Spiers, A.G., and D.H. Hopcroft. 1985. Ultrastructural studies of the spermatial and aecial stages of Melampsora larici-populina and Melampsora epitea on Larix decidua. N.Z.Journal of Botany, 23: 101-116.

Struckmeyer, E.B., and A.J. Riker. 1951. Wound periderm formation in white pine trees resistant to blister rust. Phytopathology, 41: 276-281.

Tainter, F.H. 1985. The ultrastructure of germinating aeciospores and intercellular and intracellular structures of Cronartium comandrae. Proceedings rust and hard pines working party conference. IUFRO. Athens, Georgia.

Thiery, J.P. 1967. Mise en évidence des polysaccharides sur coupes fines en microscopie electronique. J. Microsc. (Paris) 6: 987-1018.

_____. 1969. Role de l'appareil de Golgi dans la synthèse des mucopolysaccharides; étude cytochimique. I. Mise en évidence de mucopolysaccharides dans les vésicules de transition entre l'ergastoplasme et l'appareil de Golgi. J. Microsc. (Paris) 8: 689-708.

True, R. 1938. Gall development on Pinus sylvestris attacked by the Woodgate Peridermium and morphology of the parasite. Phytopathology, 28: 24-50.

Van der Kamp, B.J. 1969. Peridermium pini (Pers.) Lev. and the resin-top disease of Scots pine. II Lesion anatomy. Forestry 42: 185-201.

_____. 1970. Peridermium pini (Pers.) Lev. and the resin-top disease of Scots pine. III. Infection and lesion development. Forestry 43: 73-88.

Van der Woode, W.J. 1973. Significance of the specific staining of plant plasma membranes by treatment with chromic acid-phosphotungstic acid. Plant Physiology 51:15.

Wagner, W.W. 1964. "Facultative heteroecism'. Was it demonstrated in Peridermium harknessii in 1919-1920? Mycologia, 56: 782-785.

Walkinshaw, C.H. 1978. Cell necrosis and fungal content in fusiform rust-infected Loblolly, Longleaf, and Slash Pine seedlings. Phytopathology, 68: 1705-1710.

Walles, B. 1974. Ultrastructure of the rust fungus Peridermium pini (Pers.) Lev. Stud. For. Suec. 122: 1-30.

Ward, M.H. 1888. Illustrations of the structure and life history of Puccinia graminis, the fungus causing the "rust" of wheat. Ann.Bot. (London) 2:217-222.

Waterhouse, W.L. 1921. Studies in the physiology of parasitism. VII. Infection of Berberis vulgaris by sporidia of Puccinia graminis. Ann. Bot. (London) 35: 557-564.

Weir, J.R., and E.E. Hubert. 1917. Pycnial stages of important forest tree rusts. Phytopathology, 7: 135-139.

Welch, B.L. and N.E. Martin. 1974. Invasion mechanisms of Cronartium ribicola in Pinus monticola bark. Phytopathology 64: 1541-1546.

Wenner, N., and W. Merril. 1984. Resistance of Pinus virginiana and P. rigida X taeda seedlings to Endocronartium harknessii. (abstr.) Phytopathology, 74: 870.

Wood, P.J., and R.G. Fulcher. 1978. Interactions of some dyes with cereal β-glucans. Cereal Chem. 55: 952-966.

Woods, A.M., and J.L. Gay. 1983. Evidence for a neckband delimiting structural and physiological regions of the host plasma membrane associated with haustoria of Albugo candida. Physiol. Plant Pathol. 23: 73-88.

York, H.H. 1926. A. Peridermium new to the northeastern United States. Science 64: 500-501.

_____. 1929. The Woodgate rust. J. Econ. Entomol. 22: 482-485.

Zalasky, H., and C.G. Riley. 1963. Infection tests with two caulicolous rusts of jack pine in Saskatchewan. Can. J. Bot. 41: 459-465.

Ziller, W.G. 1974. The tree rusts of western Canada. Environment Canada, Can. For. Serv., Pac. For. Res. Cent. Publ. 1392, Victoria, B.C.